AD/A-001 524

BEHAVIOR OF STABILIZED SOILS UNDER REPEATED LOADING. REPORT 6. A SUMMARY REPORT WITH A SUGGESTED STRUCTURAL PAVEMENT DESIGN PROCEDURE

James K. Mitchell, et al

California University

Prepared for:

Army Engineer Waterways Experiment Station

October 1974

Unclassified

SECURITY CLASSIFICATION OF THIS PAGE (When Data Entered)

AD/A-001524

REPORT DOCUMENTATION PAGE

READ INSTRUCTIONS BEFORE COMPLETING FORM

1. REPORT NUMBER: Contract Report No. 3-145, Report 6
2. GOVT ACCESSION NO.
3. RECIPIENT'S CATALOG NUMBER

4. TITLE (and Subtitle): BEHAVIOR OF STABILIZED SOILS UNDER REPEATED LOADING; Report 6, A SUMMARY REPORT WITH A SUGGESTED STRUCTURAL PAVEMENT DESIGN PROCEDURE

5. TYPE OF REPORT & PERIOD COVERED: Report 6 of a series

6. PERFORMING ORG. REPORT NUMBER

7. AUTHOR(s): James K. Mitchell, Peter Dzwilewski, Carl L. Monismith

8. CONTRACT OR GRANT NUMBER(s): DA-22-079-eng-414

9. PERFORMING ORGANIZATION NAME AND ADDRESS: Department of Civil Engineering, University of California, Berkeley, California 94720

10. PROGRAM ELEMENT, PROJECT, TASK AREA & WORK UNIT NUMBERS

11. CONTROLLING OFFICE NAME AND ADDRESS: U. S. Army Materiel Command, Alexandria, Virginia 22304

12. REPORT DATE: October 1974

13. NUMBER OF PAGES: 162

14. MONITORING AGENCY NAME & ADDRESS (if different from Controlling Office): U. S. Army Engineer Waterways Experiment Station, Soils and Pavements Laboratory, P. O. Box 631, Vicksburg, Mississippi 39180

15. SECURITY CLASS. (of this report): Unclassified

15a. DECLASSIFICATION/DOWNGRADING SCHEDULE

16. DISTRIBUTION STATEMENT (of this Report)

Approved for public release; distribution unlimited.

17. DISTRIBUTION STATEMENT (of the abstract entered in Block 20, if different from Report)

18. SUPPLEMENTARY NOTES

19. KEY WORDS (Continue on reverse side if necessary and identify by block number)

Cement soil stabilization
Loads (forces)
Pavement design
Repetitive loads
Stabilized soils

20. ABSTRACT (Continue on reverse side if necessary and identify by block number)

Results of previous investigations completed in this research are briefly summarized. This summary as well as the results of other investigations completed during the period of this investigation, also summarized where appropriate, form the basis for the design procedure recommended herein. The design procedure is applicable to a two layer system - a cement stabilized layer resting on a subgrade. Stresses and deformations are estimated using layered elastic theory. Essentially the procedure consists of two phases, the first being

(Continued)

DD FORM 1 JAN 73 1473 EDITION OF 1 NOV 65 IS OBSOLETE

Unclassified

SECURITY CLASSIFICATION OF THIS PAGE (When Data Entered)

20. ABSTRACT (continued)

the selection of a thickness adequate to prevent fatigue in the cement-stabilized layer and the second a check to insure that the combination of load and thermal stresses will not crack the stabilized layer. The procedure also recognizes the fact that cement stabilized bases will crack due to shrinkage stresses shortly after construction. This is accomplished by increasing the stresses and strains in the vicinity of the cracks by 50 percent over those computed for the uncracked situation. A series of design charts are presented which permit the selection of the thickness of the cement stabilized layer for a range in base stiffnesses of 100,000 to 3,000,000 psi, a range in subgrade stiffnesses of 1500 to 20,000 psi and for the following loading conditions: highway type vehicles - 13,000 lb single wheel load, 15,000 lb single axle load (dual tires), and 18,000 lb single axle load (dual tires); aircraft - AC-1: 10,000 lb single wheel load, C-130: 40,000 lb load (single tandem), C-141: 144,700 lb load (twin tandem), and Boeing 747: 162,000 lb load (twin tandem). Base and subgrade stiffnesses either can be determined from laboratory tests or estimated by several approximate procedures briefly outlined in the report. Comparisons of thicknesses selected by this procedure for highway type loading conditions with those by existing procedures indicate that the suggested procedure produces comparable thicknesses. Generally, the thicknesses are at a level to minimize initial cracking in the pavement and may, therefore, be conservative for few repetitions of heavy loads.

PREFACE

Studies of the behavior of stabilized soils under repeated loading were initiated at the University of California, Berkeley, in August, 1964, under Contract No. DA-22-079-eng-414 for the U. S. Army Engineer Waterways Experiment Station (WES), Vicksburg, Mississippi. This work is sponsored by the U. S. Army Materiel Command, DA Project No. 1-V-0-21701-A-046-05.

Contract Reports No. 3-145, "Behavior of Stabilized Soils Under Repeated Loading" are as follows. Report 1: "Background, Equipment, Preliminary Investigations, Repeated Compression and Flexure Tests on Cement Treated Silty Clay," December 1965, describes the studies for the period 17 August 1964 - 16 August 1965. Report 2: "Behavior in Repeated Flexure, Frequency and Duration Effects, Fatigue Failure Analysis," September 1966, describes the studies for the period 17 August 1965 - 16 August 1966. Results of additional laboratory investigations conducted during the period 17 August 1966 - 16 August 1968 are presented and discussed in Report 3: "Repeated Compression and Flexure Tests on Cement and Lime-Treated Buckshot Clay, Confining Pressure Effects in Repeated Compression for Cement-Treated Silty Clay," May 1969. Report 4: "Stresses and Deflections in Cement-Stabilized Pavements," presents the results of measurements and theoretical analyses of stresses and deflections developed in two prototype cement-stabilized pavements as a result of repeated plate loadings. This work was accomplished during the latter half of 1967 and 1968. Report 5:

"Performance Evaluation of Cement-Stabilized Soil Layers and its Relationship to Pavement Design," August 1972, describes the analysis of data obtained at WES during 1963 and 1964 from field tests on four sections of cement-stabilized soils to assist in the development of design criteria and a design procedure for pavements containing soil layers stabilized with small amounts of cement and to check the validity of existing theory for prediction of behavior.

This report presents a framework for the design of cement-stabilized layers utilizing the results of the investigations described in the five previous reports as well as the results of studies of cement-stabilized materials completed by other investigators during this same period. To illustrate the basis for the procedure the results of the previous studies in this investigation as well as the appropriate results of other investigators are briefly summarized.

The investigation described herein was conducted under the supervision of Professors James K. Mitchell and Carl L. Monismith of the Department of Civil Engineering. Necessary analyses to develop the design curves (Figs. 9 - 24) were performed by Mr. Peter Dzwilewski a graduate research assistant in Soil Mechanics.

The contract was monitored by Mr. W. L. McInnis, Chief, Materiel Development Division, under the general supervision of Mr. J. P. Sale, Chief, Soils and Pavement Laboratory, WES. Contracting Officer was Col. G. H. Hilt, C.E.

TABLE OF CONTENTS

LIST OF FIGURES

SECTION I: INTRODUCTION

1. In 1964 an investigation, supported by the U. S. Army Corps of Engineers, was initiated at the University of California, Berkeley, to develop improved criteria for quality design of stabilized soils and to develop an improved structural pavement design procedure using such materials for military roads and airfields.

2. In these studies, the behavior of stabilized soils subjected to simulated traffic loads has been of primary concern. Knowledge of such response is not only of value to provide a check on criteria developed by the Corps of Engineers (based on static tests), but also to provide a basis for additional analyses of pavement structures within a theoretical framework. This, in turn, can be used in the development of new pavement thickness design procedures.

3. Previous reports in this series (Contract Report No. 3-145, Reports 1-5, dated December 1965, September 1966, May 1969, October 1970, and August 1972 respectively) have presented: (1) background information for the study; (2) description of tests for establishment of appropriate stabilization and test conditions for both a silty clay and a highly plastic clay; (3) results of repeated compression and flexural tests on cement-treated and lime-magnesium sulfate-treated soils; (4) analyses of pavement sections using measured material properties and layered-system elastic theory (to ascertain pavement thicknesses at which the treated soil will satisfy the Corps of Engineers performance criteria without traffic-load associated cracks developing in the pavement); (5) analyses

of stresses and deflections induced by repeated plate loadings in two prototype cement-stabilized pavements; and (6) analyses of results from four test sections of cement-stabilized soil constructed at the Waterways Experiment Station and trafficked under different wheel loads.

4. Section II contains a summary of the completed investigations. From these as well as studies by other investigators, references to which are subsequently included where appropriate, an improved understanding of the resilient and fatigue properties of stabilized soils has been developed. Also, it has been demonstrated that stresses and deflections in stabilized soil pavements can be predicted successfully using both elastic layer theory and a finite element analysis together with material properties determined by repeated load tests*.

5. From this information a design procedure has been developed, the framework for which is illustrated in Fig. 1. Section III contains a general outline of the procedure; much of the data which serve as the basis for the design recommendations are included in the appendices. Section IV contains the step-by-step procedure; comparisons of designs

---

* When using laboratory prepared samples of cement-stabilized materials, the test data must be modified to reflect the difference between laboratory-prepared specimens and samples of the same material mixed, compacted and cured in the field (e.g., Wang, 1968).

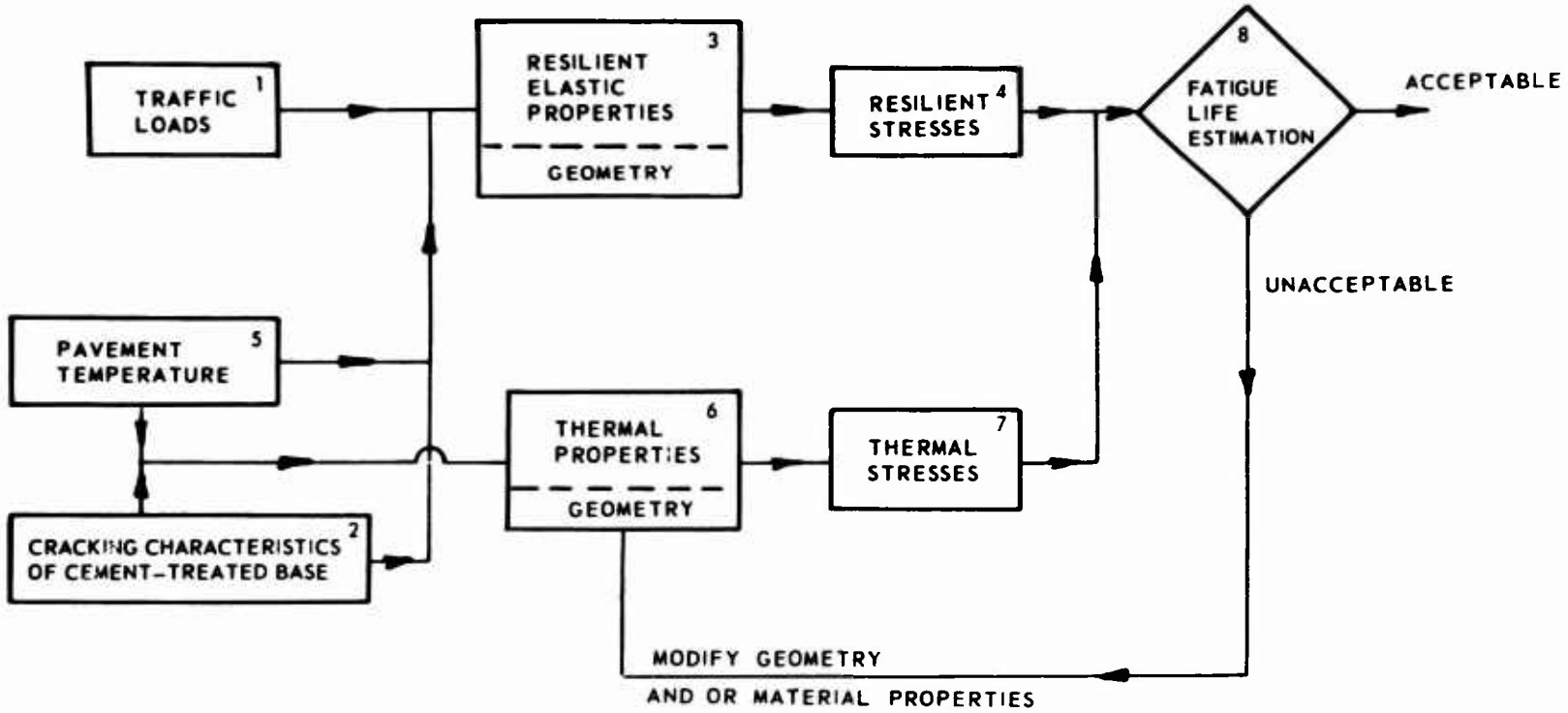

Fig. 1 Design procedure

developed by the proposed procedure with existing methodology; and suggested modifications which might be incorporated to improve and refine the procedure as experience is developed.

6. Although the emphasis of this study has been placed on cement-treated soils, the design method should have general application to soils treated with other materials as well.

SECTION II: SUMMARY OF PREVIOUS INVESTIGATIONS

7. As noted in the Introduction, this investigation has been continuing for about 10 years with results reported in five reports - the most recent of which is dated August 1972. The previous studies can be divided into three general areas:

a. Laboratory studies of cement and lime stabilized materials under the action of short-duration repeated loads simulating those applied by traffic.

b. Field tests on prototype pavements containing cement-stabilized layers using repeated load plate tests and determining the applicability of appropriate theory to predict the stresses and deformations observed in these tests.

c. Analyses of:

(1). cement-stabilized test sections constructed by the Corps of Engineers at the Waterways Experiment Station which had been subjected to actual traffic loading;

(2). pavement sections using measured material properties and layered-system elastic theory to ascertain pavement thicknesses at which treated soil will satisfy the Corps of Engineers performance criteria without cracks developing in the pavement.

8. This section contains a summary of the research completed on this project in these three areas. All of these studies, as well as the

results of other investigators, have assisted in the development of the design procedure suggested in a subsequent section.

Laboratory Studies (Reports 1 through 5)

9. The laboratory studies have included repeated compression and flexure tests on cement-treated and lime/magnesium sulfate-treated soil. Four different soils treated with cement were tested:

a. Vicksburg silty clay (CL)

b. Vicksburg buckshot clay (CH)

c. Richmond Field Station silty clay (CL)

d. Mixture of sand and clay termed ESM (SM-SC).

A summary of the soil properties prior to treatment is shown in Table 1.

Table 1 Soil Properties

Soil	Vicksburg Silty Clay	Vicksburg Buckshot Clay	Richmond Field Station Silty Clay	ESM
Liquid Limit	39.5	55.0	29.2	20.6
Plastic Limit	22.9	18.1	19.4	15.4
Plasticity Index	16.6	36.9	9.8	5.2
Specific Gravity	2.65	2.70	2.65	2.70
Unified Classification	CL	CH	CL	SM-SC

10. Some of the principal findings which have influenced the proposed design procedure are:

a. Comparison of the behavior of cement- and lime-treated soils under repeated compressive stresses indicates that although the strengths of the different soils, as measured by the CBR test prior to treatment and after a specified curing period are the same, the behavior under repeated loading may be different.

b. For the materials tested there appears to be a critical curing time less than which beneficial effects are obtained from repeated loading. This critical curing time depends, however, on the type and amount of treatment. For example, for treated buckshot clay the critical curing time is much shorter for the specific cement treatment used than for a lime-magnesium sulfate-treatment level investigated. Beyond the critical curing time, for the materials investigated, the resilient properties are relatively independent of the number of load repetitions but are more dependent on curing during repeated loading. The critical curing period also appears to depend on the mode of loading, being shorter for flexural than for compressive loading.

c. Resilient properties vary with changes in water content. However, this variation is affected by soil type and treatment. In the case of the buckshot clay, the influence of water content is more significant when the buckshot clay is treated with cement than with lime-magnesium sulfate. Such

a conclusion might suggest that at times careful control in placement conditions may be required to achieve a specific level of materials response or that if the degree of control required is not possible due to field limitations, it may be desirable to consider another type of treatment less sensitive to anticipated variations.

d. Stiffness and strength characteristics in flexure are different than in compression for the materials investigated. For example, the resilient modulus in flexure is greater than in compression.

e. The stiffness characteristics of the treated silty clays, particularly, are dependent on stress level although the sensitivity to stress is less in flexure than in compression. For repeated load compression tests, the stiffness (or resilient modulus) at a particular curing time can be expressed in an equation of the form:

$$M_R = F[I^{k1}, (\sigma_1 \text{ or } \sigma_d)^{k2}] \qquad \text{(II-1)}$$

where I is the first stress invariant, σ_1 and σ_d are the major principal and deviator stresses respectively, and k_1 and k_2 are experimentally determined coefficients.

f. The unconfined compressive strength (U.C. strength) appears to be a suitable correlating parameter for different material properties:

(1). The effect of curing on U. C. strength of a cement-stabilized soil can be expressed by:

$$(UC)_D = (UC)_{D_0} + K \log_{10} \frac{D}{D_0} \qquad \text{(II-2)}$$

where $(UC)_D$ and $(UC)_{D_0}$ are U.C. strengths after D and D_0 days curing, respectively, and K is a constant dependent on type of soil and cement content.

(2). There is no effect of compaction delay on the strength, provided water content and dry density remain the same as for samples without compaction delay, and the delay time does not extend beyond the start of permanent hydration.

(3). The U. C. strength of field undisturbed samples was about 63% of that of laboratory mixed and laboratory compacted samples. The percentage decreased with increase of cement content. A significant part of this difference was attributable to the effects of different compaction methods.

(4). A linear relationship was found between U. C. strength and flexural strength. The flexural strength was in the range of 25% to 35% of the compressive strength.

(5). CBR values, determined both in the laboratory and in the field, can be related to the unconfined compressive strength of the cement-treated material.

(6). For cement-stabilized soil, the compressive resilient modulus, M_{Rc}, can be expressed as:

$$M_{Rc} = K_c\, g(\sigma_d)\, f(\sigma_3)\, (UC)^n \qquad \text{(II-3)}$$

where K_c and n are constants dependent on material and cement content, and $g(\sigma_d)$ and $f(\sigma_3)$ are functions of the repeated deviator stress and confining pressure, respectively. The flexural resilient modulus, M_{RF} can be expressed as:

$$M_{RF} = K_F \cdot (10)^{m(UC)} \qquad \text{(II-4)}$$

where K_F and m are constants dependent on type of soil and cement content.

g. The factigue behavior of cement-stabilized soils can be expressed by:

$$S = a\, N^{-b} \qquad \text{(II-5)}$$

where S is the flexural stress level and a and b are constants dependent on the material.

Prototype Pavement Tests (Report 4)*

11. Repeated-load plate tests were conducted on two 20 ft by 20 ft by 8 in. thick pavement slabs of cement stabilized soil resting on a clay subgrade; the one section contained three percent cement and the other six percent. This investigation demonstrated conclusively that stresses and strains in cement-stabilized soil pavements resulting from

---

* Appendix C contains more detailed data on results of this phase of the project.

repeated loads of short duration can be predicted using elastic layer theory and finite element analysis together with material properties determined from laboratory repeated-load tests on undisturbed specimens taken from the test pavements.

12. It was also observed that cement-stabilized soil specimens mixed and compacted in the laboratory with the same density as the field specimens exhibited higher stiffnesses than the field specimens. This factor poses some difficulty in selecting appropriate values for use in a preliminary design.

Pavement Analyses (Reports 2 and 5)

13. Analyses of two-layered pavements-cement stabilized sections resting on untreated subgrades - suggest that:

a. Pavements stabilized to satisfy Corps of Engineers design criteria will develop traffic stresses which exceed the flexural strength of the stabilized layers. While cracking will occur, it does not imply that performance would not be adequate for forward area military operations, since in such situations, and for the short design lives specified, the formation of cracks and even the development of ruts may not impede the movement of vehicles.

b. The method of analysis for the probability of fatigue crack formation for different strength, curing time, cement content, and pavement thickness conditions suggested in Report 2 appears useful to serve as the basis for a design procedure for pavements containing stabilized layers. Moreover, an approach of this type

which combines experimentally measured properties under one set of conditions with theoretical analyses for the prediction of stresses and properties under another set of conditions, is potentially useful for the study of the effects of stabilized soil quality variations on performance.

14. Performance analyses of the test sections at WES showed that:

a. A failure criteria could be defined according to the rut depth in the test sections.

b. The equivalency between different wheel loads could be represented by:

$$EWL = \left(\frac{P}{P_o}\right)^{4.5} \qquad \text{(II-6)}$$

where EWL is the equivalent number of repetitions of wheel load, P_o, for one repetition of wheel load, P.

c. A linear relationship existed between pavement thickness and log of number coverages at failure.

d. The effect of thickness on the performance was more significant for low-strength subgrade than for high-strength subgrade.

e. The subgrade strength had less influence on the performance of thicker pavements than on that of thinner ones.

f. The higher the strength of the subgrade and the thicker the pavement, the more pronounced the effect of the cement content on the performance.

g. For a given number of coverages, the required thickness of pavement decreased significantly with increasing cement content up to about 6% cement, but only minor improvement in performance was obtained for cement contents higher than 6%.

h. Design curves for the test sections can be expressed in the following terms:

$$T = F\left(\frac{p}{S_p} \cdot Rr\right)$$

or (II-7)

$$T = F\left(\frac{r}{R}, \frac{p}{S_s}\right)$$

where T is the stabilized layer thickness, S_p is the unconfined pavement strength, p is the tire pressure, r is the radius of the loaded area, S_s is the unconfined subgrade strength, and R is the ratio Sp/Ss.

Summary

15. In general, these results, as well as information developed by other investigators, suggest the framework for a design procedure for pavements containing stabilized layers. The studies conducted as a part of this investigation indicate some of the material variables to be considered, a means through the use of the unconfined compressive strength of the stabilized material to establish reasonable material characteristics necessary for the analysis, and the fact that layered elastic analysis is a suitable procedure to represent the response of pavements to moving wheel loads.

16. The investigations also indicate that laboratory determined properties may not be used without modification to represent the behavior of the same material in-situ.

17. One of the most difficult questions to answer is concerned with performance determinants. For example, how much cracking is tolerable before the pavement is considered unserviceable. Analysis of the WES sections have permitted a direct correlation between design parameters and a measure of performance defined by the judgement of the WES staff (influenced in a large measure by rutting observations). To make the design procedure more generally applicable it is desirable to have some relationship between specific forms of distress and performance, for example the aerial extent of cracking and a measure of the ability of the pavement to carry the traffic satisfactorily.

18. In the design procedure described in Section III, initial cracking is considered to be the damage determinant. It must be recognized that this is a conservative estimate of performance since there will be an additional indeterminable number of load repetitions which can be carried beyond the initial cracking. As a start, however, and considering the other variables which will be incorporated into the design framework, it appears worthwhile to detail what we consider an "improved" design procedure, that is one which builds on the experience acquired to date and, hopefully, extends the capability to design for situations for which no experience exists.

SECTION III: DESIGN SYSTEM

19. The pavement system for which the design procedure has been developed consists of two layers -- a stabilized layer resting on a subgrade (Fig. 2)*. This type of system is representative of some military roads in forward areas and of some airfield pavements in the theater of operations. Although the design procedure presented herein is limited to layers stabilized with portland cement the procedure is sufficiently general so that lime-or asphalt-stabilized materials could be incorporated in place of the cement-stabilized material if the required material characteristics were available.

20. An outline of the procedure is illustrated by the flow diagram shown in Fig. 1. The major factors controlling structural behavior of cement-stabilized layers appear to be taken into account in this design subsystem. In the procedure it is assumed that shrinkage cracking will develop a short time after construction. After development of this type of cracking, stresses due to shrinkage have been shown to be comparatively small (Pretorius, 1970) and are, therefore, neglected in the analysis.

---

*The pavement system considered would also be applicable to sections containing asphalt surface treatments or other thin surface layers that contribute little or no load carrying capabilities to the pavement.

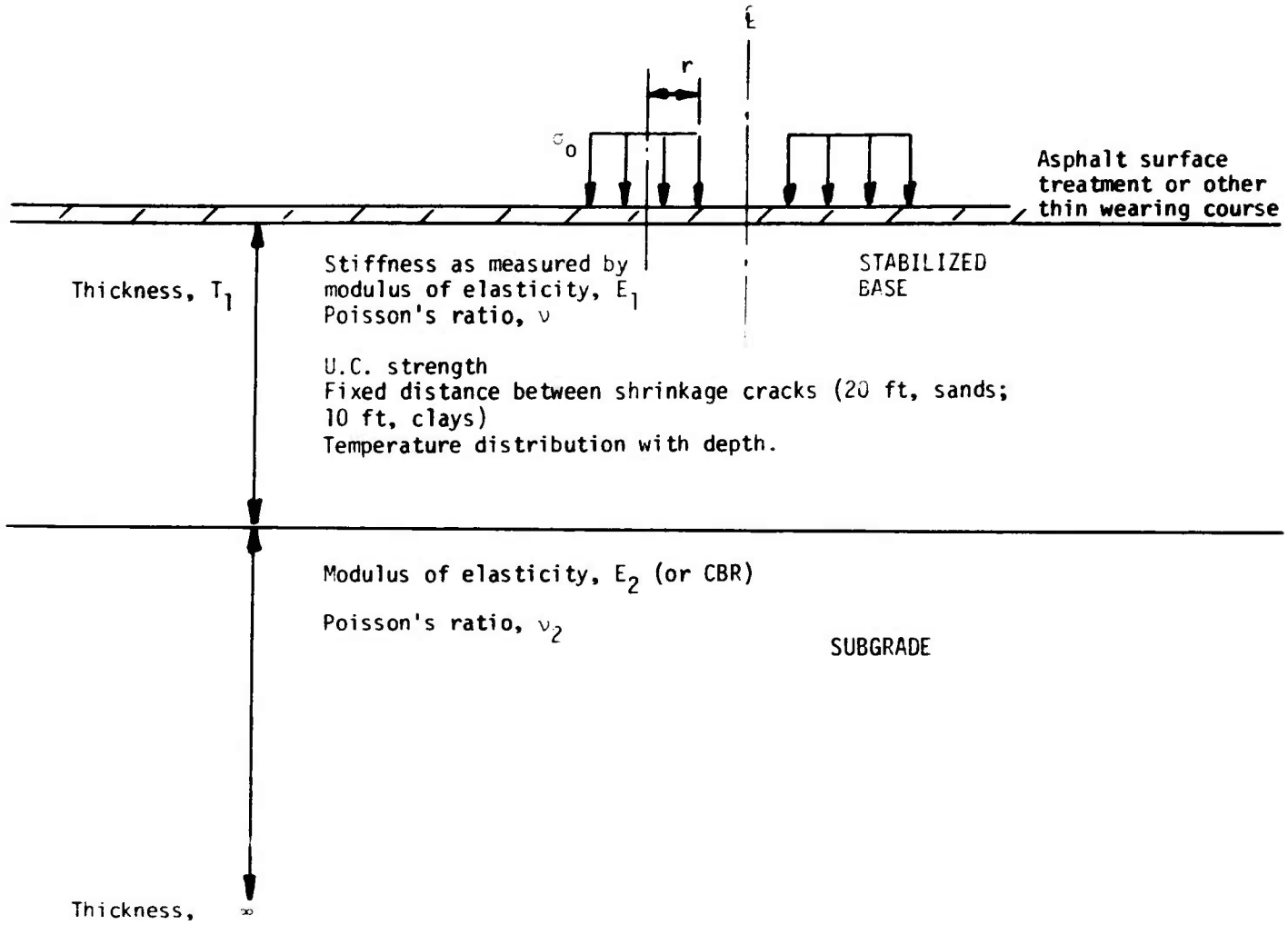

Fig. 2 Pavement System

21. Stresses considered in design are those resulting from traffic loading and temperature fluctuations which, when compared to the fatigue characteristics of the material, permit selection of a suitable thickness.

22. The following sections briefly describe the various inputs required and the design procedure.

Traffic Data (Block 1)

23. Characteristics of military vehicles and aircraft for which design curves have been developed are summarized in Table 2 (Corps of Engineers, 1963). In addition, corresponding data have been included for an 18,000 lb. single axle (representative of conventional highway loadings) and for the Boeing 747 aircraft. The characteristics included in the table are used as input to the design procedure.

Pavement Temperature, Thermal Properties (Blocks 5, 6)

24. As a part of the design procedure, it is necessary to estimate the distribution of temperature in the pavement section both with depth and as a function of time. For cement-stabilized materials, temperature distribution with depth influences thermal stresses which may be developed. If an asphalt-bound layer were used, knowledge of the temperature distribution with time and depth are important since the stiffness of an asphalt mixture is dependent on temperature -- stiffness in turn influences the development of stresses due to traffic loads.

25. Three procedures are available to estimate temperatures, all based on a solution of a form of the heat-conduction equation in which

temperature input is assumed independent of the x and y coordinates, i.e.,

$$\frac{\partial^2 \Phi}{\partial z^2} = \frac{\gamma c}{k} \frac{\partial \Phi}{\partial t} \qquad \text{(III-1)}$$

where:

Φ = temperature field

c = specific heat of the material

k = thermal conductivity

γ = unit weight of material

t = time

z = depth

In one procedure equation (III-1) is solved in closed form (Barber, 1957) while in the others numerical techniques, either finite difference (Christison and Anderson, 1972) or finite element (Pretorius, 1970) are used.

26. The Barber solution is recommended for use as a part of the design procedure. A detailed summary of the procedure together with justification for its use are presented in Appendix A.

27. In this method as well as in the finite element and finite difference procedures, the thermal conductivity, k, and the specific heat, c, for the materials being analysed are required. For asphalt-bound materials (e.g., asphalt concrete) the available data indicate that the thermal conducitivity is on the order of 0.7 BTU · ft/hr/ft^2/F deg, and the specific heat is on the order of 0.2 BTU/lb/F deg (Finn, 1967).

28. Typical values of thermal conductivity for soil-cement using different soil types are (HRB, 1961):

Soil Type	Thermal Conductivity, k
Sandy soil	0.67
Silty soil	0.33
Clayey soil	0.31

29. Since the temperature distribution is not sensitive to wide variations in k (Fig. A6,Pretorius, 1970), a value of k equal to 0.5 BTU · ft/hr/ft^2/F deg should be acceptable for most analyses. No values could be found in the literature for the specific heat for cement-treated soil, but a value for c of 0.2 BTU/lb/F deg should be reasonable since c_{clay} = 0.22 and $c_{concrete}$ = 0.16.

30. Absorptivity of the surface to solar radiation, b is also required. For a black surface (e.g., asphalt concrete), b = 0.95 (Barber, 1957). No values of b were available for cement-treated soil, but b = 0.65, which is the value for sand and gravel concrete (Barber, 1957), is considered to be appropriate for cement-treated soil

Pavement System (Block 3)

Geometry

31. Geometry of the pavement system is specified in terms of the thickness of the cement-treated base, a semi-infinite subgrade layer and an assumed distance between shrinkage cracks. A summary of crack spacings reported in the literature is summarized in Appendix B.

Based on these data, representative crack spacings of 20 ft for treated granular materials and 10 ft for treated fine-grained materials were selected for design purposes.

Loading conditions

32. Loads are assumed to be applied to circular areas, the radii of which are based on the contact areas and tire pressures shown in Table 2.

33. In Appendix B it is demonstrated that edge-loading conditions result in larger stresses than those occurring at the interior of a slab. For convenience the layered elastic analysis (which assumes interior loading) has been used. To account for the larger stresses resulting from edge loading, stresses computed for the interior condition have been multiplied by a factor of 1.5.

Resilient elastic properties

34. For the analysis of layered systems, the modulus of elasticity E, and Poisson's ratio, ν, are needed for each layer. Due to the nature of the traffic loads, elastic properties determined by repeated load tests are more representative than properties determined by static loading. Although repeated load test data are desirable, such tests are more difficult to perform than some of the more conventional tests and the necessary equipment may not be available. Therefore, an effort was made in this study to correlate resilient elastic properties with more readily measured characteristics.

35. Subgrade. The modulus can be obtained directly from a repeated load triaxial compression test, by approximation from California Bearing

Ratio (CBR) test results, or by approximation from plate bearing test results.

36. In the repeated load triaxial compression test, the sample is subjected to a confining pressure and deviator stress that approximates the expected in-situ state of stress. The test was first developed by Seed and Fead (1960) and step-by-step procedures are available (Monismith and McLean, 1971).

37. Heukelom and Foster (1960) have suggested that the modulus may be estimated from the CBR by the relationship:

$$E\ (psi) = 1500\ CBR \qquad \text{(III-2)}$$

This is used by Shell (Dormon and Metcalf, 1965) as a part of their pavement design procedure.

38. If the plate bearing value is available, the modulus can be estimated from the correlation shown in Fig. 3 (Asphalt Institute, 1973). In this correlation the plate bearing value was determined using the ASTM D 1195 procedure.

39. Alternatively, if no strength test data are available for the usbgrade, an approximate modulus can be estimated from the FAA soil classification as shown in Table 3 developed by the Asphalt Institute (1973). An approximate relationship between the CBR and the FAA classification is shown in Table 4*.

---

* Table 3 was in all proabability deduced from Table 4 and equation III-2.

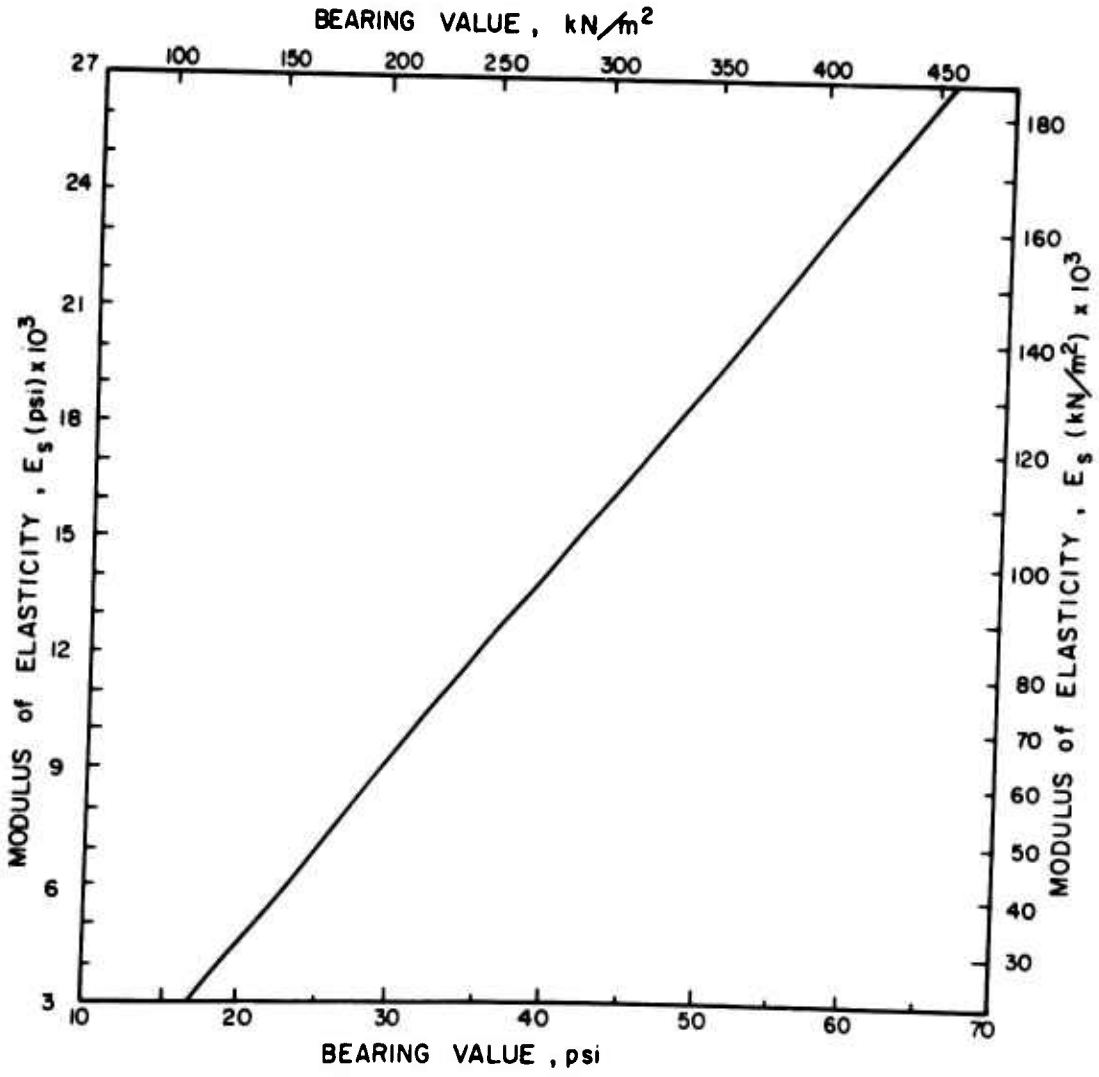

Fig. 3 Approximate relationship between plate bearing value and modulus of elasticity, E (Asphalt Institute, 1973)

40. Poisson's ratio, ν, for subgrades range from 0.5 for saturated clays to 0.35 for sands. The structural analysis of a pavement system is not sensitive to variation in the Poisson's ratio of the subgrade. From a number of analyses it was found that for a decrease in Poisson's ratio of the subgrade from 0.5 to 0.3, tensile strains in the cement-treated base were reduced, but not by more than 10 percent. For thick and stiff cement-treated bases,Poisson's ratio had essentially no influence on tensile strains. Therefore, a Poisson's ratio of 0.5 is recommended for the subgrade and is the value which was used to prepare the design curves presented herein.

41. Cement-treated base. The resilient modulus of cement-treated soils in flexure can be determined by subjecting beam samples to repeated loading (Mitchell et al, 1965). This type of test is recommended for use in this procedure because it duplicates field-loading conditions more reasonable than other tests, although the effect of confining pressure is not taken into account. If a flexure test is performed, the resilient modulus in flexure, M_{RF}, can be approximated (assuming that confining pressure has no effect) by the following equation (Mitchell, Ueng, and Abboud, 1973):

$$M_{RF} = K_F \, (10)^{m.UC} \qquad \text{(III-3)}$$

where:

K_F = material constant

C = cement content (percent) by weight

$m = 0.04 \, (10)^{-0.186C}$

UC = unconfined compressive strength

42. A relationship between M_{RF} and the unconfined compressive strength is shown in Fig. 4 for Vicksburg silty clay treated with 3 percent cement. The material constant, K_F^* for this stabilized soil is 10,090.

43. Poisson's ratios for cement-treated soil have been reported in the range from 0.1 to greater than 0.5 (Balmer, 1958; Fossberg, 1970; Pretorius, 1970; Larsen et al, 1969; HRB, 1961). At working stress levels, the data indicate that Poisson's ratio is generally in the range of 0.1 to 0.2 for treated granular soils, independent of cement content or curing time. Treated fine-grained soils generally exhibit somewhat higher values, with a typical range of 0.15 to 0.35; although Balmer (1958) reported values in the range of 0.1 to 0.15 for an A-4 soil (AASHO soil classification) at several cement treatment levels.

44. It should be noted, however, that the structural anslysis of the pavement system is not sensitive to variations in the Poisson's ratio of the cement-treated base. Hadley et al. (1972) reported that for a range of Poisson's ratio, from 0.125 to 0.375, the maximum differences in tensile stresses and strains were 15 percent and 8 percent, respectively. Similarly, Fossberg (1970) reported that varying Poisson's ratio between 0.12 and 0.24 resulted in only an 11 percent variation in the maximum tensile stress in the base.

---

*K_F varies with cement content and soil type; see Report 5 in this series.

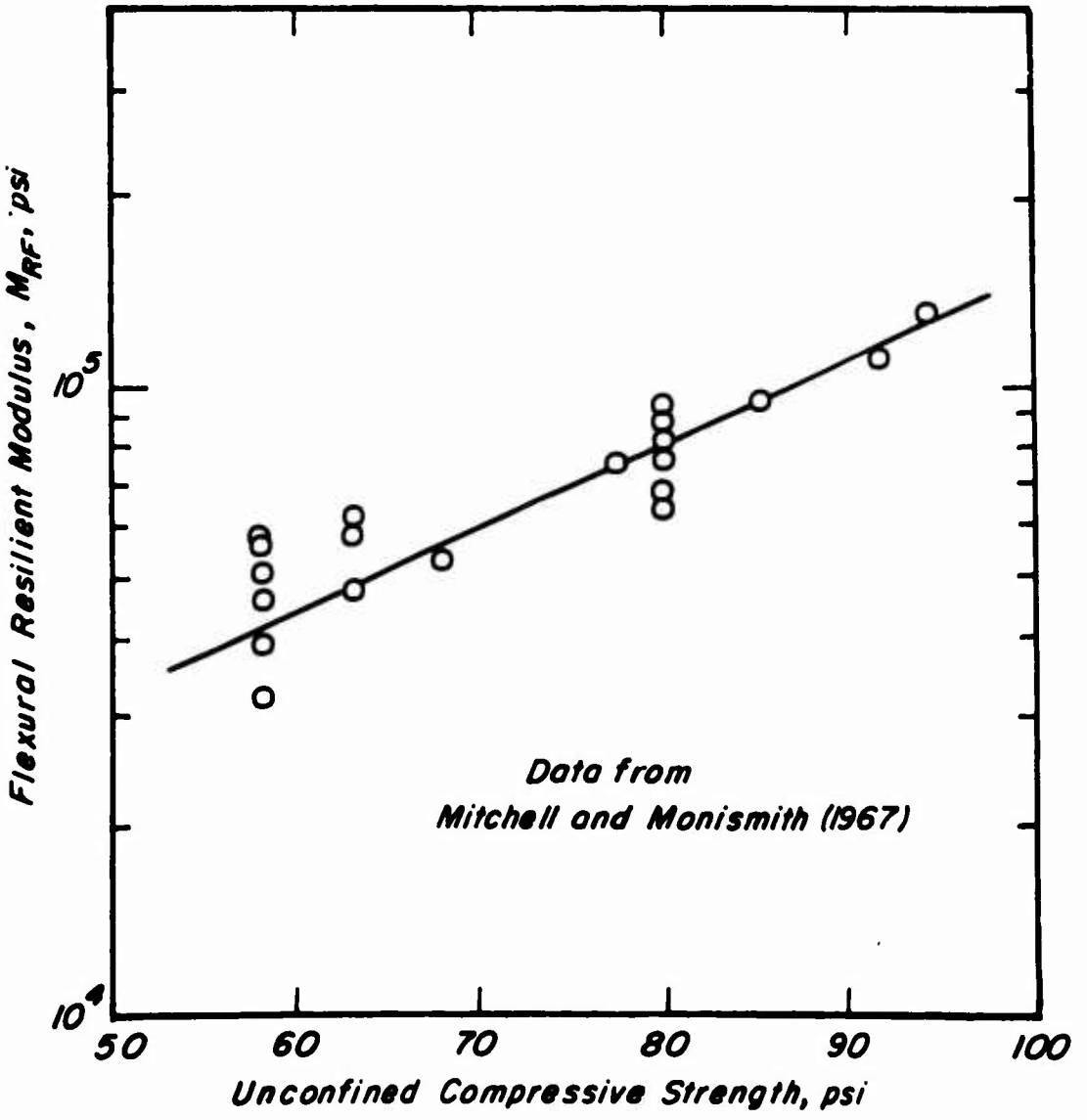

Fig. 4 The relationship between the unconfined compressive strength and resilient modulus in flexure for Vicksburg silty clay with 3 percent cement

45. To develop the design curves presented here, a Poisson's ratio of 0.15 was used.

Thermal properties

46. To calculate the thermal stresses caused by nonuniform temperature distributions, a coefficient of thermal expansion for the cement-treated soil is required. Table 5 summarizes available experimental data; these data provide a basis for selecting an appropriate value. It would appear that a thermal coefficient of 5×10^{-6} in/in./ deg F should be adequate for most analyses.

Traffic Associated Stresses and Strains (Block 4)

47. The design procedure presented herein is similar to that developed by Shell (Dormon and Metcalf, 1965) in which the thicknesses of the various components are selected to insure that critical stresses and strains are maintained within limits set by analyses of test roads and in-service pavements. To minimize the probability of fatigue cracking in the cement-stabilized layer, tensile stresses and strains on the underside of the layer are limited to values established from laboratory test data.

48. The pavement is assumed to respond elastically to ascertain the stresses and strains resulting from traffic loading. A summary of two studies considered to justify this assumption is contained in Appendix C.

49. Either multilayer elastic theory or the finite element procedure can be used to estimate the stresses and deformations resulting from

traffic loading. For a number of reasons including ease of computation and minimal computer time, multilayer theory was selected. Some of the assumptions associated with this solution are:

a. The pavement materials are elastic, isotropic, and homogeneous within each layer.

b. Continuity exists between layers.

c. All layers are infinite in lateral extent.

50. The design curves were determined using the program developed by G. Ahlborn of the University of California Berkeley and termed ELSYM 5. This program permits computation of stresses, strains and displacements for any chosen point in the pavement system. The pavement can have up to five layers. Loads are applied to circular areas (one to ten in number) with uniform contact pressures. To use this program the following input data are needed:

a. Load configuration and tire pressure or contact area.

b. The modulus of elasticity and Poisson's ratio for each layer.

c. The thickness of each layer. The bottom layer (subgrade) can either be semi-infinite or be underlain by a rigid base.

51. As noted earlier, to account for the increased stresses resulting from loading at edge of the slab (at a transverse crack), the stresses determined from the elastic layer solution were increased 50 percent.*

---

*It is possible to solve the edge loading problem directly as noted in Appendix B using the prismatic space finite element idealization. The computer time (and therefore the cost) is large, however, thus making it unattractive for routine design purposes.

Thermal Stresses (Block 7)

52. Cement-stabilized layers may be subjected to thermal stresses as are portland cement concrete pavement slabs. As these stresses may amount to an appreciable percentage (30 to 50 percent) of the traffic stresses (see Appendix D), they should therefore be considered in design.

53. The procedure suggested by Bradbury (1938) for determining stresses due to temperature differentials is recommended for use as a part of this design procedure.

54. The curling (or warping) stress along the edge of the slab is calculated by:

$$\sigma_{xe} = \frac{C_x E \alpha t}{2} \qquad \text{(III-4)}$$

while the stresses in the interior of the slab are calculated by:

$$\sigma_x = \frac{E \alpha t}{2} \cdot \frac{C_x + \nu C_y}{1 - \nu^2} \qquad \text{(III-5)}$$

$$\sigma_y = \frac{E \alpha t}{2} \cdot \frac{C_y + \nu C_x}{1 - \nu^2} \qquad \text{(III-6)}$$

where:

σ_{xe} = maximum temperature-curling stress at the edge of the slab in the direction of slab length (x-direction), in psi.

σ_x = maximum temperature-curling stress in the interior of the slab in the direction of slab length, in psi.

σ_y = maximum temperature-curling stress in the interor of the slab in the direction of slab width (y-direction), in psi.

E = modulus of elasticity of the cement-treated base, in psi.

ν = Poisson's ratio for the cement-treated base.

α = thermal coefficient of expansion and contraction of the cement-treated base, in in./in./F degrees.

t = difference in temperature between top and bottom of the slab in degrees F.

C_x and C_y = coefficients that relate slab length and the relative stiffness of slab and subgrade to temperature-curling stresses. Values of C_x and C_y in terms of L_x/ℓ and L_y/ℓ, respectively are given in Fig. 5.

L_x = length of slab in inches.*

L_y = width of slab in inches.*

ℓ = radius of relative stiffness, which measures the stiffness of the slab in relation to that of the subgrade. It is expressed by the equation:

$$\ell = \sqrt[4]{\frac{E\,h^3}{12(1-\nu^2)\,k}}$$

h = thickness of the cement-treated base, in inches.

k = the subgrade modulus, or resistance of subgrade to deformation, in pci.

---

* For this procedure both L_x and L_y are 20 ft for granular materials and 10 ft for fine-grained soils.

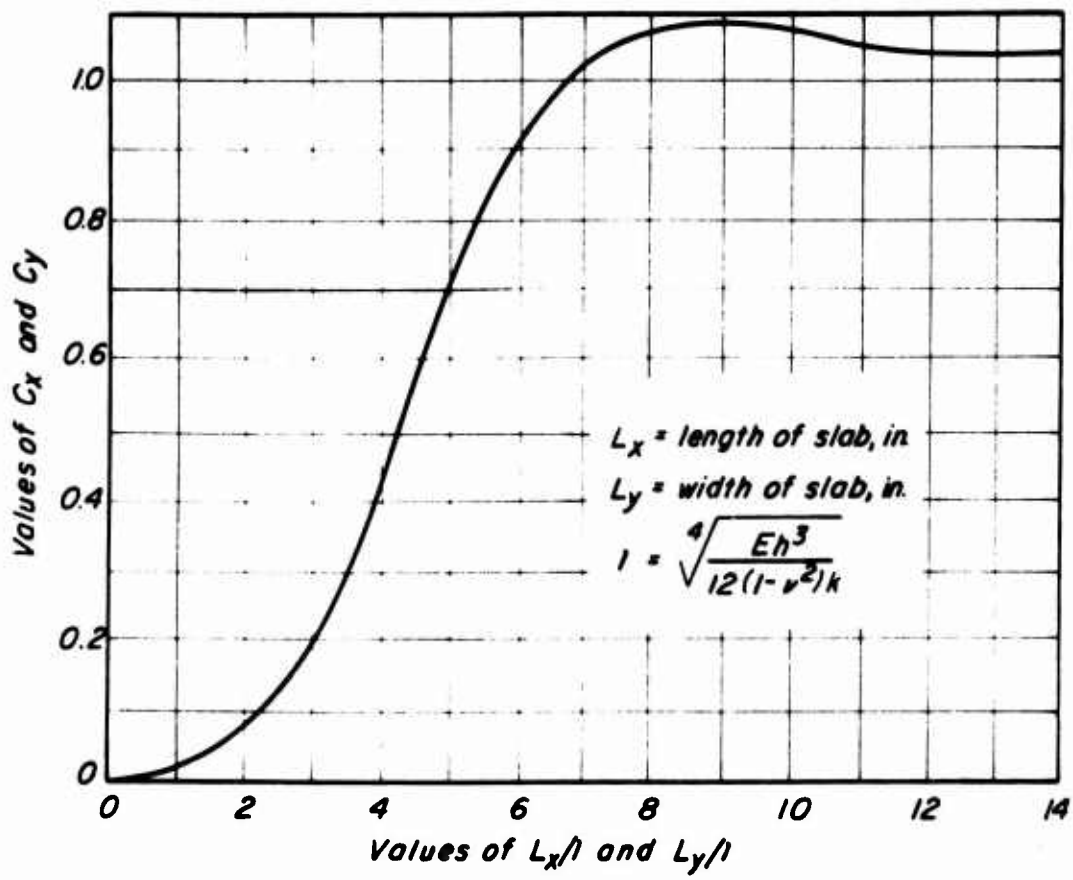

Fig. 5 Values of C_x and C_y for use in equations III-7 (Bradbury, 1938)

55. For square slabs, equations 4, 5 and 6, simplify to equation (III-7) for edge stresses, and to equation (III-8) for interior stresses:

$$\sigma_e = \frac{C\ E\alpha t}{2} \qquad \text{(III-7)}$$

$$\sigma_i = \frac{E\alpha t\ C}{2\ (1-\nu)} \qquad \text{(III-8)}$$

56. As the maximum value of the coefficient, C, is approximately equal to one, the maximum possible warping stresses can be simply calculated from the following:

For edge stresses:

$$\sigma_e = \frac{E\alpha t}{2} \qquad \text{(III-9)}$$

For interior stresses:

$$\sigma_i = \frac{E\alpha t}{2(1-\nu)} \qquad \text{(III-10)}$$

57. Using equations (III-9) and (III-10) will provide the upper bound temperature stresses, while equations (III-4) to (III-6) or equations (III-7) and (III-8) will permit computation of the actual stresses developed. If the temperature stresses determined using equations (III-9) and (III-10) are acceptable, there is no need to use equations (III-4) - (III-7).

58. In these equations the temperature differential may be determined from the Barber solution (Appendix A) for the particular environment in which the design is being developed. The differential to be used is that which will produce a tensile stress in the bottom of the

the slab which may be additive to the traffic stress. This will occur for the situation where the top of the slab is warmer than the bottom.

59. As noted above if the designer wishes to use equations (III-4) through (III-7) it is necessary to have a measure of the modulus of subgrade reaction, k. The quantity can be estimated from the following expression (equation D1, Appendix D):

$$k = (pci) = 0.0565\ E\ (psi)$$

Appendix D contains some discussion illustrating the validity of such a relationship.

Distress Characteristics(Block 8)

Fatigue response

60. In this design procedure, cracking of the pavement slab due to repetitive traffic loading (termed fatigue) is the principal design criterion. Appendix E contains a series of analyses which indicate that the tensile strain in the cement-stabilized layer is the governing factor in the thickness selection process for the type of pavement structure considered herein.

61. The strain vs repetitions to failure relationship used for the design procedure is shown in Fig. 6. Analyses of various data (Appendix E) indicate this to be a reasonable relationship for design purposes.

Fracture characteristics

62. Although the thermal stresses are not used for fatigue life determination, they must still be calculated to insure that the combination

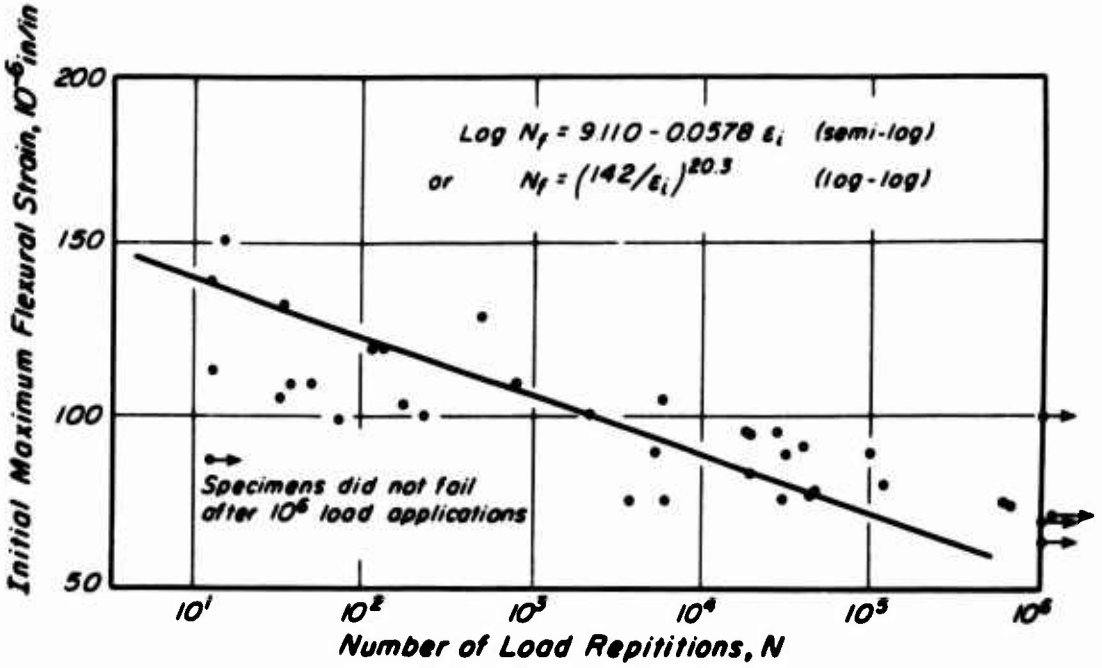

Fig. 6 Fatigue life of flexural specimens (After Pretorius, 1970)

of the maximum tensile thermal stress and the maximum traffic stress do not exceed the flexural strength of the cement-treated base. If the flexural strength is exceeded, the base could crack under one load application. To avoid the necessity of performing flexural strength tests, the following equation relating flexural strength to unconfined compressive strength (Mitchell et al, 1973) is recommended for use. Figs. 7 and 8 contain data on which the relationship is based.

$$f = 0.5\ (UC)^{0.88} \qquad \text{(III-11)}$$

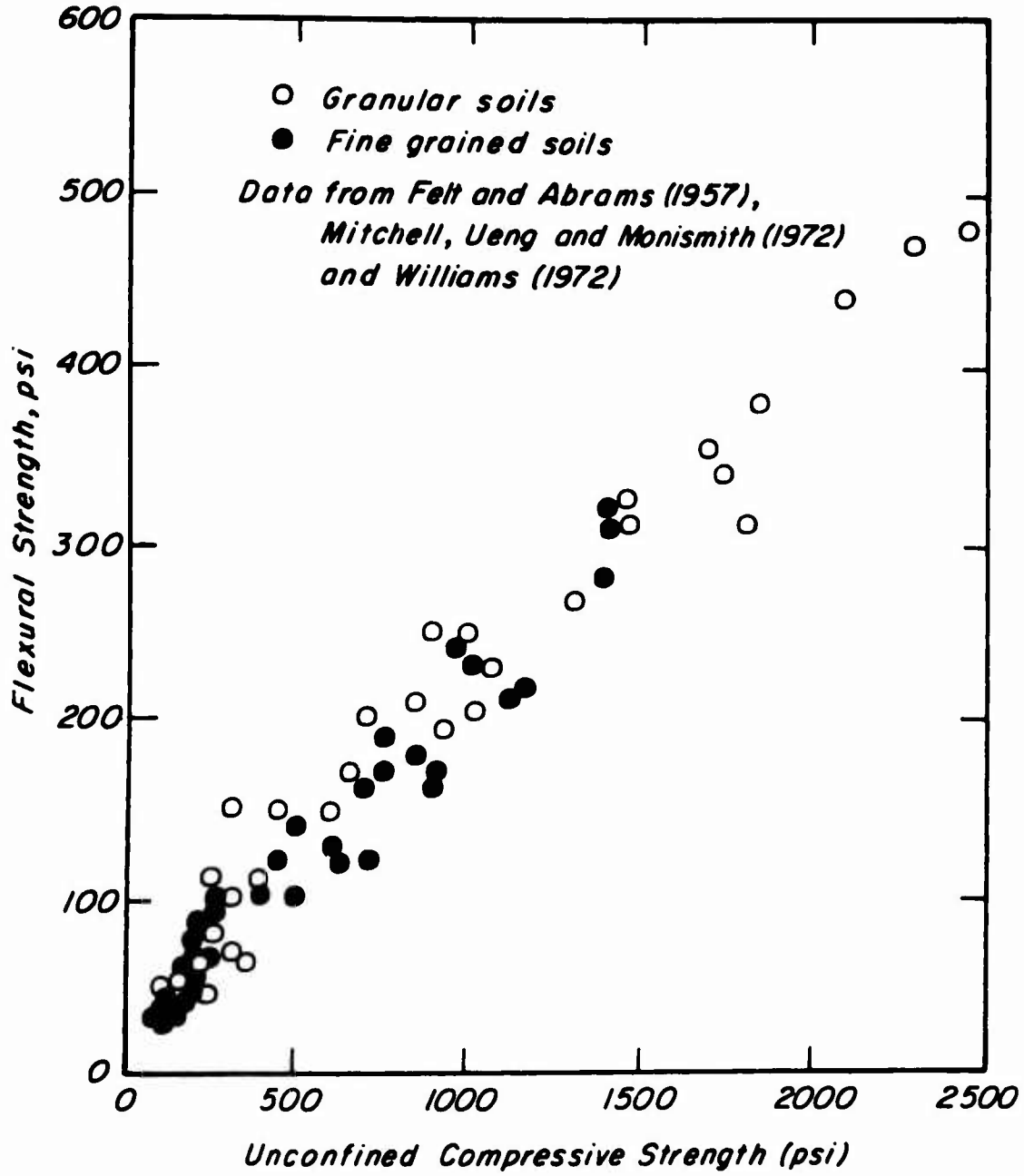

Fig. 7 The relation between the unconfined compressive strength and the flexural strength of soil and cement mixtures

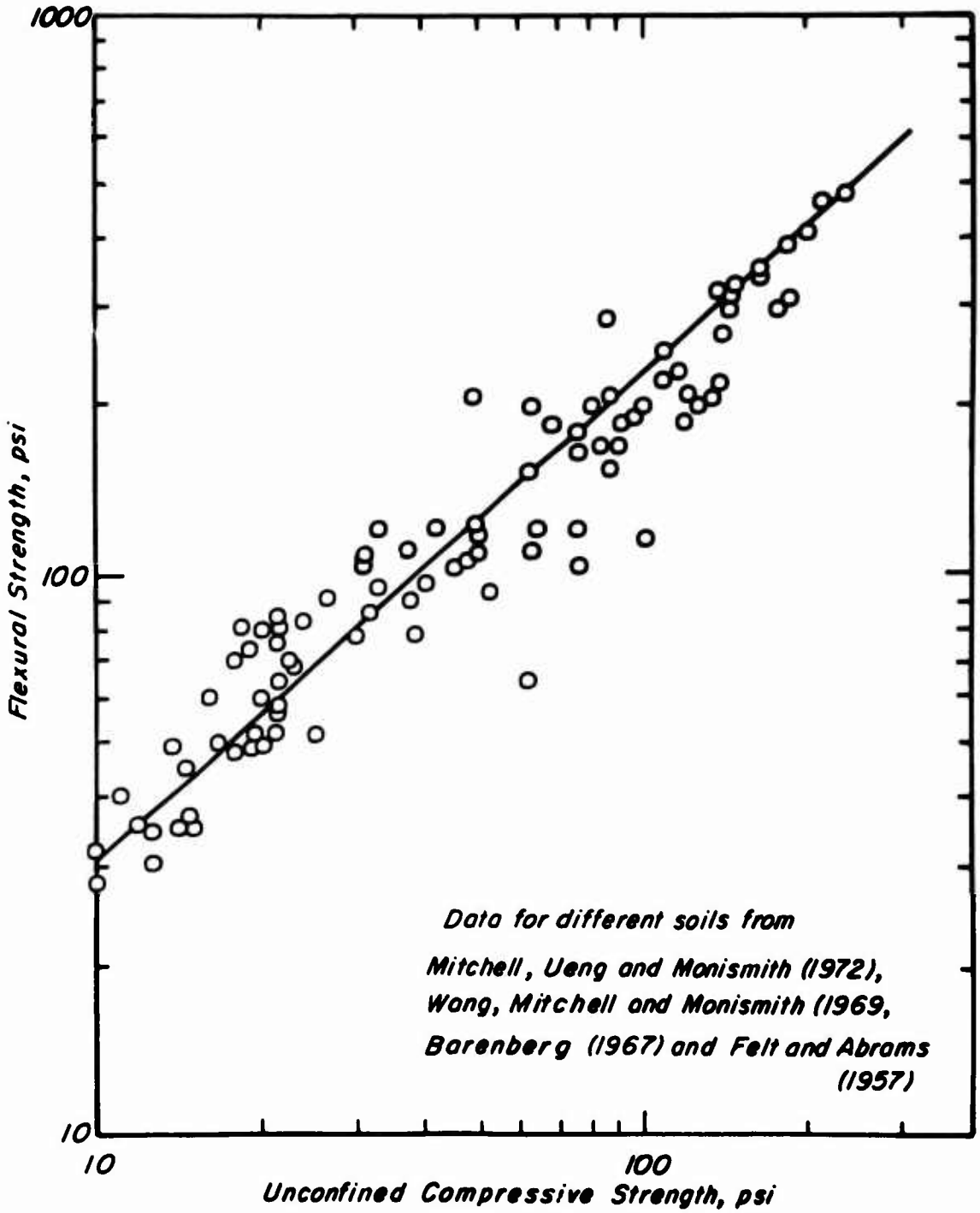

Fig. 8 The relation between the unconfined compressive strength and the flexural strength of soil and cement mixtures

SECTION IV: DESIGN PROCEDURE

Description

63. The design procedure incorporates the material presented in the previous section and utilizes the step-by-step procedure listed below. Essentially it consists of two phases, the first being the selection of a thickness adequate to prevent fatigue in the cement-stabilized layer and the second a check to insure that the combination of load and thermal stress will not crack the stabilized layer.

a. Select a thickness adequate to preclude fatigue in the cement-treated layer.

(1) After choosing the design life of the road or airfield in terms of number of load repetitions obtain the corresponding tensile strain from the fatigue curve in Fig. 6.

(2) With this tensile strain, the modulus of the subgrade and cement-treated base, and the traffic load (Table 2) determine the thickness of the cement-treated base from the appropriate design curves (Figs. 9 - 16)*. To account for edge loading effects use the appropriate scale on the ordinate.**

---

* Appendix F contains a brief description of the development of the design charts.

** The ordinates labeled edge in Figs. 9 - 16 are 1.5 times those labeled interior, the reason for this having been discussed in Section III.

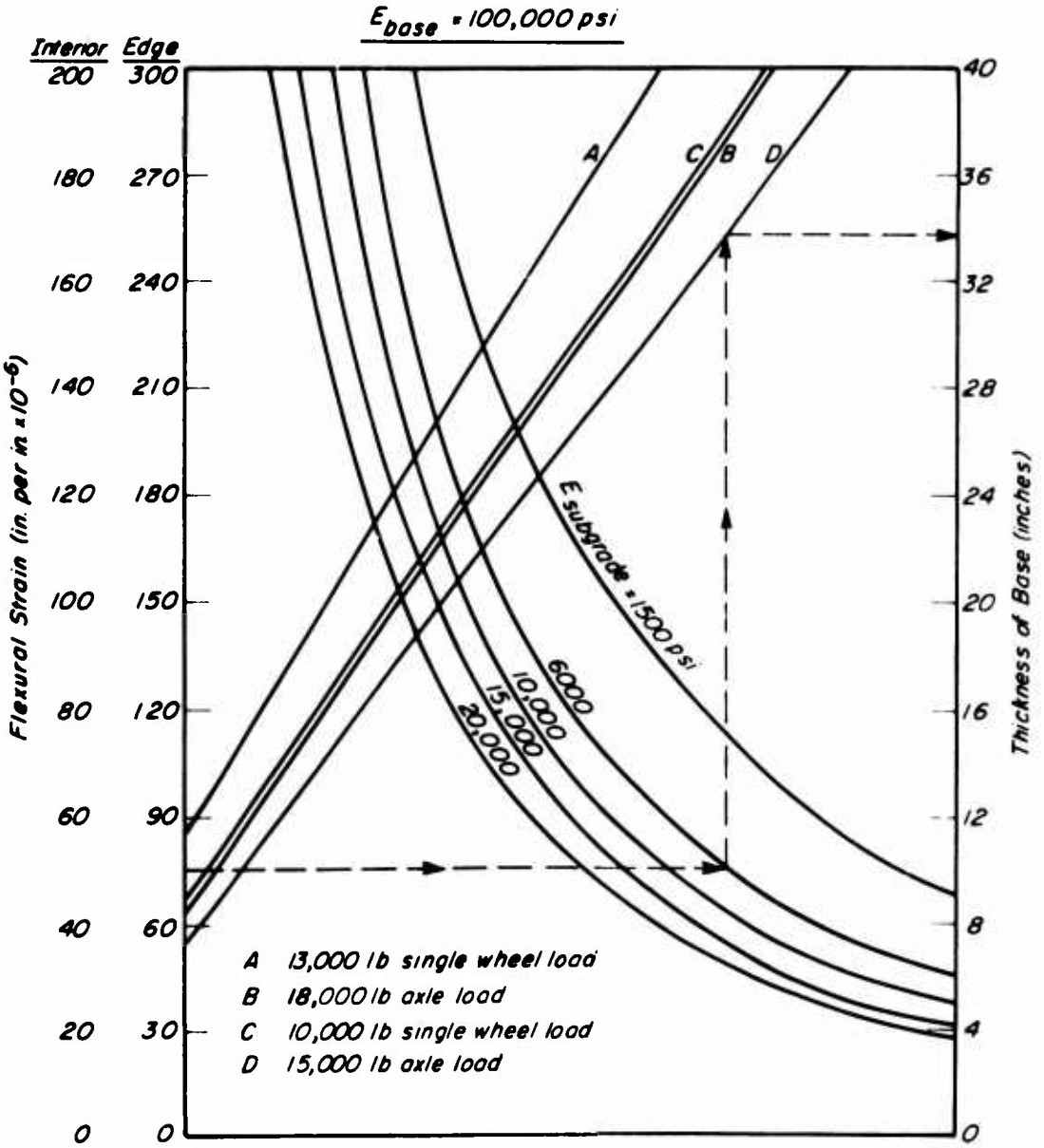

Fig. 9 Relationship between tensile strain and base thickness for various single and dual-wheel loads, E_{base} = 100,000 psi

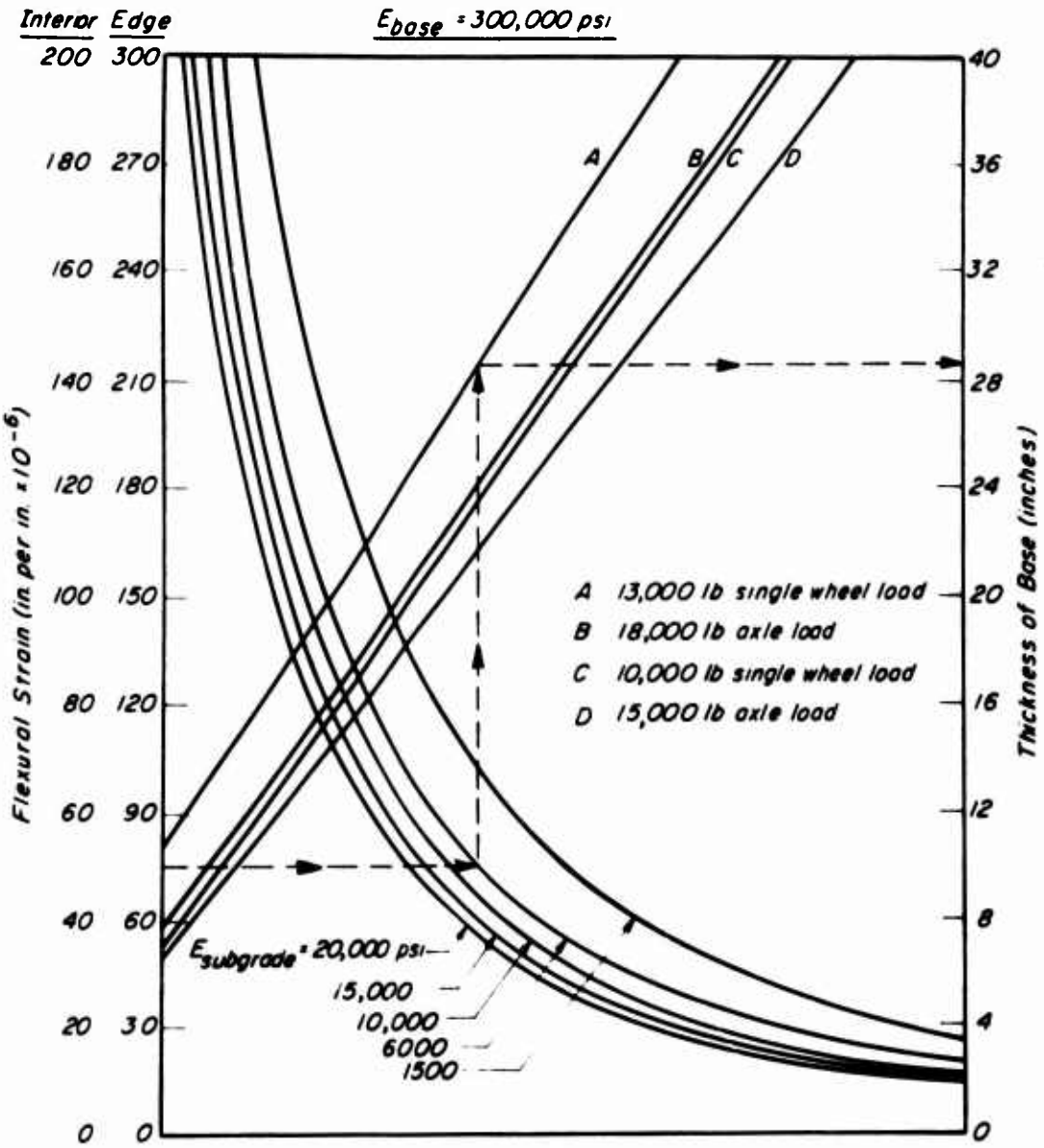

Fig. 10 Relationship between tensile strain and base thickness for various single and dual-wheel loads, E_{base} = 300,000 psi

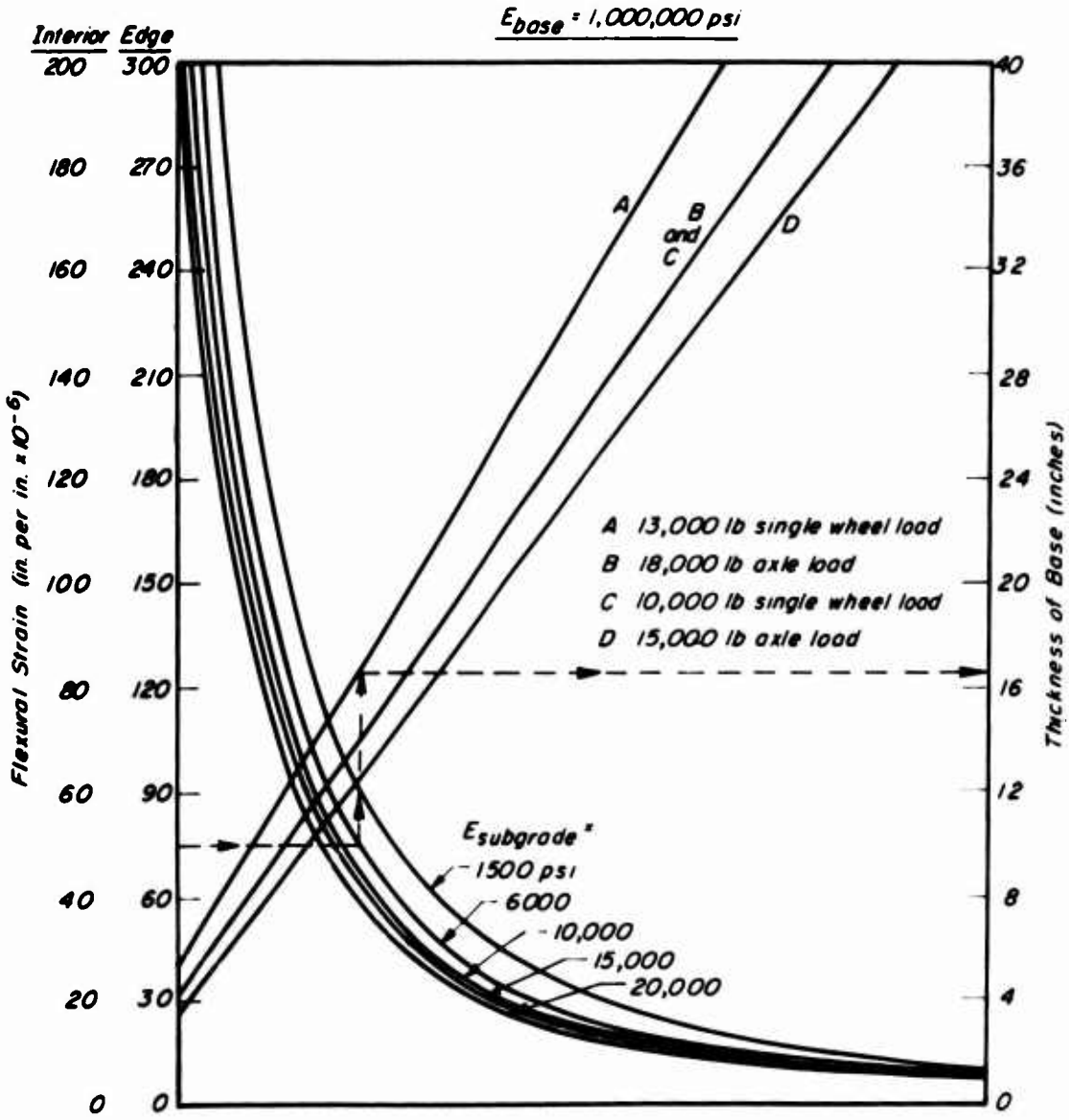

Fig. 11 Relationship between tensile strain and base thickness for various single and dual-wheel loads, E_{base} = 1,000,000 psi

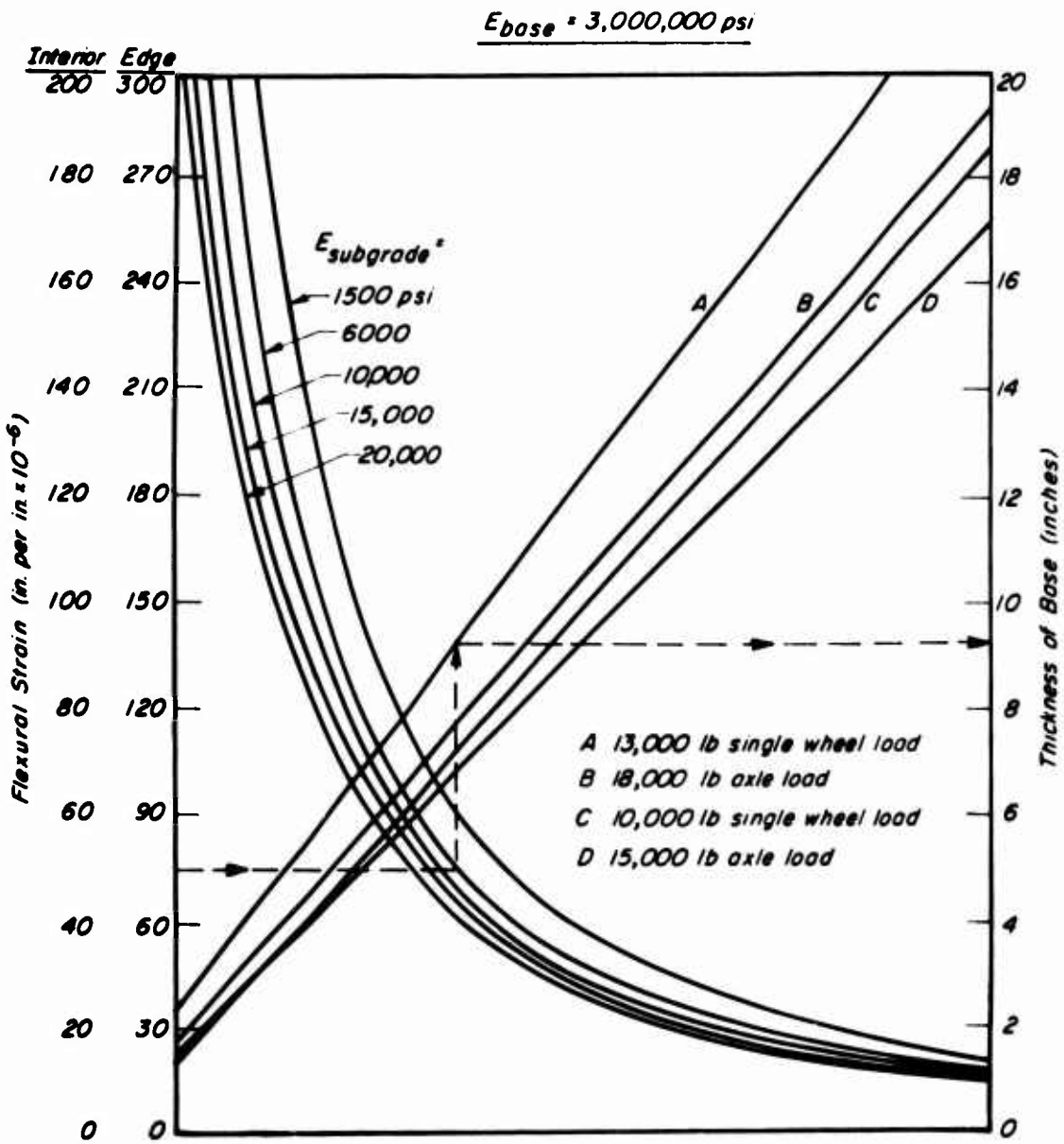

Fig. 12 Relationship between tensile strain and base thickness for various single and dual-wheel loads, E_{base} = 3,000,000 psi

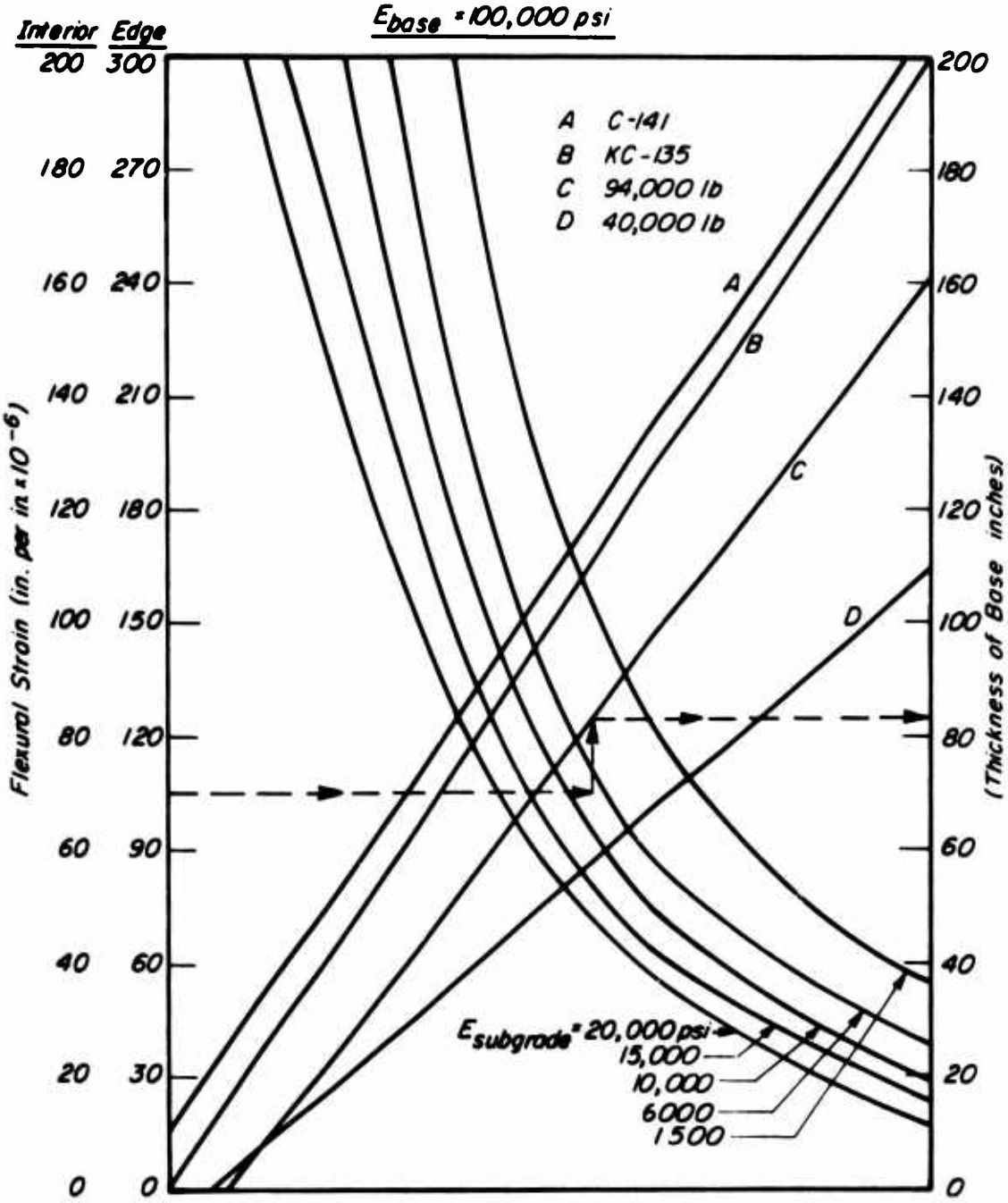

Fig. 13 Relationship between tensile strain and base thickness for various aircraft loads, E_{base} = 100,000 psi

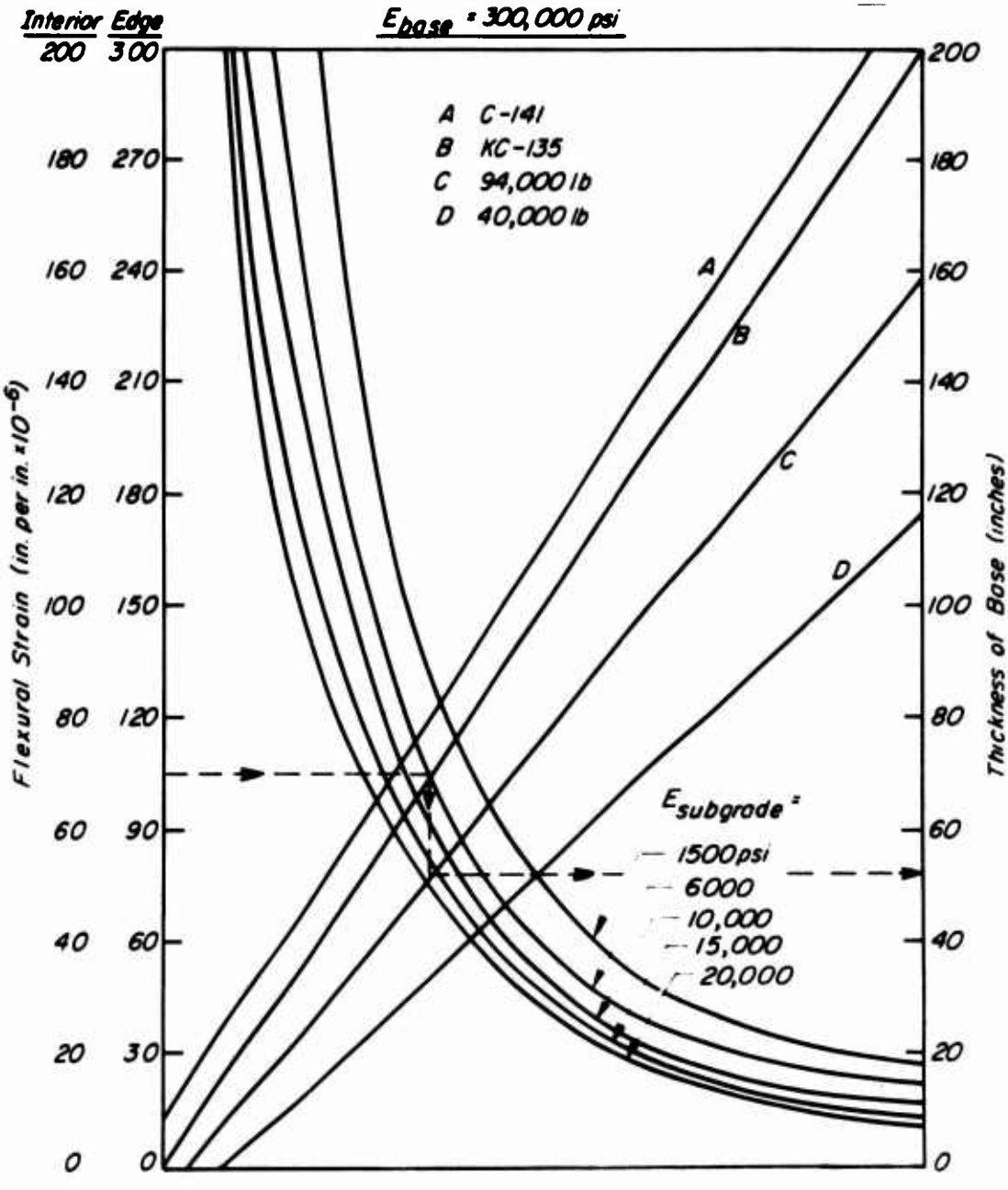

Fig. 14 Relationship between tensile strain and base thickness for various aircraft loads, E_{base} = 300,000 psi

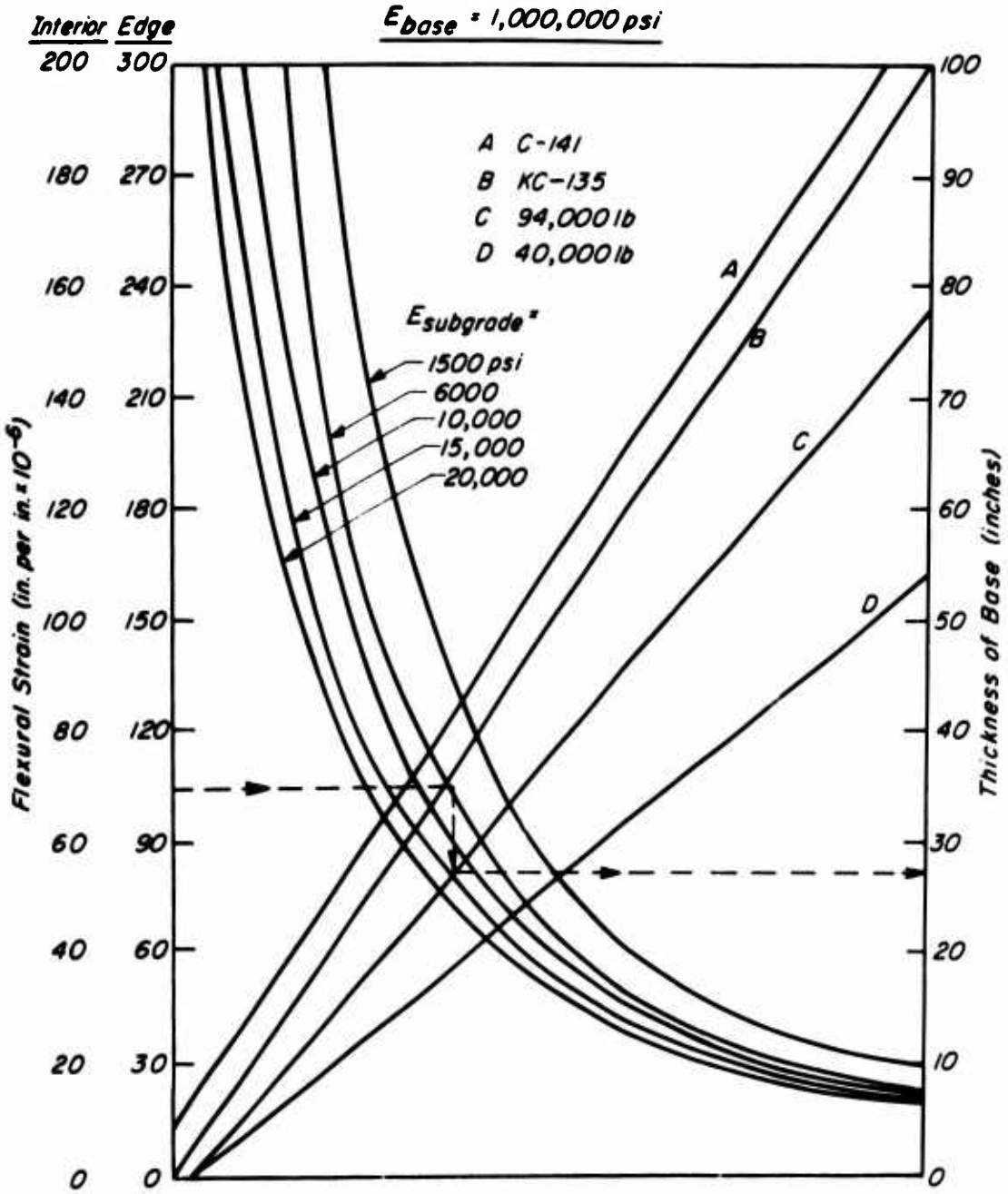

Fig. 15 Relationship between tensile strain and base thickness for various aircraft loads, E_{base} = 1,000,000 psi

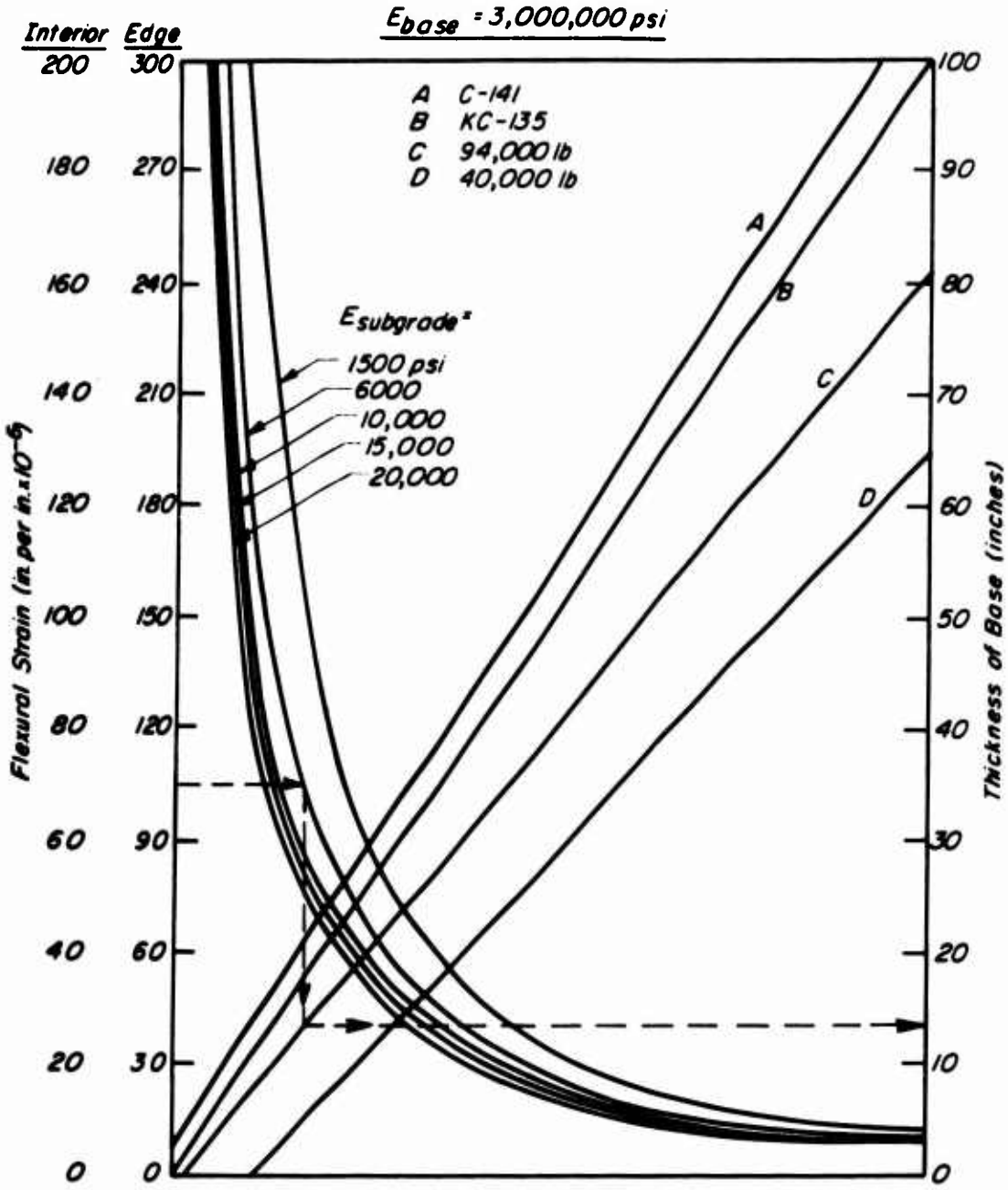

Fig. 16 Relationship between tensile strain and base thickness for various aircraft loads, E_{base} = 3,000,000 psi

b. Check to ascertain whether the load stress plus thermal stress will exceed the fracture strength of the stabilizer layer.

(1) Determine the flexural stress due to traffic loading from Figs. 17 - 24.

(2) Calculate the thermal stresses that will constitute the most severe conditions expected.

(3) Add the thermal stress calculated in Step 2 with the traffic stress from Step 1.

(4) Compare the combined stresses with the flexural strength of the base material. If the flexural strength is greater than the combined stresses, the thickness of cement-treated base is adequate. If note, increase the thickness and recheck the combined stress.

Comparison with Existing Procedures

64. To assess the reasonableness of the proposed procedure, thicknesses selected for highway loading conditions have been compared with a few of the procedures summarized in Appendix G. For convenience, only an 18,000 lb axle load and one subgrade stiffness (CBR = 2.5, E = 3750 psi) were considered. Results are summarized in Table 6 and in Fig. 25.

65. In the Asphalt Institute method, the thicknesses of asphalt concrete were converted to equivalent thicknesses of cement-treated materials and variations with repetitions of traffic are shown in Fig. 25. In making these conversions a substitution ratio of 1.2 in. of cement-treated base equal to 1.0 in. of asphalt concrete was used*.

---

*See footnote next page.

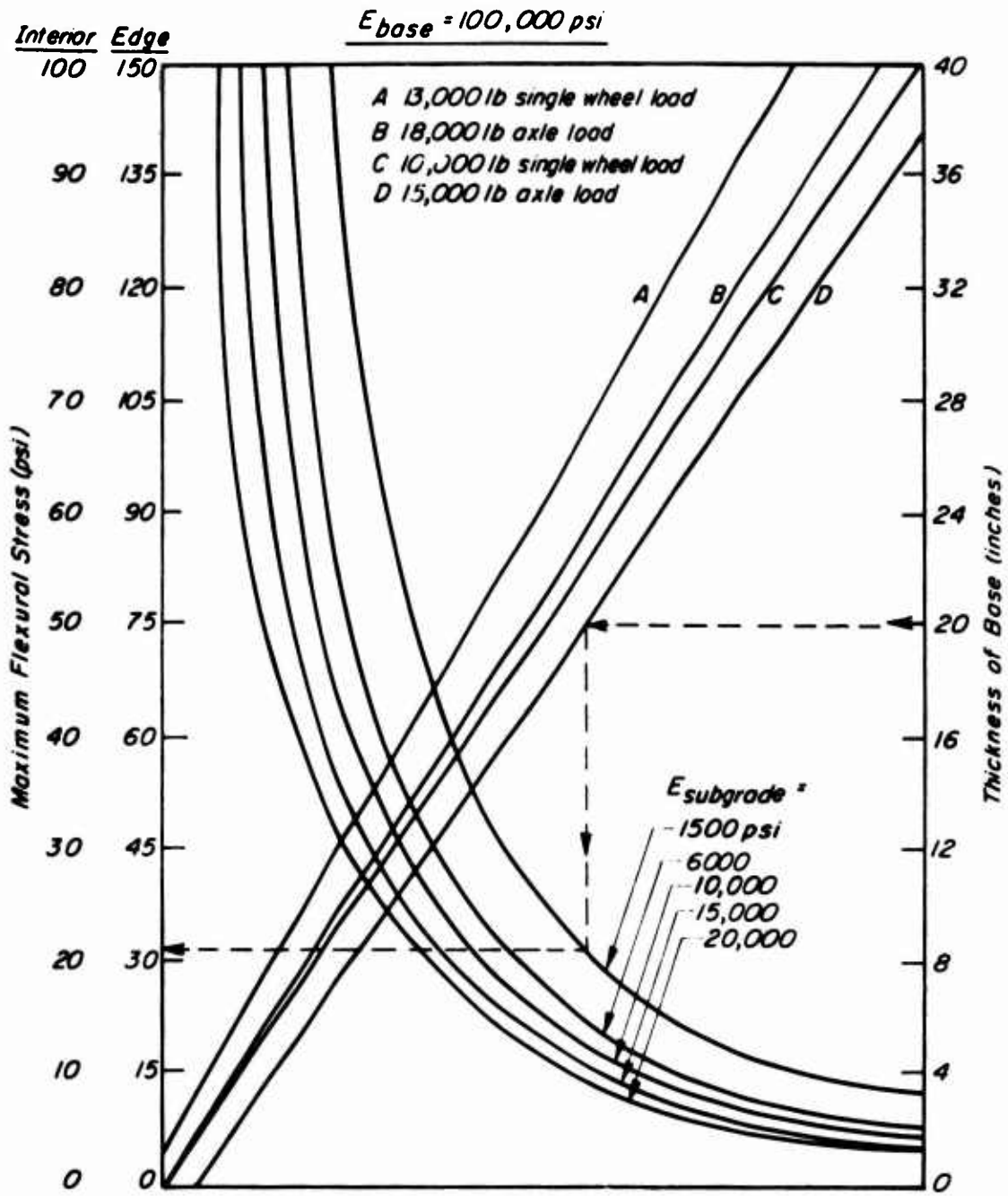

Fig. 17 Relationship between tensile stress and base thickness for various single and dual-wheel loads, E_{base} = 100,000 psi

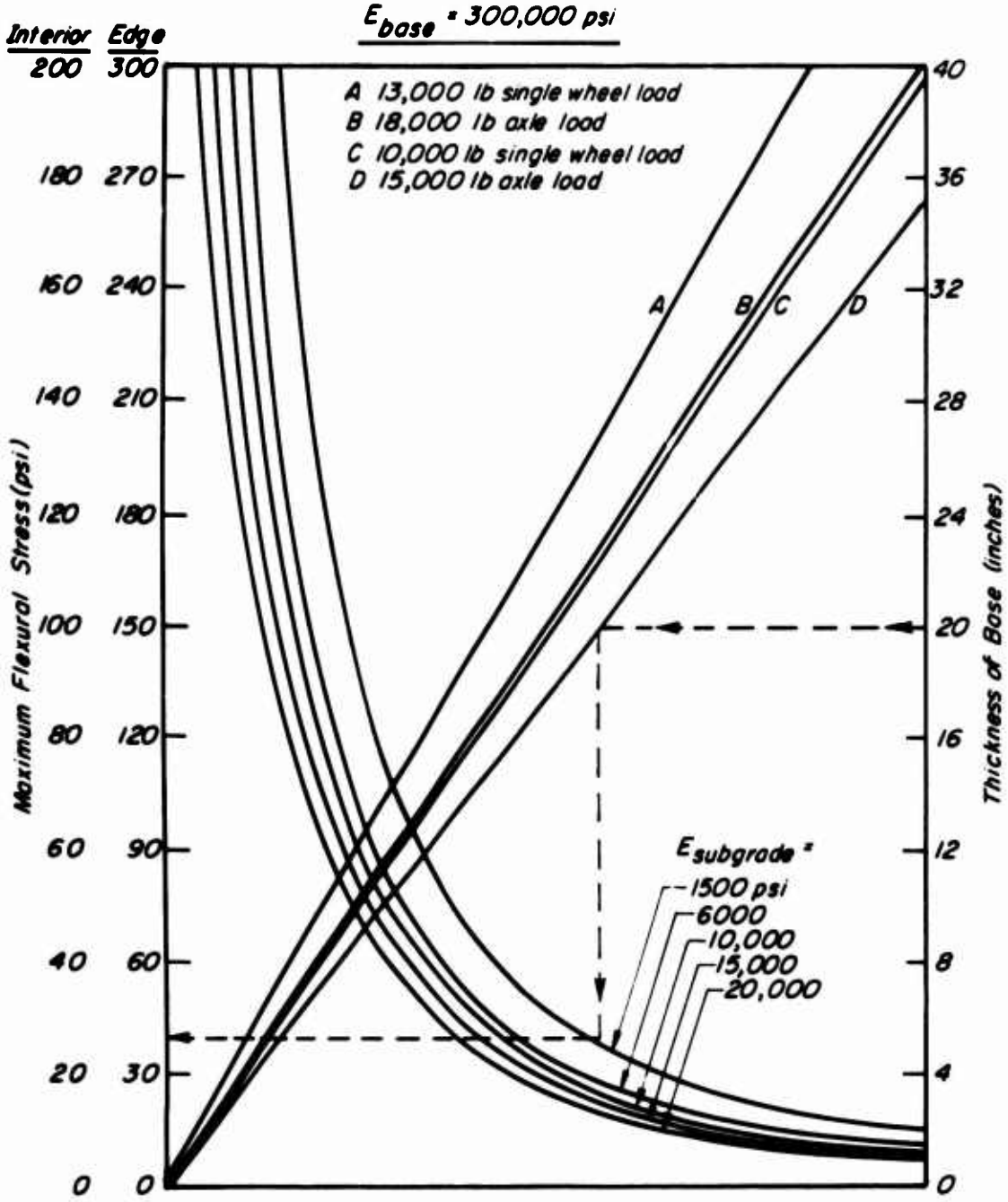

Fig. 18 Relationship between tensile stress and base thickness for various single and dual-wheel loads, E_{base} = 300,000 psi

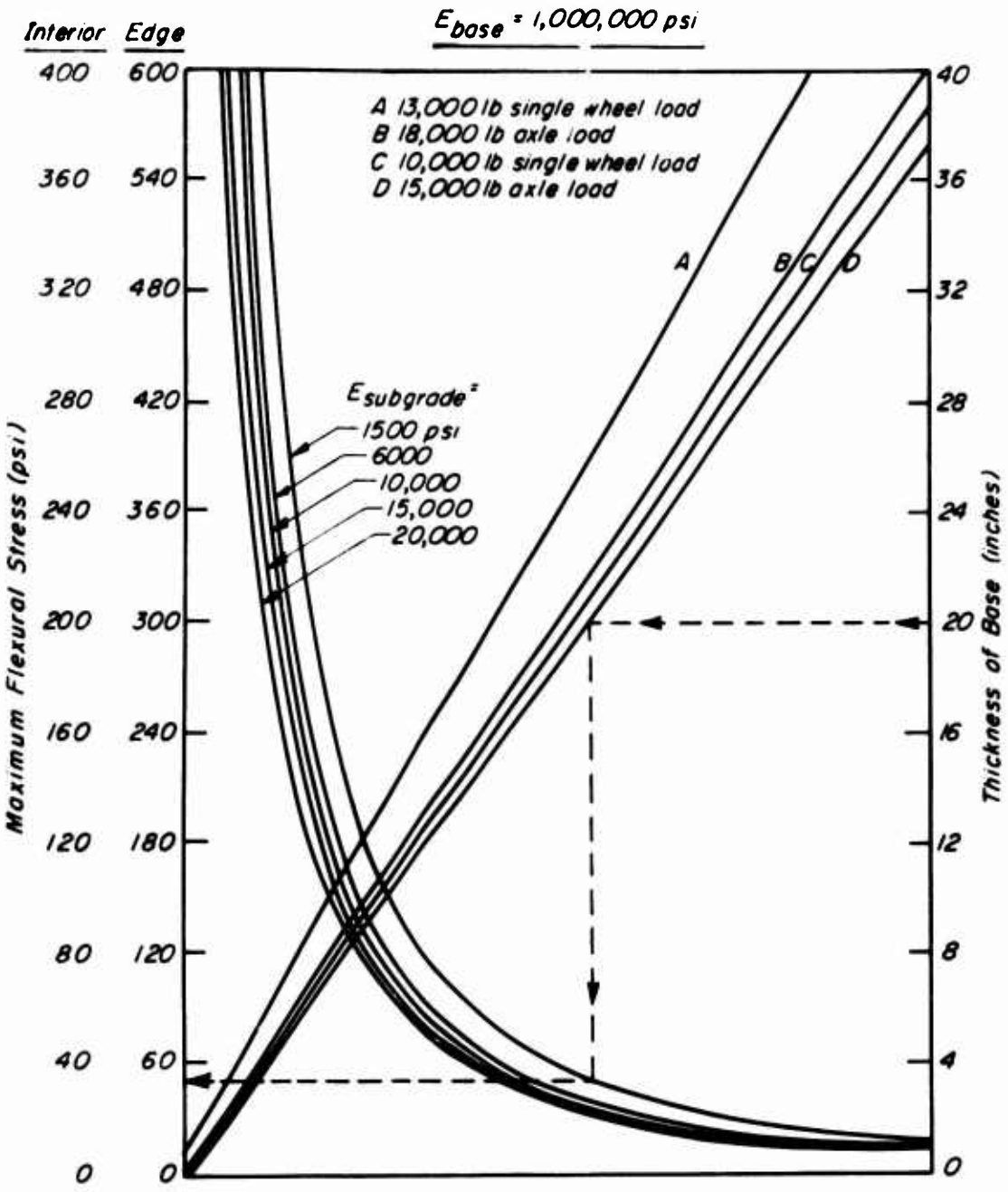

Fig. 19 Relationship between tensile stress and base thickness for various single and dual-wheel loads, E_{base} = 1,000,000 psi

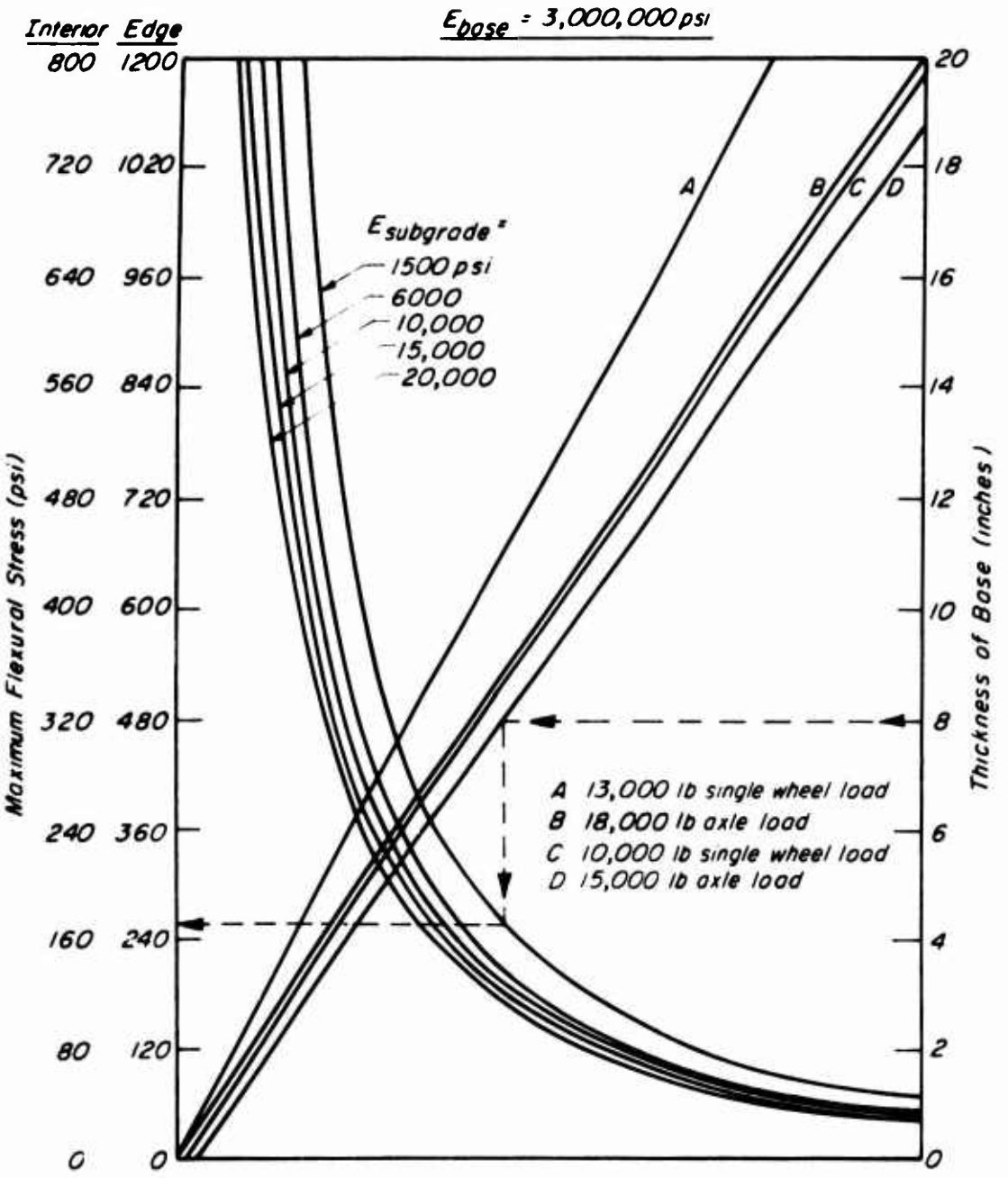

Fig. 20 Relationship between tensile stress and base thickness for various single and dual-wheel loads, E_{base} = 3,000,000 psi

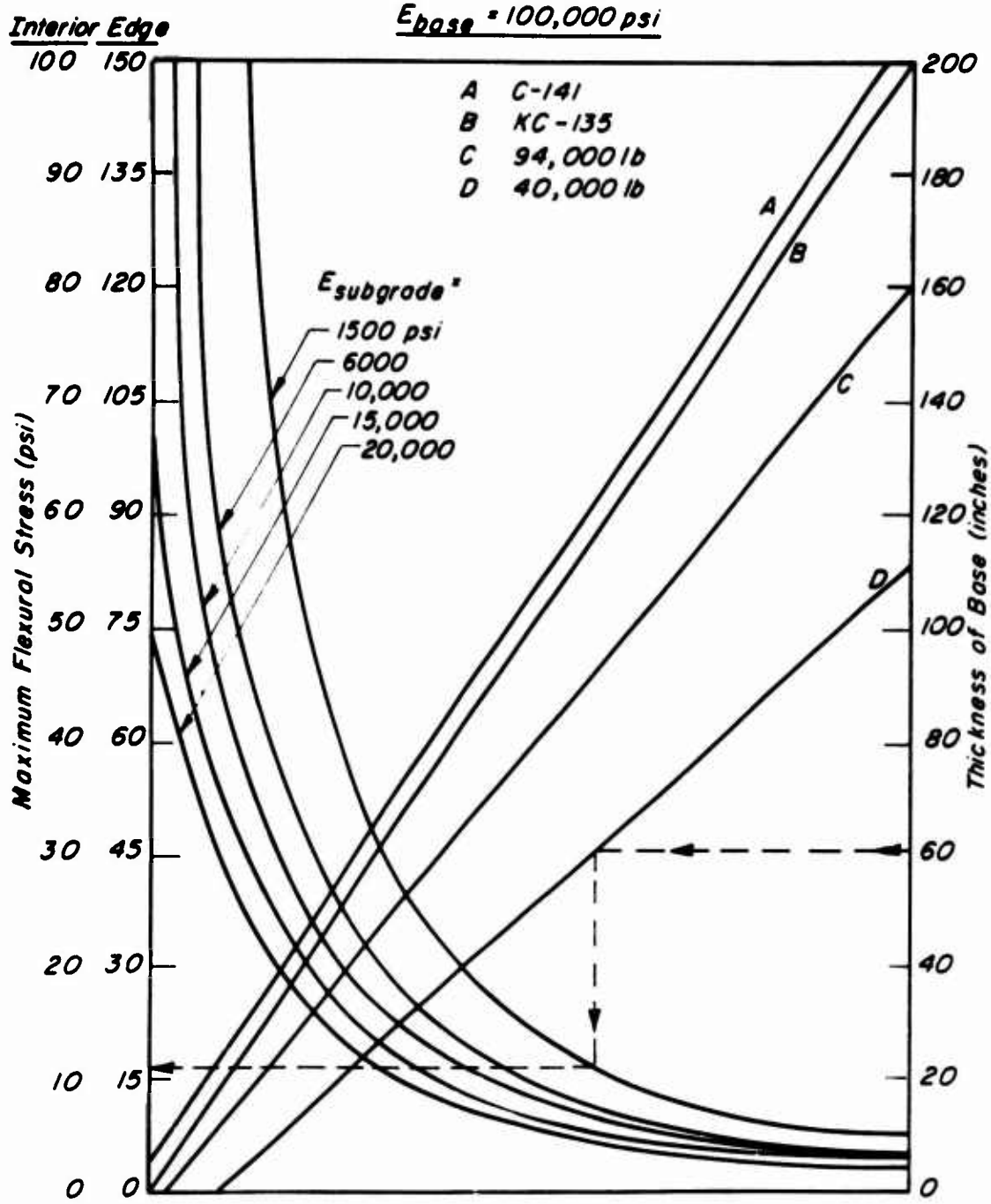

Fig. 21 Relationship between tensile stress and base thickness for various aircraft loads, E_{base} = 100,000 psi

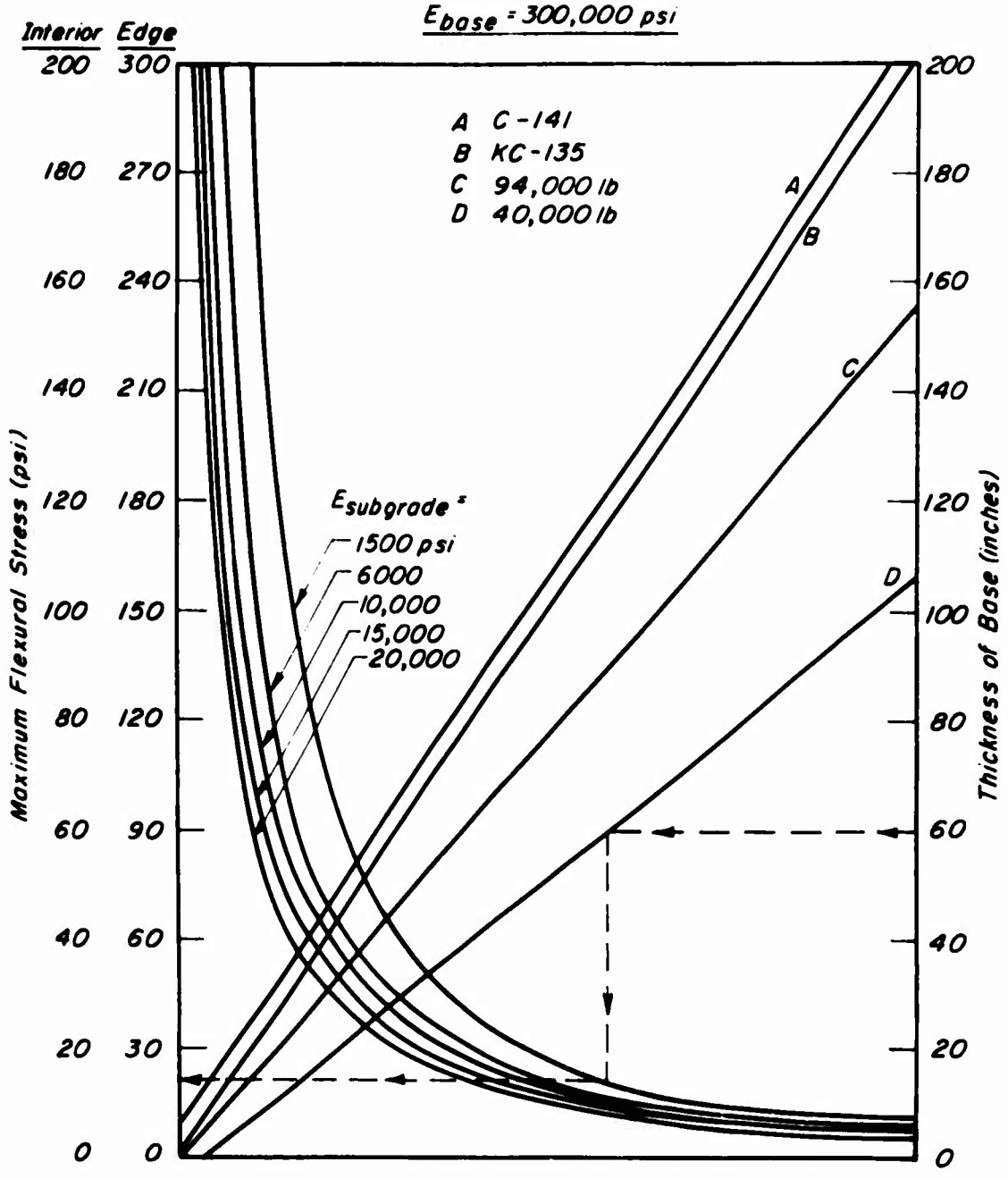

Fig. 22 Relationship between tensile stress and base thickness for various aircraft loads, E_{base} = 300,000 psi

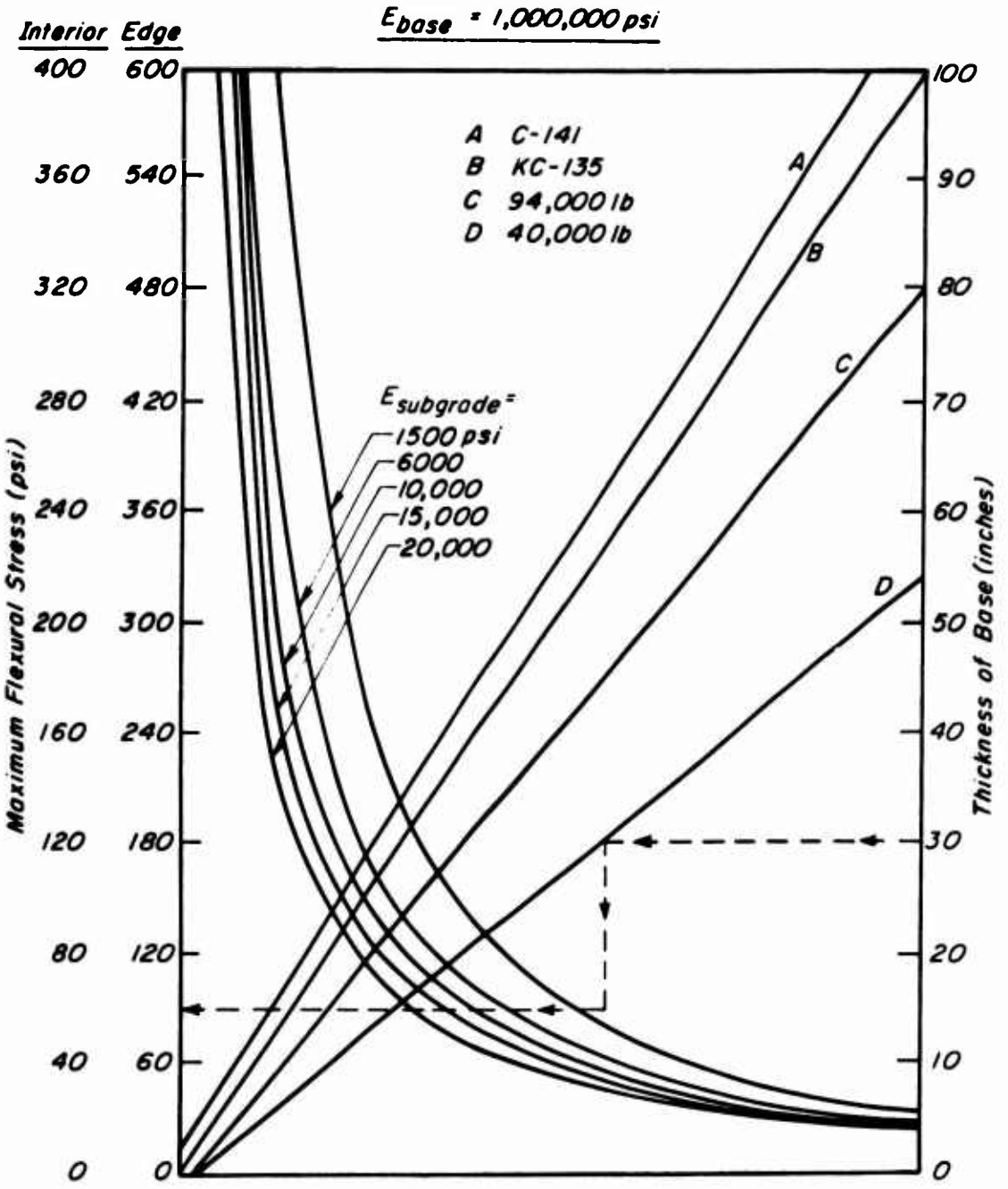

Fig. 23 Relationship between tensile stress and base thickness for various aircraft loads, E_{base} = 1,000,000 psi

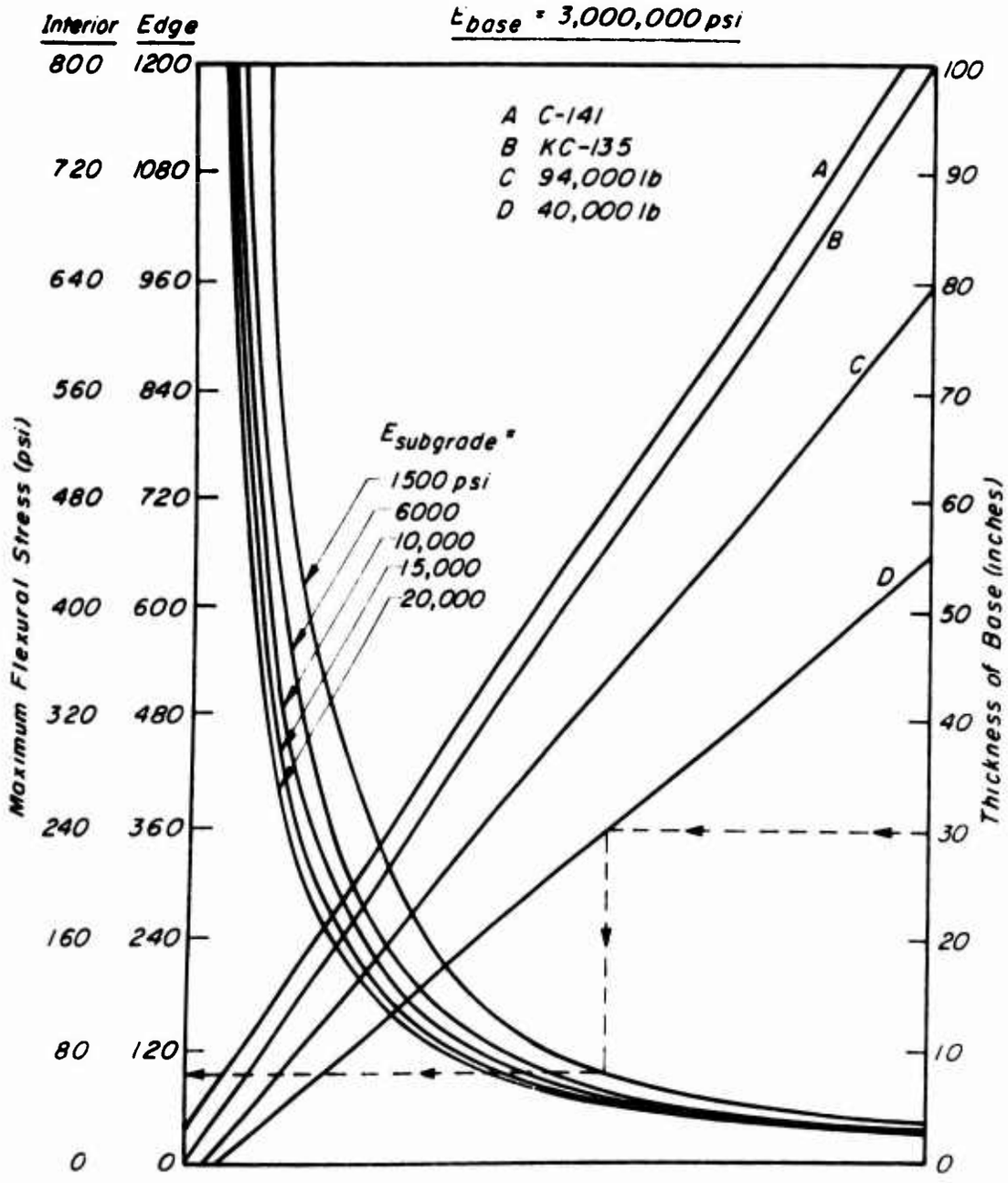

Fig. 24 Relationship between tensile stress and base thickness for various aircraft loads, E_{base} = 3,000,000 psi

66. With the Shell procedure, two conditions were selected: one for the all-asphalt concrete case, the other for the condition which would tend to maximize the use of untreated aggregate. Again by using substitution ratios for asphalt concrete and untreated aggregate base*, a range of thicknesses were obtained; these also are shown in Fig. 25.

67. To use the proposed design procedure allowable strain values were obtained from Fig. 6 and the thicknesses of cement-treated material were determined using the design curves of Figs. 9 - 16. Since the substitition ratios reported for highway loading conditions correspond to relatively high quality treated materials, only stiffnesses of 1×10^6 psi and 3×10^6 psi were used for the design based on the procedure presented herein. The resulting thicknesses are also shown in Fig. 25.

68. It will be noted that the thicknesses determined by the proposed procedure bound the results determined from the Shell and Asphalt Institute methods. While this is not conclusive proof for the validity of the design procedure it does indicate that the results are reasonable in the engineering sense for highway loadings.

---

* Substitution ratios of 1.2 in. of cement-treated base for 1.0 in. of asphalt concrete and 1.7 in. of granular base for 1.0 in. of cement-treated base represent average values used in practice (AASHO, 1961; State of California, 1964).

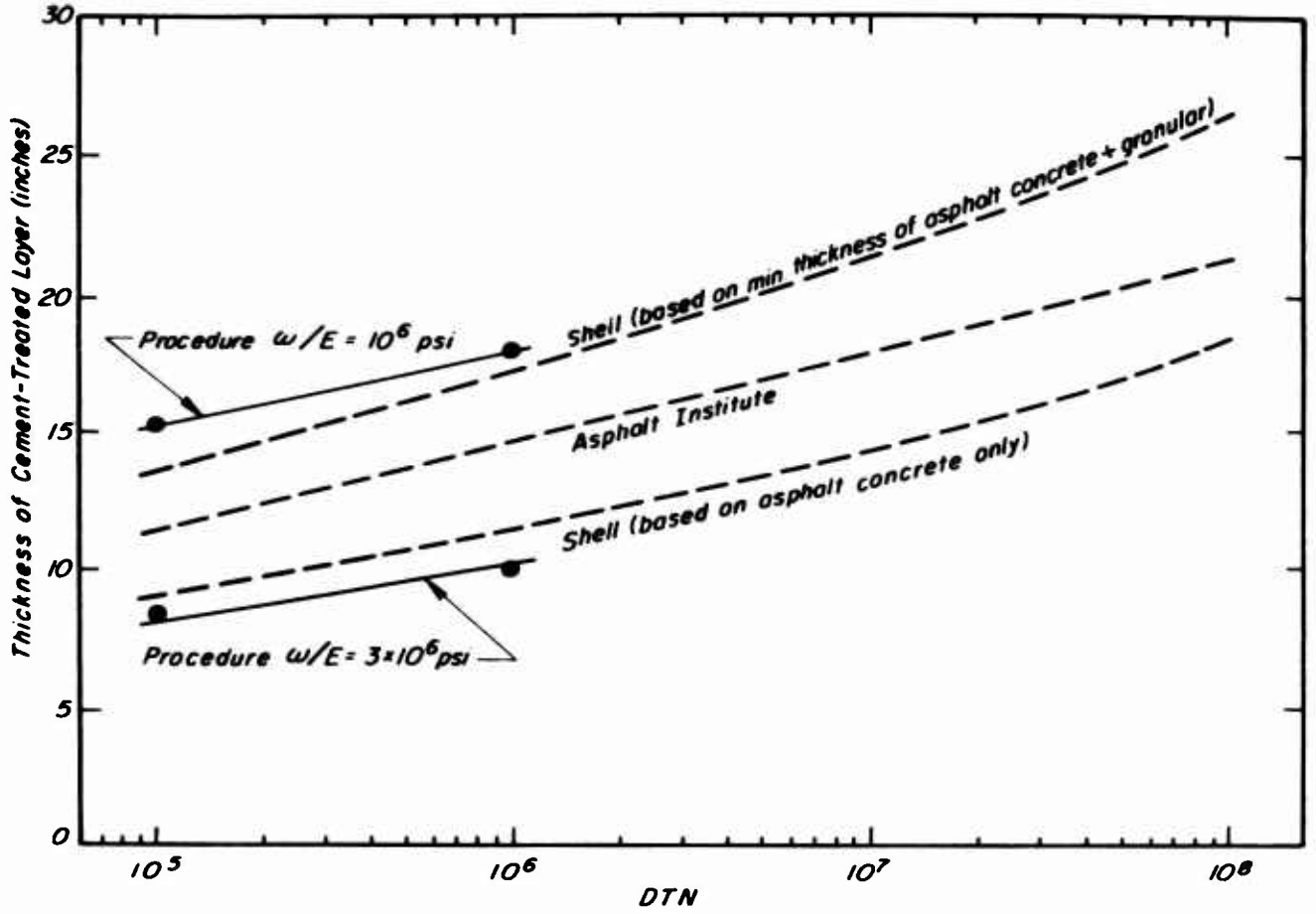

Fig. 25 Comparison of thicknesses of cement stabilized layer by various design procedures for a range in 18,000 lb single axle load applications.

60. Comparisons of thicknesses determined by this procedure with those developed from the WES test sections for airfield loadings indicate that the design charts provide very conservative estimates. This, it must be emphasized, is related to the distress criterion used - in this case initial cracking.

70. Recognizing such limitations and the fact that such a design procedure can be modified as improved distress criteria become available, the proposed procedure has considerable advantage when compared to existing methodology since actual properties of the cement-stabilized soil layer can be utilized within a reasonable engineering framework.

Future Modifications

71. It must be emphasized that the procedure presented herein is applicable to a pavement consisting of a cement-stabilized soil layer resting on an untreated subgrade. If a wearing surface is included, (e.g., a surface treatment on a thin asphalt bound layer), it is assumed to offer no structural stiffness to the section.

72. It is possible to extend this procedure to consider a three-layer system with an asphalt concrete surface layer which offers structural capabilities (Monismith et al, 1970). When an asphalt concrete layer is included, however, temperature has a significant influence on the streses and deformations resulting from traffic loadings since the stiffness characteristics of asphalt concrete depend on temperature. This presents no difficulties since, as already seen, pavement temperatures can be estimated from weather data (Appendix A); accordingly such effects could be included in the design procedure.

73. The linear summation of cycle ratios concept (Appendix E) permits design of the pavement structure for mixed traffic conditions rather than for a specific wheel load. Its inclusion would thus appear to be a step forward. This same cumulative damage hypothesis will also be useful for analyzing pavements with thick asphalt-bound surface layers since it permits inclusion of a more realistic assessment of environmental influences; that is, different stresses (or strains) resulting from changed asphalt concrete stiffnesses can be summed throughout the year.

74. Use of the modified Goodman diagram (Appendix E) in the design process to consider the superposition of steady state stresses on the fluctuating stresses caused by traffic loading would also appear to be a worthwhile modification.

75. Relative to the distress criteria, only one fatigue curve has been included. It is probable that different materials will exhibit different response characteristics and that various treatment levels for the same material would result in a series of fatigue curves. Inclusion of such data, however, only awaits their development.

76. Asphalt-stabilized or lime-stabilied materials can also be included in the design procedure. Presumably lime-treated materials could be analyzed in a manner similar to the cement-treated materials described herein; it would be necessary, however, to have the necessary stiffness and fatigue characteristics for such materials. The same data will be required for asphalt-treated materials. For such materials,

as noted above, temperature effects are significant and must therefore be included in the design procedure. Guides, however, for such methodology already exist (Monismith et al, 1970).

TABLE 2 CHARACTERISTICS OF THE LOADS USED FOR THE DEVELOPMENT OF THE DESIGN CURVES

Representative Vehicles (Truck or Aircraft)	Maximum Single-Axle Load lb.	Configuration	Tire Pressure p.s.i.
	Roads		
Military Cargo Trucks up to 5 tons	13,000 with single wheel	--	70
Military Cargo Trucks up to 5 tons	15,000 with dual wheels	12 in. c-c	70
Conventional Single Axle Load	18,000 with dual wheels	12 in. c-c	80
	Airfields		
AC-1* AO-1* U1-A L-Series	10,000 (single wheel)	--	35
C-130* C-131 C-119 C-123 F-100 Series	40,000 (single tandem)	60 in. c-c, 400 sq. in. contact area	50
C-124*	94,000 (twin tandem)	44 in. c-c, 630 sq. in contact area	75
KC-135	134,000 (twin tandem)	60" x 36"	134
C-141	144,700 (twin tandem)	48" x 32.5"	172
Boeing 747	162,000 (twin tandem)	64" x 46"	207

* Critical aircraft for which the gear load, configuration, and tire pressure are given.

TABLE 3 APPROXIMATE RELATIONSHIP BETWEEN ELASTIC MODULUS AND THE FAA SOIL CLASSIFICATION*

FAA Classification	E_S psi	E_S KN/M^2
F10	5,500	37,900
F9	6,500	44,800
F8	7,700	53,100
F7	8,900	61,400
F6	10,800	74,500
F5	12,600	86,900
F4	14,600	100,700
F3	16,600	114,500
F2	19,900	137,200
F1	22,700	156,500
Fa	31,000	213,700

* After the Asphalt Institute (1973).

TABLE 4

RELATIONSHIP BETWEEN CBR AND FAA SUBGRADE CLASS*

Subgrade Class	CBR
F10	3.5
F9	4.5
F8	5.5
F7	6.5
F6	7.5
F5	8.5
F4	10
F3	12
F2	14.5
F1	18
Fa	20

* After FAA (1973)

TABLE 5 SUMMARY OF DATA

ON COEFFICIENT OF THERMAL EXPANSION OF HARDENED CEMENT-TREATED SOIL*

Description of Soil	Cement Content	Coefficient of Thermal Expansion (in./in. deg F) x 10^{-6}
Sandy loam	2.5 to 10%	4.5 to 5.8
Silty loam	2.5 to 10%	4.1 to 5.6
Silty clay loam	2.5 to 10%	3.9 to 6.1
Loam	2.5 to 10%	4.6 to 6.3
Sand-shell	2.8 sks/cu yd	3.5
Sandy loam (A-2)	8%	6.9
Silty clay loam	14%	6.2
Clay (A-6-7)	12%	5.7
Several types	Not given	5.1 to 8.7

* (Highway Research Board, 1961)

TABLE 6 COMPARISON PAVEMENT THICKNESSES BY VARIOUS DESIGN PROCEDURES

	Asphalt Institute		Shell[a]					Proposed	
			Method A		Method B				
N	Thickness of Asphalt Concrete in.	Thickness of CTB[a] in.	Thickness of Asphalt Concrete in.	Thickness of CTB[b] in.	Thickness of Asphalt Concrete in.	Thickness of Granular Base in.	Thickness of CTB[c]	$E=1\times10^6$ psi	$E=3\times10^6$ psi
10^5	9.5	11.4	7.3	9.1	5	13	13.6	15.2	8.5
10^6	12.2	14.7	9.5	11.4	5	20	17.8	18.0	10.0

a. In Shell procedure, two designs have been selected:

Method A - all asphalt concrete

Method B - asphalt concrete + granular base

b. Based on equivalency of 1.0 in. of asphalt concrete equal to 1.2 in. of cement-stabilized material.

c. Based on equivalency of 1.7 in. of gravel equal to 1.0 in. of cement-stabilized material.

REFERENCES

Asphalt Institute, Thickness Design - Asphalt Pavement Structures for Highways and Streets, 7th Edition, Manual Series No. 1. College Park, Maryland: 1963.

Asphalt Institute, Documentation of the Asphalt Institute's Thickness Design Manual, 7th Edition, Research Series No. 14. College Park, Maryland: August, 1964.

Asphalt Institute, Thickness Design - Full Depth Asphalt Pavement Structures for Highways and Streets, 8th Edition, Manual Series No. 1. College Park, Maryland: 1970.

Asphalt Institute, "Full-Depth Asphalt Pavements For Air Carrier Airports," Manual Series No. 11 (MS-11), January 1973 Edition, 168 pp.

A.S.T.M. Standards (1966) Part 30, Designation: E206-66, May, 1966.

Bolmer, G. G., "Shear Strength and Elastic Properties of Soil Cement Mixtures Under Triaxial Loading," ASTM Proc. 58, pp. 1187-1204, 1958.

Barber, Edward S., "Calculation of Maximum Pavement Temperatures From Weather Reports," Highway Research Board, Bulletin 168, Washington, D. C., 1957, pp. 1-8.

Barenberg, E. J., "Evaluating Stabilized Materials," Report to National Cooperative Highway Research Program, HRB, Department of Civil Engineering, Engineering Experiment Station, University of Illinois, 1967.

Bradbury, Royal D., Reinforced Concrete Pavements, Wire Reinforcement Institute, 1938.

Corp of Engineers, U. S. Army Engineer Waterways Experiment Station, Vicksburg, Mississippi, "Soil Stabilization Requirements For Military Roads and Airfields in the Theater of Operations", Miscellaneous Paper No. 3-605, Oct. 1963.

Dormon, G. M., J. M. Edwards, and J. E. D. Kerr, "The Design of Flexible Pavements," Paper prepared for presentation to the annual general meeting of the Engineering Institute of Canada, May, 1964, Banff, Alberta, Canada.

Dormon, G. M. and C. T. Metcalf, "Design Curves for Flexible Pavements Based on Layered System Theory," Highway Research Board, Highway Research Record No. 71. Washington, D. C.: 1965.

Edwards, J. M. and C. P. Valkering, Structural Design of Asphalt Pavements for Heavy Aircraft. Shell International Petroleum Company, Limited, London, 1970.

Felt, E. J. and Abrams, M. S., "Strength and Elastic Properties of Compacted Soil-Cement Mixtures," ASTM, STP 206, 1957.

Finn, Fred N., "Factors Involved in the Design of Asphaltic Pavement Surfaces," Washington, D. C., Highway Research Board, NCHRP, Report 39, 1967, 112 pp.

Fossberg, P. E., "Load-Deformation of Three-Layer Pavements Containing Cement-Stabilized Base," Ph.D. Thesis, University of California, Berkeley, 1970.

George, K. P., "Cracking in Cement-Treated Bases and Means of Minimizing It", HRB Record 255, 1968, pp 59-71.

George, K. P, "Cracking in Pavements Influenced by Viscoelastic Properties of Soil-Cement," HRB Record 263, 1969, pp 47-59.

George, K. P., "Shrinkage Cracking of Soil-Cement Base: Theoretical and Model Studies," HRB Record 351, 1971, pp 115-132.

George, K. P. and Davidson, P. T., "Development of a Freeze-Thaw Test for Design of Soil-Cement," HRB Record 36, 1963, pp 77-96.

Hadley, W. O., Hudson, W. R., and T. W. Kennedy, "A Comprehensive Structural Design for Stabilized Pavement Layers," Research Report 98-13, Center for Highway Research, University of Texas at Austin, April, 1972, 203 pp.

Harr, M. E. and G. A. Leonards, "Warping Stresses and Deflections in Concrete Pavements," Proceedings HRB, 1959, pp 286-320.

Heukelom, W.and C. R. Foster, "Dynamic Testing of Pavements," ASCE, Journal of Soil Mechanics and Foundation Division, V. 86, No. SM1, February 1960, Part I, pp 1-28.

Heukelom, W.and A. G. J. Klomp, "Consideration of Calculated Strains at Various Depths in Connection with the Stability of Asphalt Pavements," Proceedings of the Second International Conference on the Structural Design of Asphalt Pavements. University of Michigan, Ann Arbor: 1968.

Highway Research Board, Bulletin 292, "Soil Stabilization with Portland Cement," 1961, 212 pp.

Hilsdorf, A. E. and C. E. Kesler, "Fatigue Strength of Concrete Under Varying Flexural Stresses," Journal of the American Concrete Institute, October 1966.

Hveem, F. N. and R. M. Carmany, "The Factors Underlying the Rational Design of Pavements," Proceedings, Highway Research Board, Vol. 28, 1948.

Hveem, F. N., "Pavement Deflections and Fatigue Failures," Design and Testing of Flexible Pavements, Highway Research Board Bulletin 114. Washington, D. C.: 1955, pp 43-87.

Hveem, F. N. and G. B. Sherman, "Thickness of Flexible Pavements by the California Formula Compared to AASHO Road Test Data," Flexible Pavement Design, Highway Research Board, Highway Research Record No. 13. Washington, D. C.: 1963, pp 142-166.

Kasianchuk, D. A., "Fatigue Considerations in the Design of Asphalt Concrete Pavements," Ph.D. Dissertation, University of California, Berkeley, 1968.

Klomp, A. G. J. and G. M. Dormon, "Stress Distribution and Dynamic Testing in Relation to Road Design," Proceedings, Australian Road Research Board, Vol. II, 1964.

Larsen, T. J. and P. J. Nussbaum, "Fatigue of Soil-Cement," Journal of the Portland Cement Association Research and Development Laboratories, Vol. 9, No. 2, pp 37-50, May, 1967.

Larsen, T. J., P. J. Nussbaum, and B. E. Colley, "Research on Thickness Design for Soil-Cement Pavements," Portland Cement Association, Development Department Bulletin No. D 142, 1969.

Lettier, J. A. and C. T. Metcalf, "Application of Design Calculations to 'Black Base' Pavements," Proceedings of the Association of Asphalt Paving Technologists, Vol. 33, 1964.

Liddle, W. J. "Application of AASHO Road Test Results to the Design of Flexible Pavement Structures," Proceedings, International Conference on the Structural Design of Asphalt Pavements, University of Michigan, Ann Arbor: 1963.

Lister, N. W., "Design and Performance of Cement-Bound Bases," Journal of the Institution of Highway Engineers, Vol. XIX, No. 2, February, 1972 pp 21-33.

Materials Research and Development, "AASHO Interim Guide for Design of Pavement Structures," Highway Research Board, Draft Final Report, National Cooperative Highway Research Program Project 1-11. Washington, D.C.: October, 1971.

McCullough, B. F., C. J. VanTil, B. A. Vallerga, and R. G. Hicks, "Evaluation of AASHO Interim Guide for Design of Pavement Structures," Highway Research Board, Final Report, National Cooperative Highway Research Program Project 1-11. Washington, D. C.: December, 1968.

Mitchell, J. K. and C. L. Monismith, Behavior of Stabilized Soils Under Repeated Loading, Report 2, Behavior in Repeated Flexure, Frequency and Duration Effects, Fatigue Failure Analyses, Contract Report No. 3-145 for U. S. Army Engineer Waterways Experiment Station, Vicksburg, Mississippi, 1967.

Mitchell, J. K, C. K. Shen, and C. L. Monismith, Behavior of Stabilized Soils Under Repeated Loading, Report 1, Background, Equipment, Preliminary Investigations, Repeated Compression and Flexure Tests on Cement-treated Silty U. S. Army Engineer Waterways Experiment Station, Vicksburg, Mississippi, 1965, 122 pp.

Mitchell, J. K., T. S. Ueng, and M. Abboud, "The Properties of Cement-Stabilized Soil," Unpublished Report, 1973.

Mitchell, J. K., T. S. Ueng, and C. L. Monismith, "Behavior of Stabilized Soils Under Repeated Loading, Report 5, Performance Evaluation of Cement-Stabilized Soil Layers and Its Relationship to Pavement Design, Contract Report No. 3-145 for U. S. Army Engineers Waterways Experiment Station, Vicksburg, Mississippi, August 1972, 166 pp.

Monismith, C. L. and D. B. McLean, Design Considerations for Asphalt Pavements, Report No. TE 71-8, University of California, Berkeley, December 1971.

Murdock, J. W. and C. E. Kesler, "Effect of Range of Stress on Fatigue Strength of Plain Concrete Beams," Journal of the American Concrete Institute, August, 1958.

Oglesby, C. H. and L. I. Hewes, Highway Engineering, John Wiley and Sons, Inc., New York, 2nd Edition, 1959, 783 pp.

Otté, E., "A Tentative Approach to the Design of Pavements Having Cement-Treated Layers," NIRRPCI Symposium on Cement-Treated Crusher-Run Bases," Preprint, Johannesburg, Feb., 1973, 27 pp.

Otté, E., "The Performance of Two Pavements Containing Cement-Treated Crusher-Run Bases," NIRR-PCI Symposium on Cement-Treated Crusher-Run Bases, Preprint, Johannesburg, Feb. 1973, 29 pp.

Nakayama, H. and R. L. Handy, "Factors Influencing Skrinkage of Soil-Cement," Highway Research Board, Highway Research Record No. 86, 1965, pp. 15-27.

Nielsen, J. P., "Thickness Design Procedure For Cement-Treated Sand Bases," Journal of the Highway Division, ASCE, Vol. 94, No. HW2, Nov. 1968, pp. 141-159.

Norling, L. T., "Minimizing Reflective Cracks in Soil-Cement Pavements - A status Report of Laboratory Studies and Field Practices," PCA, Presented at the 52nd Annual Meeting of HRB, Washington, D. C., January 1973.

Packard, R. G., Design of Concrete Airport Pavements, Portland Cement Association, Chicago, 1973.

Peutz, M. G. F., H. P. M. VanKempen, and A. Jones, "Layered Systems Under Normal Surface Loads," Highway Research Board, Highway Research Record 228, Washington, D. C.: 1966.

Pickett, G. and G. K. Ray, "Influence Charts For Concrete Pavements," Transactions, ASCE, Vol. 116, Paper No. 2425, 1951, pp. 49-73.

Pretorius, P. C., "Design Considerations for Pavements Containing Soil-Cement Bases," Ph.D. Dissertation, University of California, Berkeley, 1970, 210 pp.

Pretorius, P. C. and C. L. Monismith, "Prediction of Shrinkage Stresses in Pavements Containing Soil-Cement Bases," HRB Record 362, 1971, pp 63-86.

Pretorius, P. C. and C. L. Monismith, "Fatigue Crack Formation and Propogation in Pavements Containing Soil-Cement Bases," HRB Record 407, 1972, pp. 102-115.

Raithby, K. D. and A. C. Whiffin, "Failure of Plain Concrete under Fatigue Loading -- A Review of Current Knowledge," Road Research Laboratory, Ministry of Transport, RRL Report LR 231.

Reddy, A. S., G. A. Leonards, and M. E. Harr, "Warping Stresses and Deflections in Concrete Pavements: Part III," HRR No. 44, 1963, pp. 1 - 24.

Seed, H. B. and J. W. N. Fead, "Apparatus For Repeated Load Tests on Soils, ASTM Special Technical Publication No. 254, 1960, Papers on Soils 1959 Meetings, pp. 78 - 87.

Sanan, B. K. and K. P. George, "Viscoelastic Shrinkage Stress in Soil-Cement Base," ASCE, Journal of Soil Mechanics and Foundations Division paper No. 9454, Vol. 98, SM 12, pp. 1375 - 1395, December 1972.

Shell Oil Company, Shell 1963 Design Charts for Flexible Pavements. New York: 1963.

Sherman, G. B., "Recent Changes in the California Design Method for Structural Sections of Flexible Pavements," Proceedings, First Annual Highway Conference, College of Pacific, Stockton, California: 1958.

Shook, J. F. and F. N. Finn, "Thickness Design Relationship for Asphalt Pavements," Proceedings, International Conference on Structural Design of Asphalt Pavements, University of Michigan, Ann Arbor: 1963.

Shook, J. F., "Development of Asphalt Institute Thickness Design Relationships," Proceedings of the Association of Asphalt Paving Technologists, Vol. 33, 1964).

State of California, Division of Highways, Materials Manual, Vol. I, "Test Method No. Calif. 301-F" September, 1964.

Thomlinson, J., "Temperature Variations and Consequent Stresses Produced by Daily and Seasonal Temperature Cycles in Concrete Slabs," Concrete and Construction Engineering, Vol. XXXV, No. 6, June 1940, pp 298-307.

U. S. Federal Aviation Administration, "Airport Paving," Advisory Circular AC 150/5320-6B, 1973.

Wang, M. C., "Stress and Deflections in Cement-Stabilized Soil Pavements, Ph.D. Dissertation, University of California, Berkeley.

Wang, M. C. and J. K. Mitchell, "Stress-Deformation Prediction in Cement-Treated Soil Pavements," pp. 93 - 11, HRR 351, 1971.

Wang, M. C. J. K. Mitchell, and C. L. Monismith, "Behavior of Stabilized Soils Under Repeated Loading; Report 4: Stresses and Deflections in Cement-Stabilized Pavements," Contract Report No. 3-145 to U. S. Army Corps of Engineers, Waterways Experiment Station, Vicksburg, Miss., 1970.

Williams, A. A. B. and G. L. Dehlen, "The Performance of Fullscale Base and Surfacing Experiments on National Route 3-1, at Key Ridge, after the First Six Years," First Conference on Asphalt Pavements for Southern Africa, Durban, August 1969.

Wilson, E. L., "The Determination of Temperatures within Mass Concrete Structures," Report No. 68-17, Structures and Materials Research, Department of Civil Engineering, University of California, Berkeley, 1968.

Zube, E., C. G. Gates, E. C. Shirley and H. A. Munday, Jr.; "Service Performance of Cement-Treated Bases as Used in Composite Pavements," HRB Record 291, pp. 57 - 69, 1969.

APPENDIX A: PAVEMENT TEMPERATURE DETERMINATIONS

1. As noted in the main body of the report three procedures are available to solve the heat conduction equation:

a. Closed form - uniform material with depth (Barber, 1957).

b. Finite difference - layered structure (Christensen and Anderson, 1972).

c. Finite element - layered structure (Pretorius, 1970).

Only the first (Barber) procedure will be described in detail in this section.

2. The Barber method uses available weather data to calculate temperatures in a semi-infinite mass in contact with a sinusoidally varying air temperature. The effects of solar radiation, cloud cover, and wind velocity are also included in the analysis.

3. For a semi-infinite mass in contact with air at temperature: $T_M + T_V \cdot \sin \frac{2\pi}{24} t$, the 24 hour periodic temperature of the semi-infinite mass is:

$$T = T_M + T_V \frac{He^{-xC}}{\sqrt{(H+C)^2 + C^2}} \cdot \sin \left(\frac{2\pi}{24} t - xC - \arctan \frac{C}{H + C}\right) \qquad (A\text{-}1)$$

where:

T = temperature of mass, °F

T_M = mean effective air temperature, °F

T_V = maximum variation in temperature from mean, °F

$H = h/k$

h = surface coefficient, BTU/ft^2/hr/F deg

k = conductivity, BTU · ft/hr/ft^2/f deg

x = depth below surface, ft.

C = 0.131/d

d = diffusivity, ft^2/hr = k/C·W

c = specific heat, BTU/lb/F deg

w = density, lb/ft^3

4. To include the other effects noted above:

a. The effects of forced convection due to wind and average reradiation from the surface are accounted by stating the surface coefficient as:

$$h = 1.3 + 0.62\ V^{0.75} \qquad \text{(A-2)}$$

where: V = wind velocity, miles/hour

b. The effect of solar radiation is included by defining the effective air temperature to include solar radiation as:

$$T_E = T_A + \frac{bI}{h} \qquad \text{(A-3)}$$

where:

T_E = effective air temperature, °F

T_A = air temperature, °F

b = absorptivity of surface to solar radiation

I = solar radiation, BTU/sq ft/hour

Solar radiation on a horizontal surface is reported in Langleys per day. One Langley/day = one calorie/cm^2/day or 3.69 BTU/ft^2/day.

There is an average net loss by long-wave reradiation of about one-third, so that R, the average contribution to effective air temperature, is:

$$R = 0.67\ b\ \frac{3.69L}{24\ h}$$

where:

L = solar radiation, Langleys/day

The deviation of the radiation from this average may be roughly approximated by a sine wave with a half-amplitude of 3R. Combining this with the air temperature, which is approximated by a sine wave with amplitude equal to the daily range in temperature, gives a sinusoidal effective temperature. The pavement temperature may then be calculated from equation (A1), using:

$$T_M = T_A + R \qquad \text{(A-5)}$$

and

$$T_V = 0.5\ T_R + 3R \qquad \text{(A-6)}$$

where:

T_R = daily range in air temperature, °F

c. The effect of cloud cover is included by decreasing solar radiation in terms of Langleys per day according to:

$$L_{adj} = \left[1 - \frac{\text{Hours cloud cover}}{\text{Total daylight hours}}\right] L \qquad \text{(A-7)}$$

5. Agreement between observed pavement temperature and those calculated by the Barber method is extremely good. Barber showed good agreement between observed and calculated bituminous pavement surface temperatures (Fig. A1) and also between observed and calculated maximum

temperatures of a concrete pavement (Fig. A2). For a 12-inch thick asphalt layer, (Kasianchuk,1968) showed good agreement between measured and calculated temperatures at different depths in the layer (Fig. A3 and A4).

6. A drawback of the Barber method is its lack of generality in that it fails to distinguish among layers with different thermal properties. This problem, which may be important for pavements with cement-treated bases, is overcome by use of the finite element method. Pretorius, (1970) compared measured temperatures in a 10-inch asphalt concrete layer with those predicted by both the finite element method and the Barber method (Fig. A5). He then used the finite element method to determine the temperature distribution in the pavement containing a cement-treated base (Fig. A6). From his analyses, Pretorius concluded that the Barber method can be used for a two- or three-layer system, using the thermal properties of the top layer. The main reasons are: the analysis is not sensitive to conductivity of the different layers; the thermal properties of asphalt concrete and cement-treated base are similar; and the effects of the subgrade thermal properties are negligible. The Barber method is particularly attractive as it lends itself to hand calculation and therefore is recommended to determine temperature distributions in pavements. The sophistication of the finite element method, which necessitates use of a computer, is not necessary for this analysis.

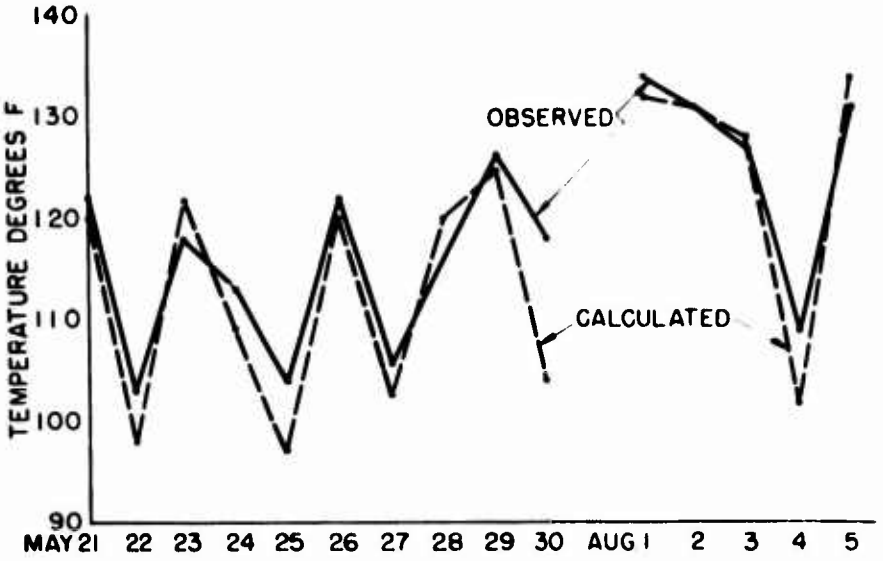

Fig. A1 Comparison of observed and calculated asphalt concrete pavement surface temperatures (After Barber, 1957)

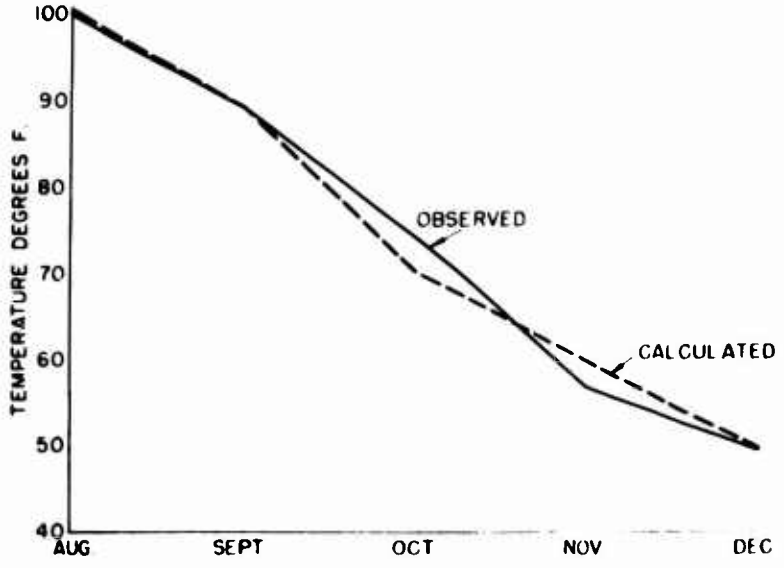

Fig. A2 Comparison of observed and calculated maximum temperatures of a concrete pavement (After Barber, 1957)

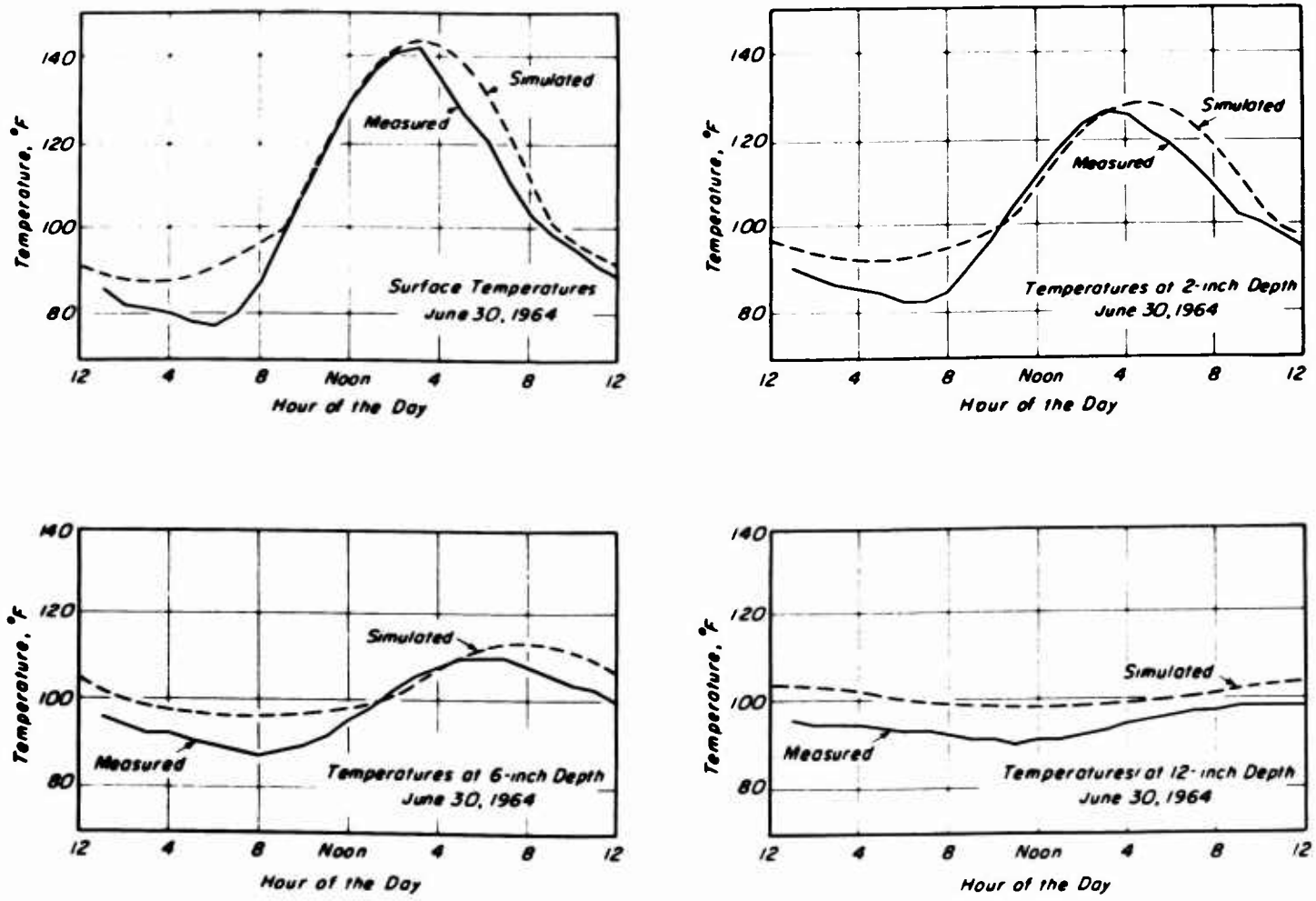

Fig. A3 Comparison of computed and measured daily temperature variation in a 12 in. asphalt concrete layer (After Kasianchuk, 1968)

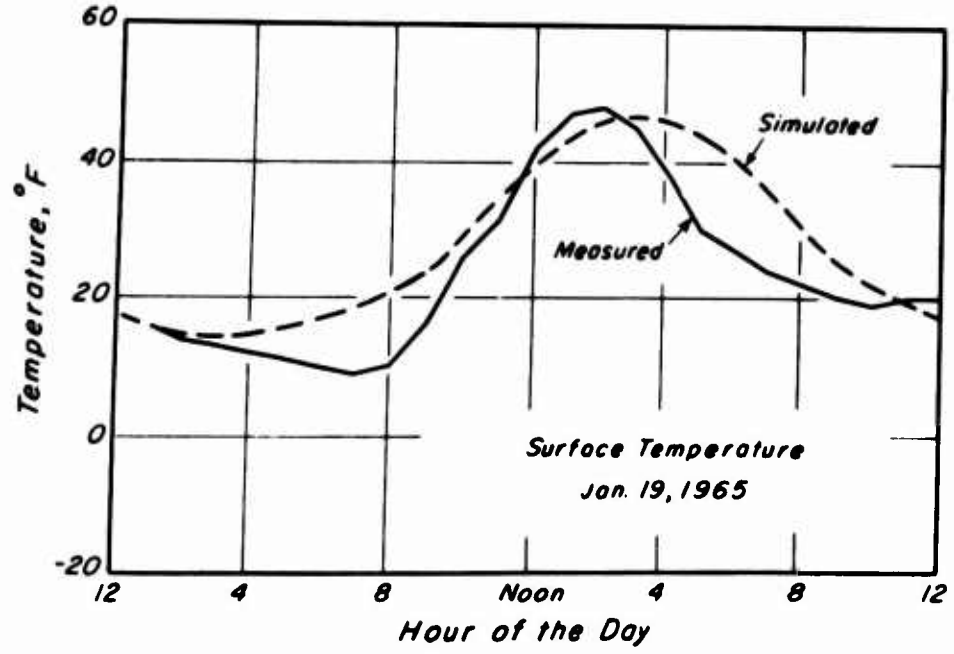

a.

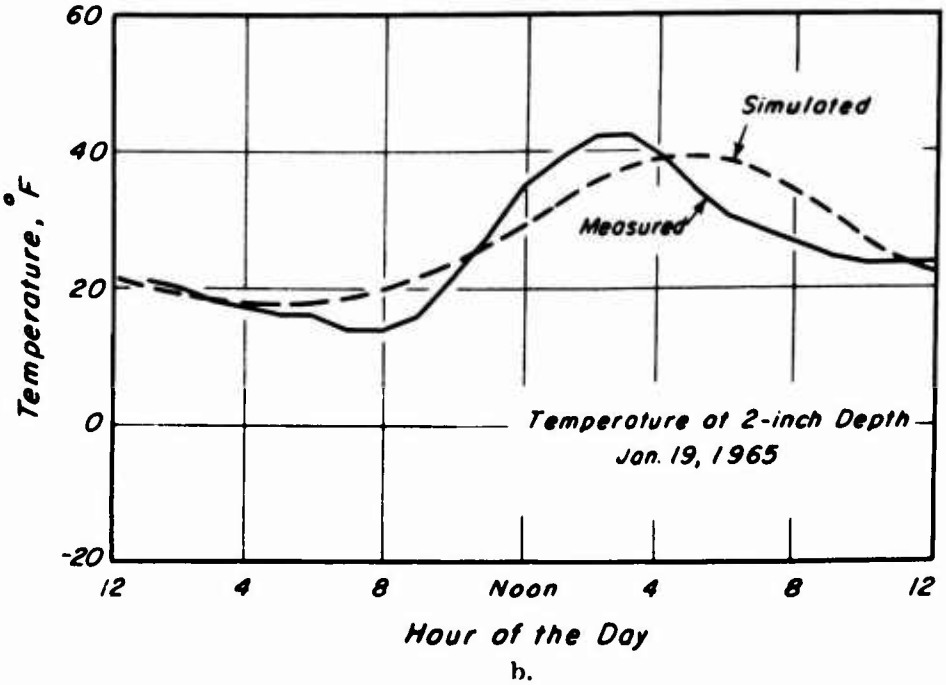

b.

Fig. A4 Comparison of computed and measured daily temperature variation, 12 in. asphalt concrete layer, College Park, Maryland (After Kasianchuk, 1968)

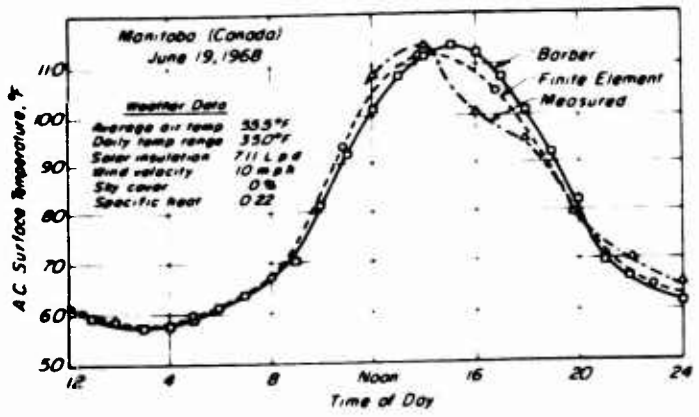

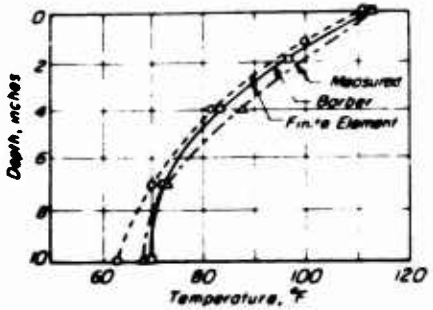

Fig. A5 Comparisons of recorded and predicted temperatures in a 10-in. asphalt concrete layer

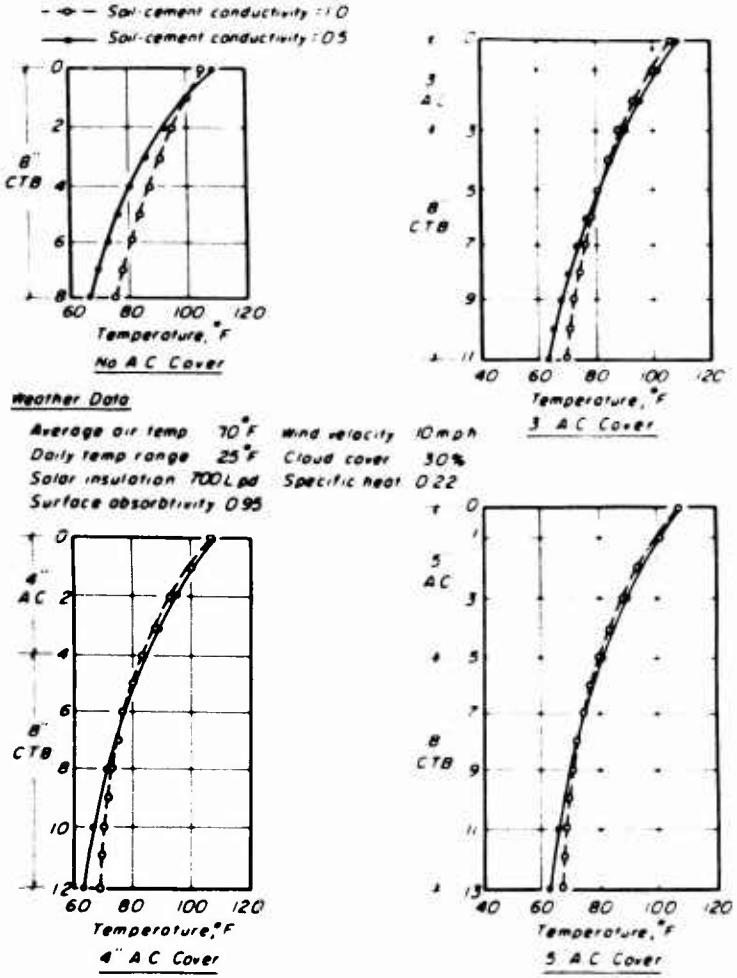

Fig. A6 Influence of soil-cement conductivity on pavement temperature

APPENDIX B: SHRINKAGE CRACKING AND EDGE LOADING EFFECTS

1. Shrinkage is an inherent property of cement-treated soils, and cracking is a characteristic of cement-treated bases (George and Davidson, 1963; Nielsen, 1968; Zube et al., 1969; Norling, 1973; and Otté, 1973). The analysis of the shrinkage of a cement-treated base is difficult. Solutions for the developed shrinkage stresses are given in the literature (George, 1968, 1969, 1971; Pretorius, 1970; Pretorius and Monismith, 1971; and Sanan and George, 1972). Although the theoretical solutions are important in understanding the shrinkage and cracking phenomena, the effects of shrinkage cracks on the stresses and strains in the pavement system are of more importance for design.

2. The presence of shrinkage cracks may have four effects;

a. Transverse cracks will give rise to edge loading, which may be more critical than interior loadings.

b. Water may infiltrate cracks, thereby weakening the subgrade.

c. Residual shrinkage stresses may exist.

d. The spacing of the shrinkage cracks will in part determine the magnitude of the warping stresses developed due to temperature differentials across the cement-treated layer.

Of these four consequences, only the edge loading effects and the crack spacing are important as will be demonstrated below.

Crack Spacing

3. The magnitude of warping stresses due to temperature differential across the cement-treated base is in part determined by the lateral

dimensions of the slab and hence the crack spacing. Some crack spacings reported in the literature are given in Table B1.

TABLE B1 TYPICAL CRACK SPACING

Type of Stabilized Soil	Crack Spacing ft	Reference
Cement-treated sand	20	Zube et al., 1969
By states, type of soil unspecified		HRB, 1961
Georgia	0.5 - 14	
Idaho	15 - 400	
Iowa	25	
Maine	50 - 80	
Maryland	8 - 10	
Montana	10 - 15	
Cement-treated crusher-run bases	10 - 20	Otté, 1973
Cement-treated sand	10 - 20	HRB, 1961
Cement-treated clay	2 - 10	
Lean concrete base	8 - 20 10 (mean)	Lister, 1972

4. Based on these data, a crack spacing of 20 ft has been assumed to be representative for cement-treated granular material and 10 ft for cement-treated fine-grained soils.

Edge Loading Effects

5. Pretorius (1970) and Pretorius and Monismith (1972) investigated the effects of edge loading on both fatigue crack formation and propagation for a three-layered pavement system. The pavement system, composed of three inches of asphalt concrete and eight inches of a stiff soil-cement base resting on a clay subgrade, was subjected to an 18,000 lb axle load (Fig. B1). For the interior loading condition, the tensile stress at the bottom of the soil-cement base was calculated using the Chevron layered elastic program which permits determination of stresses and deformations in up to five layers. Manual summation of the stresses induced by each tire is required when this program is used. Figs. B2 and B3 show the resulting stresses.

6. Once shrinkage cracks form, a different set of circumstances exists. Increased stresses may be expected because of the loss of continuity and the possibility that water infiltration may weaken the subgrade (Williams and Dehlen, 1969). Because the shrinkage cracks form early in the life of the pavement, the cracked condition is the one of importance for design purposes. For the pavement system used by Pretorius (1970), uniform shrinkage would cause cracking in one day for an ambient relative humidity of 65 percent, and in three days for an ambient relative humidity of 90 percent. Sanan and George (1972) also predicted early cracking using a viscoelastic model to characterize the shrinkage of soil-cement. Their analytical results showed that the maximum shrinkage stresses occurred at an age between 40 and 100 hours, which also was confirmed by their scale model experiments.

7. To determine the effects of edge loading, Pretorius used the prismatic space finite-element method (Wilson, 1968). The approach is essentially two-dimensional, with the third dimension introduced into the idealization by expressing the load as Fourier series in this direction. A finite element discretization of the structure is shown in Fig. B4. The structure is solved for every Fourier term necessary to adequately represent the load. The x- and y-displacements vary cosinusoidally and stresses sinusoidally in the z-direction which enables a complete stress solution at any desired z- position.

8. The finite element representation of the pavement system that was analyzed for edge loading is shown in Fig. B5. The transverse shrinkage cracks were placed at 20-ft intervals (Table B1). The maximum stress was found to be parallel to the edge at position B (Fig. B6), which is midway between the dual tires. For the 1600 psi subgrade (subgrade condition (b) in Fig. B7), the maximum tensile stress at the bottom of the base is 130 psi (Fig. B8), which is approximately 60 percent greater than that for the corresponding axisymmetric case. For a stronger subgrade (10,000 psi, condition (d), in Fig. B7), the maximum interior tensile stress is 75 psi and the maximum tensile stress for edge loading is 110 psi (Fig. B8), an increase of approximately 45 percent.

9. In a field study, Fossberg (1970) reported that measured horizontal tensile strains parallel to a crack were 40 percent to 50 percent greater than strains for interior loading.

10. Simiarly, analysis of edge loading on two-layered systems (base over subgrade) using Westergaard's representation and influence charts developed by Pickett and Ray (1951) showed that the edge stresses from an 18,000 lb axle load ranged from 40 percent to 90 percent larger than interior stresses (Fig. B9). It should be noted that the ratio of edge to interior stresses is dependent upon the radius of relative stiffness. For cement-treated bases, the radius of relative stiffness will usually be less than forty, which implies that the edge stresses will be at most 70 percent larger than the interior stresses,(Fig. B9).

11. Based on these analyses the decision was made to increase the stresses determined for interior loading conditions (uncracked slabs) by 50 percent to account for edge-loading effects.

Water Infiltration into Snrinkage Cracks

12. To investigate the effects of water infiltration through cracks, Pretorius (1970) considered four conditions with varying degrees of subgrade softening (Fig. B7). It was found that the stress contours and distributions differ very little for the various subgrade conditions (Fig. B8). This result is partially explained by considering the displacement profiles presented in Fig. B10. While the deflections decrease with improved subgrade condition, there is very little difference in the radii of curvature. This is due to the very high ratio of the cement-treated base modulus to subgrade modulus (approximately 280). The significance of this finding is that although water infiltration will cause increased deflection and possibly pumping, the stress in the cement-treated base will be relatively unaffected.

Shrinkage Stresses

13. Although shrinkage cracking is inevitable and is accepted in the design procedure, it is important to determine the effects of the residual shrinkage stresses on the performance of the cement treated base. To calculate the shrinkage stresses for the pavement system represented in Fig. B11, Pretorius (1970) and Pretorius and Monismith (1971) used a constant strain axisymmetric finite element program with the following assumptions.

a. Linear viscoelasticity is applicable to failure

b. Continuity exists between all layers.

14. Two solutions are presented in Fig. B12, one for uniform shrinkage, which is the lower bound solution, and the other for differential shrinkage, which is the upper bound solution. From Fig. B12 it can be seen that the assumed real stress is low, especially after long times (30 days) and hence will not have much influence on the response of the system. In fact, the shrinkage stresses may be beneficial since, at the bottom of the base, the differential shrinkage stresses are compressive while the traffic stresses are tensile. In the design procedure presented in the report, the shrinkage stresses were considered negligible and are not included in the analysis of the pavement system. This appears to be a conservative assumption.

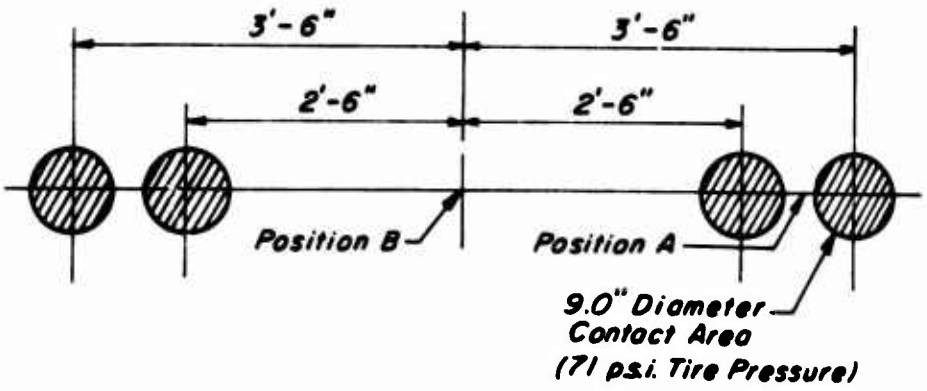

Fig. B1 Assumed wheel spacing for 18 kip axle load

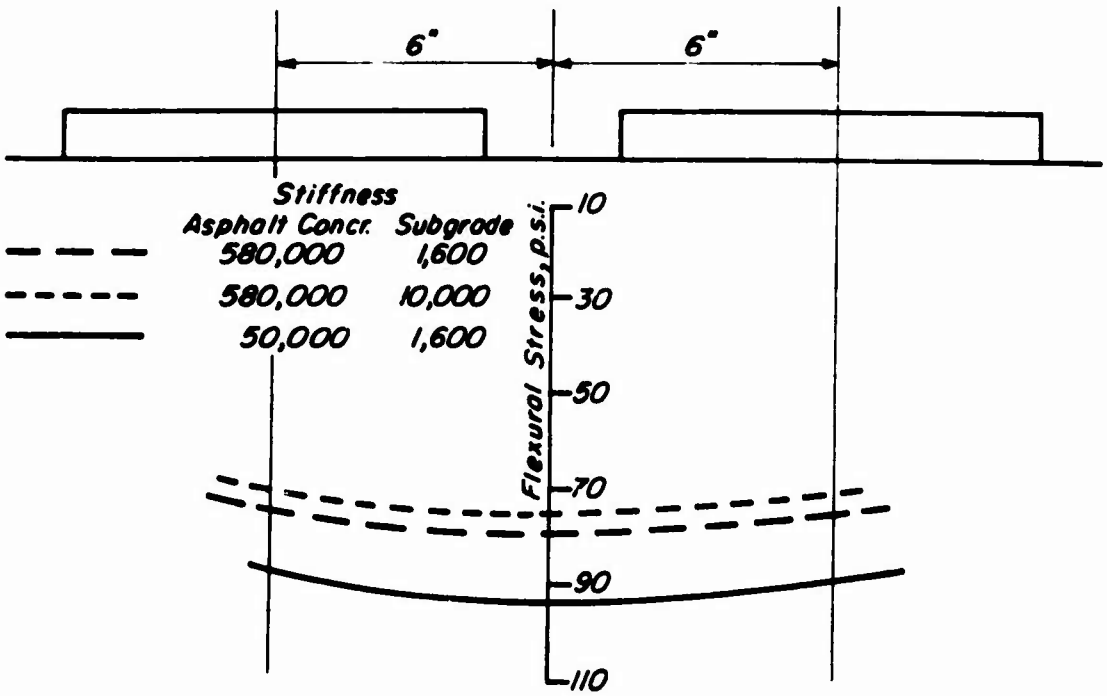

Fig. B2 Maximum tensile stress at bottom of soil-cement base at position A

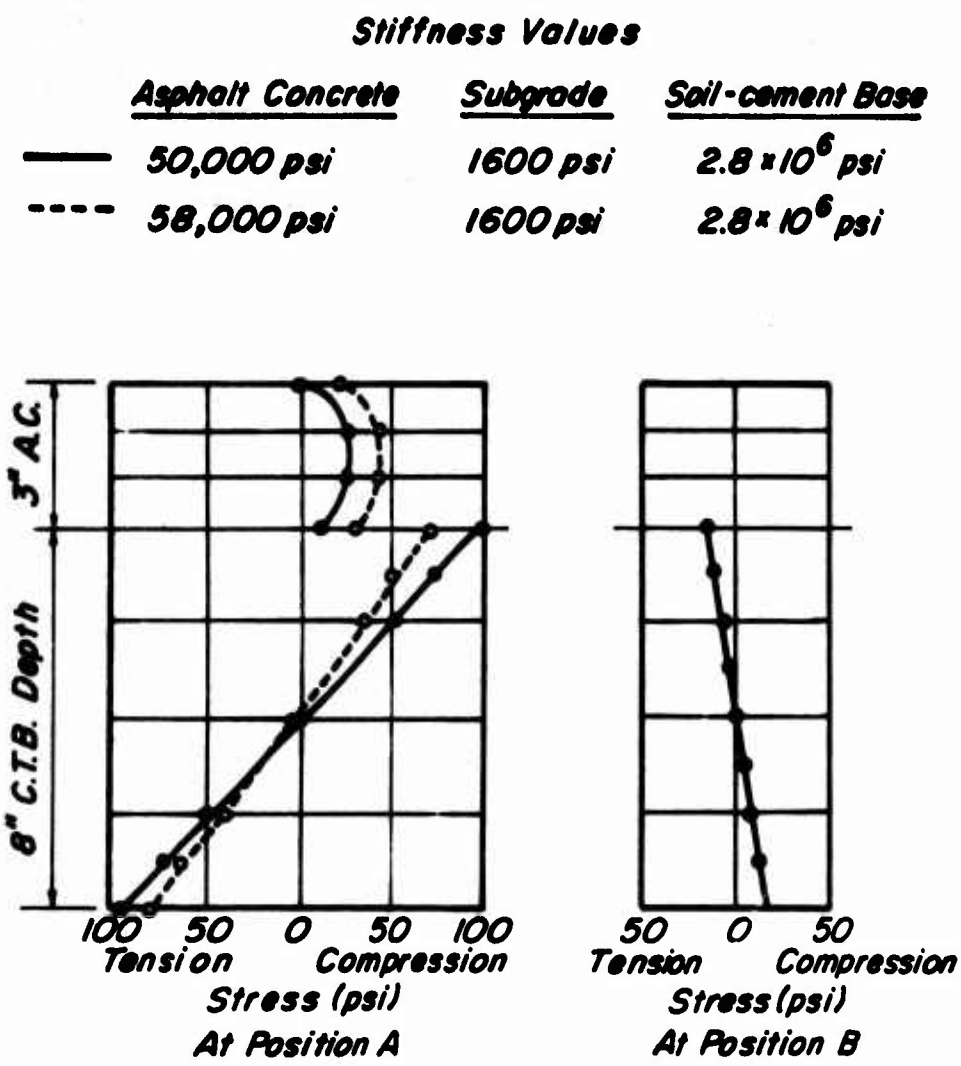

Fig. B3 Maximum stress distribution for an interior loading position

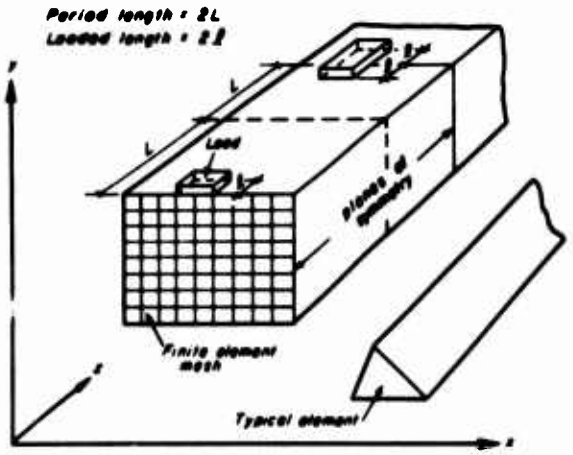

Fig. B4 Prismatic space finite element representation

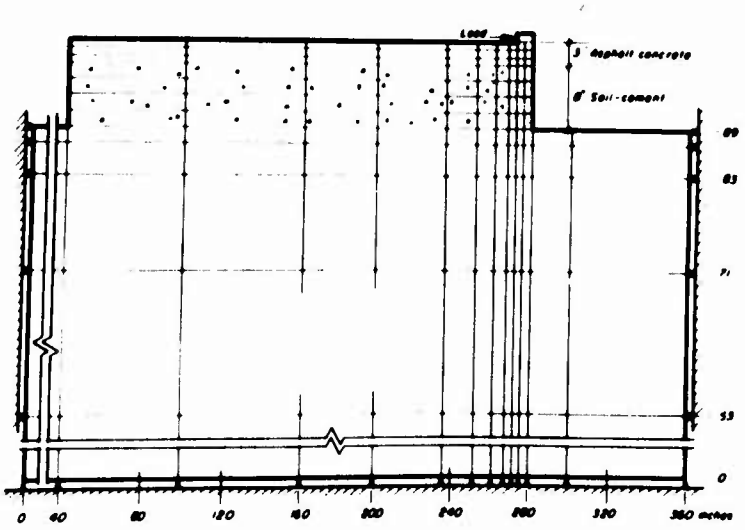

Fig. B5 Finite element mesh for load at an edge

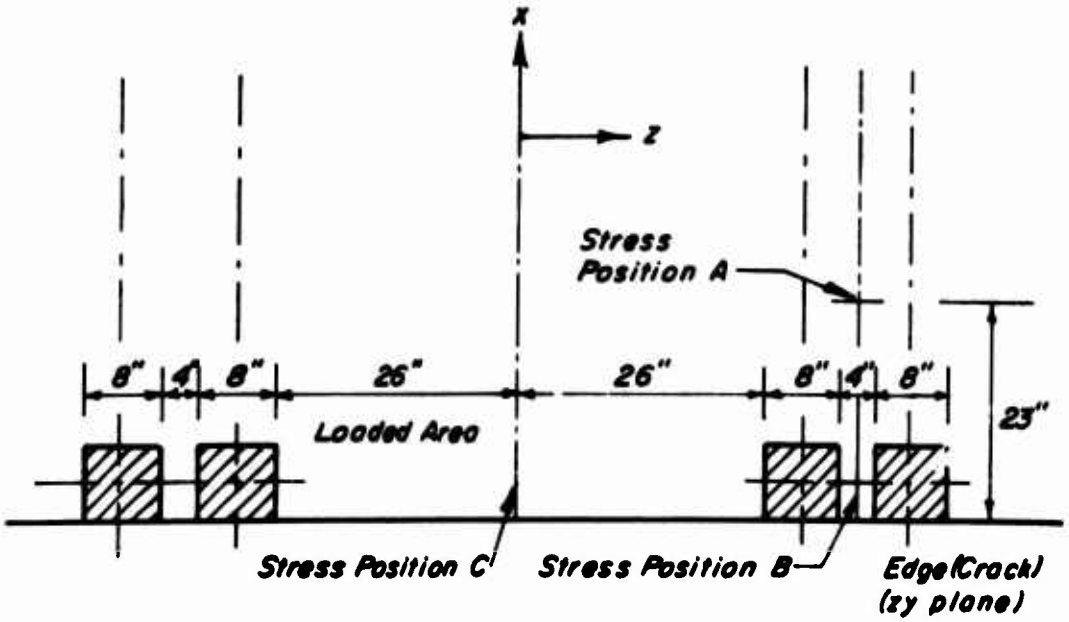

Fig. B6 Loading position for edge effect considerations

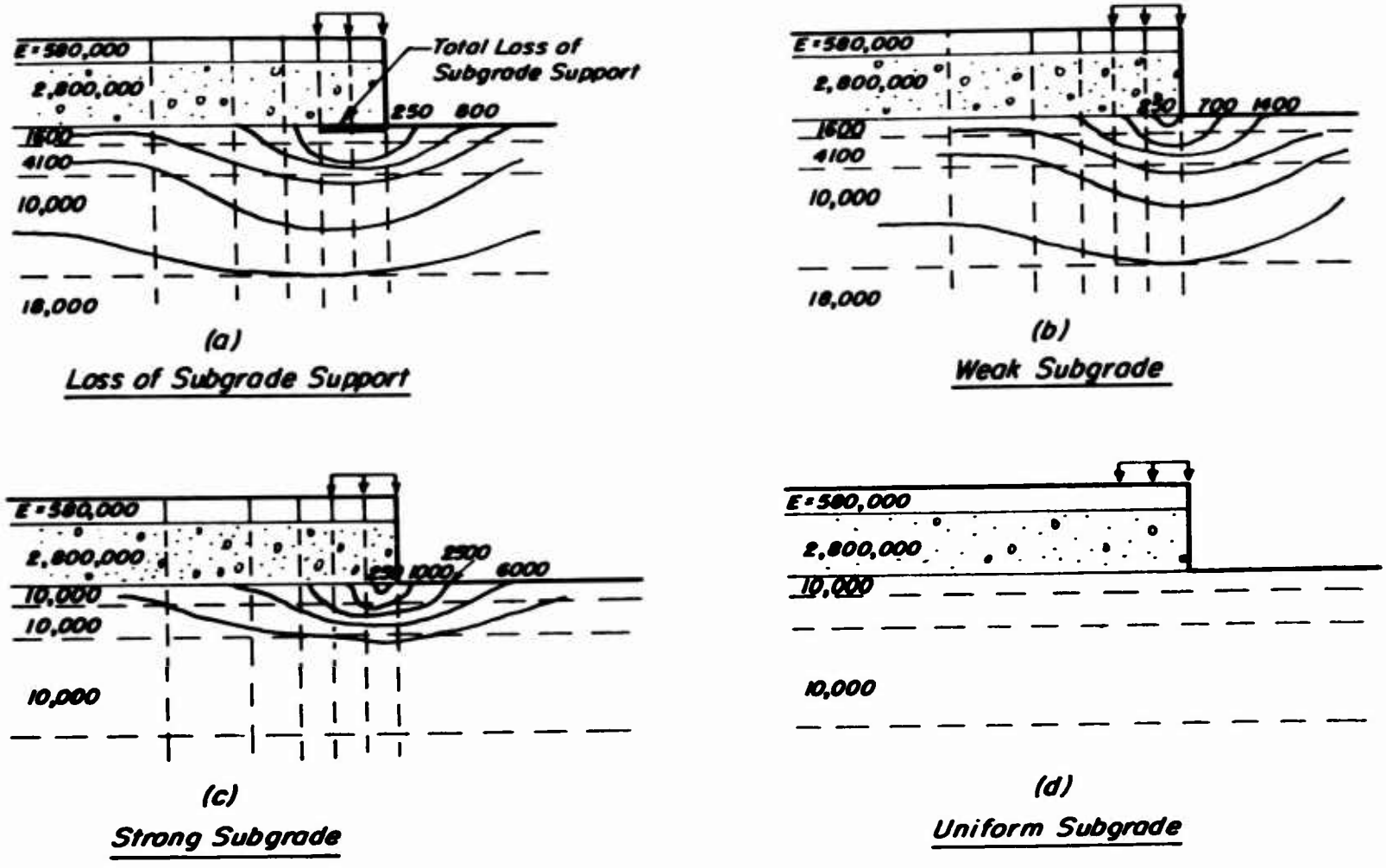

Fig. B7 Subgrade support conditions

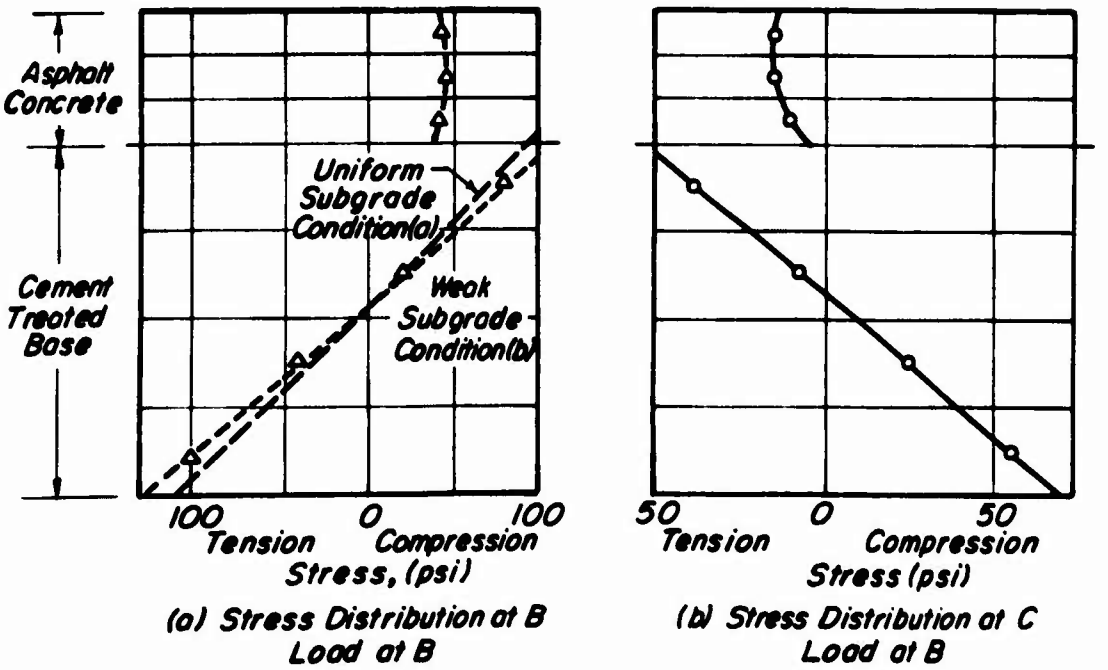

Fig. B8 Variation of tensile stress with depth

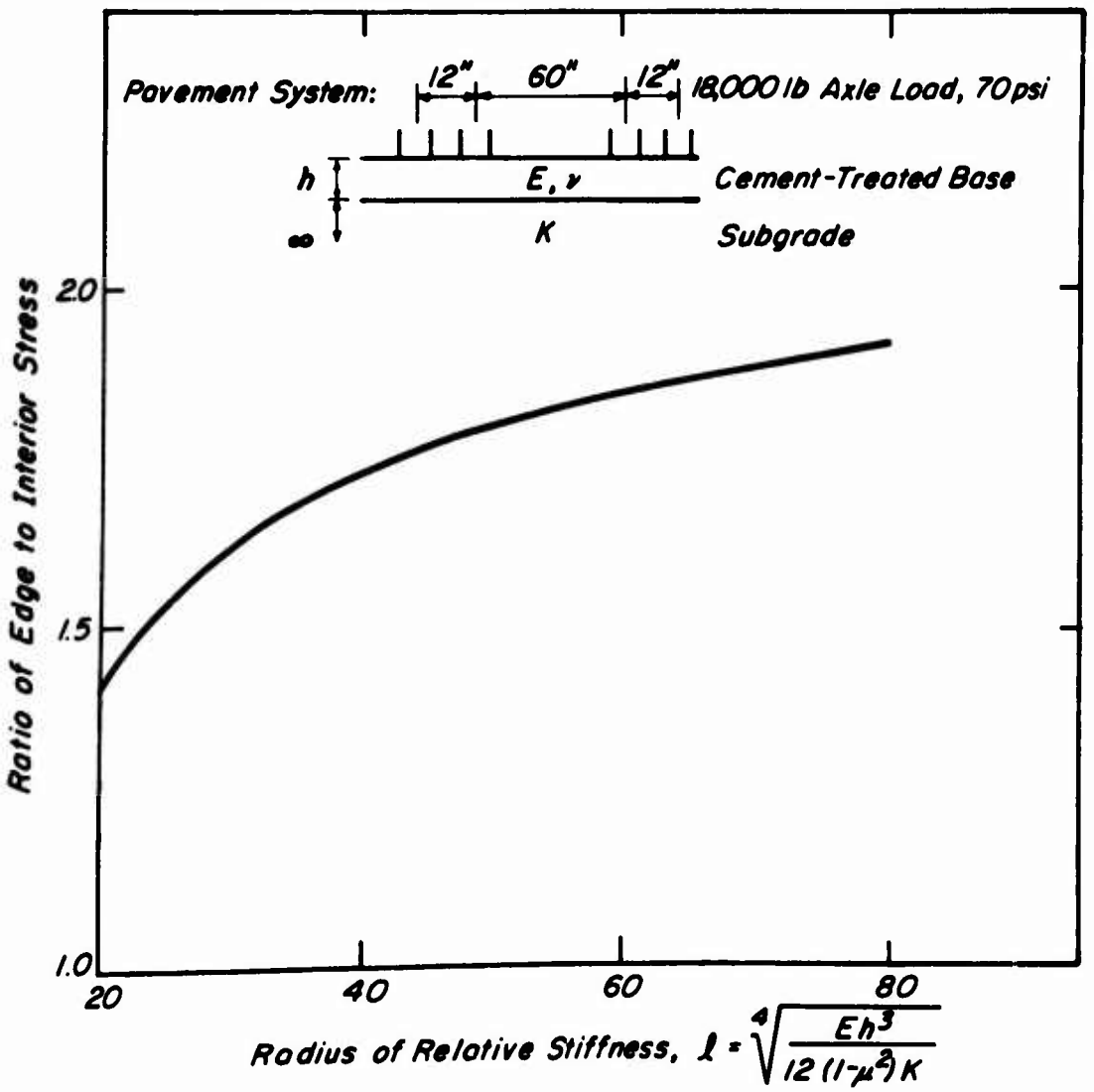

Fig. B9 Comparison of edge and interior stresses for a two-layered system using Westergaard's theory

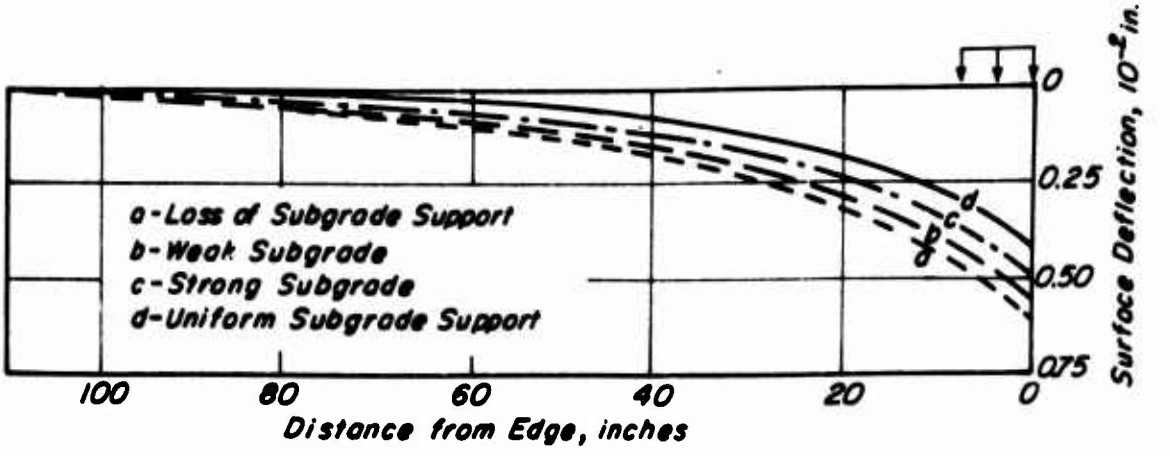

(b)

Surface Deflection Profile for 4500 lb Wheel Load at Position BB

Fig. B10 Surface deflection profile for 4500 lb wheel load at position BB

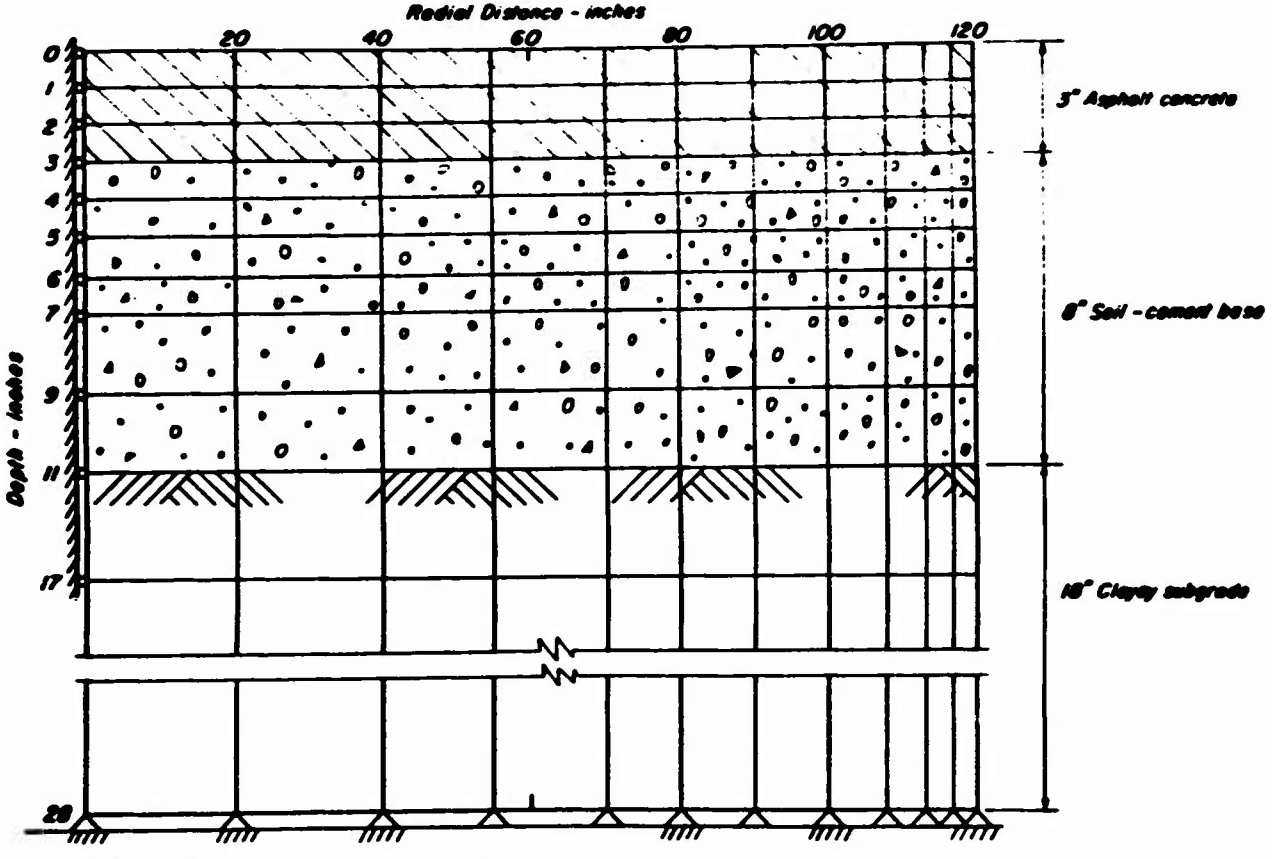

(Note: Vertical scale is four times the horizontal scale)

Fig. B11 Finite element mesh for shrinkage stress calculation

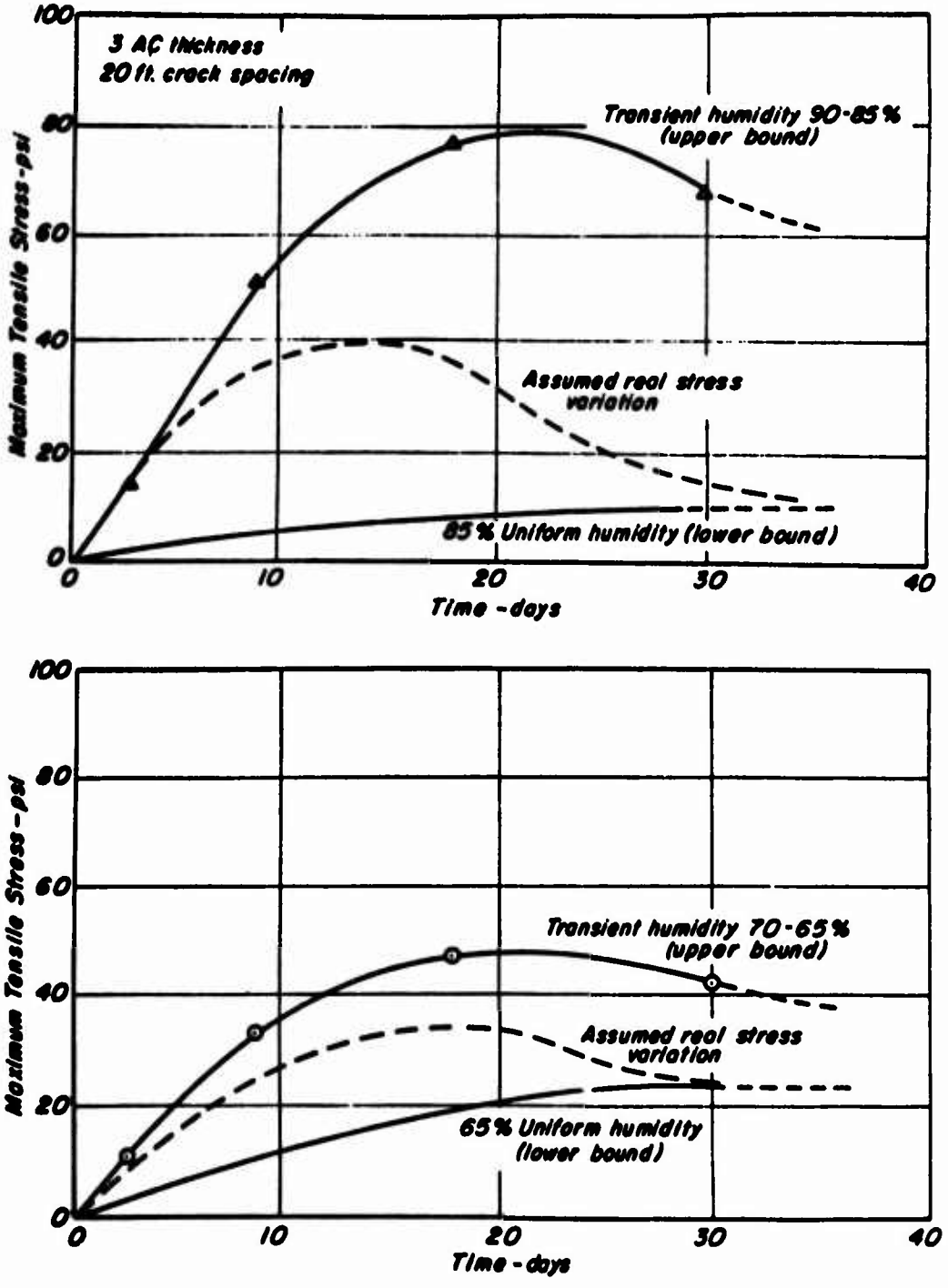

Fig. B12 Time variation of shrinkage stresses in the cement-treated base

APPENDIX C: VALIDITY OF APPLICATION OF ELASTIC THEORY

1. In the design procedure presented in this report, the pavement structure is represented as a layered elastic structure. To establish the validity of this assumption, results of two studies of prototype pavements are summarized in this section. These studies indicate that a pavement structure can be represented as a multilayer elastic system or by means of a finite element idealization (Wang, 1968; Wang et al., 1970, Wang and Mitchell, 1971; and Fossberg, 1970).

2. In the first study (Wang, 1968 and Wang et al., 1970, Wang and Mitchell, 1971), two test pavements, each 20 by 20 ft in plan and 8 in. in thickness, were constructed over a natural clay subgrade using a silty soil stabilized with 3 percent cement (pavement 1) and 6 percent cement (pavement 2). Each test pavement contained nine test locations to permit plate load testing for a range of curing times. Stress and strain gages for measurement of vertical compressive stress on the top of the subgrade and radial strain at the bottom of the stabilized layer were installed during construction in both pavements.

3. Repeated load plate tests were conducted on the 8-in. thick cement-treated base after various curing periods using a range of plate sizes and pressures. Measurements included:

a. surface deflection,

b. subgrade deflection,

c. radial strain at the bottom of the stabilized layer, and

d. vertical compressive stress at the top of the subgrade.

4. Repeated load tests were conducted in the laboratory on both triaxial compression and beam specimens using both undisturbed pavement and subgrade samples taken from the test pavements and laboratory compacted samples. The field behavior was then predicted using the measured properties with both layered elastic theory and the finite element method.

5. Fig. C1 compares predicted and measured values of resilient surface deflection for the pavement treated with 3 percent cement and cured for 2 days. Best agreement in this case was obtained with the values predicted by multilayer elastic theory. Resilient deformations of the same pavement after curing periods of 23 and 100 days are shown in Fig. C2. Similar results for pavement 2 are shown in Fig. C3 for curing period of 17 and 93 days. In the case of the extended curing periods, it is seen that the finite element procedure gave predictions in excellent agreement with the measured values.

6. Predicted and measured values of radial strain at the base of the stabilized layer for pavement 1 are compared in Fig. C4.with reasonable agreement indicated. Fig. C5 illustrates strain comparisons for different plate sizes for pavement 2. While not shown herein, comparisons were also made for the vertical compressive stress at the top of the subgrade, and agreement between predicted and measured values was satisfactory.

7. In the second study (Fossberg, 1970) two soil-cement test sections each 8.5 in. thick and with asphalt concrete surface layers up

to 5 in. in thickness were constructed. Gages enabled measurements of stresses and strains at several points in both pavements and complete surface deflection data were obtained. Reasonable agreement between measured and predicted stresses and strains were also obtained in this study using both multilayer elastic theory and the finite element procedure. For example, comparison between predicted and measured radial and tangential strains in the cement-treated base with a range in thicknesses of asphalt concrete are shown in Figs. C6 - C9.

8. Because of greater facility in analysis, multilayer elastic theory was selected in preference to the finite element procedure for incorporation into the design procedure presented in this report.

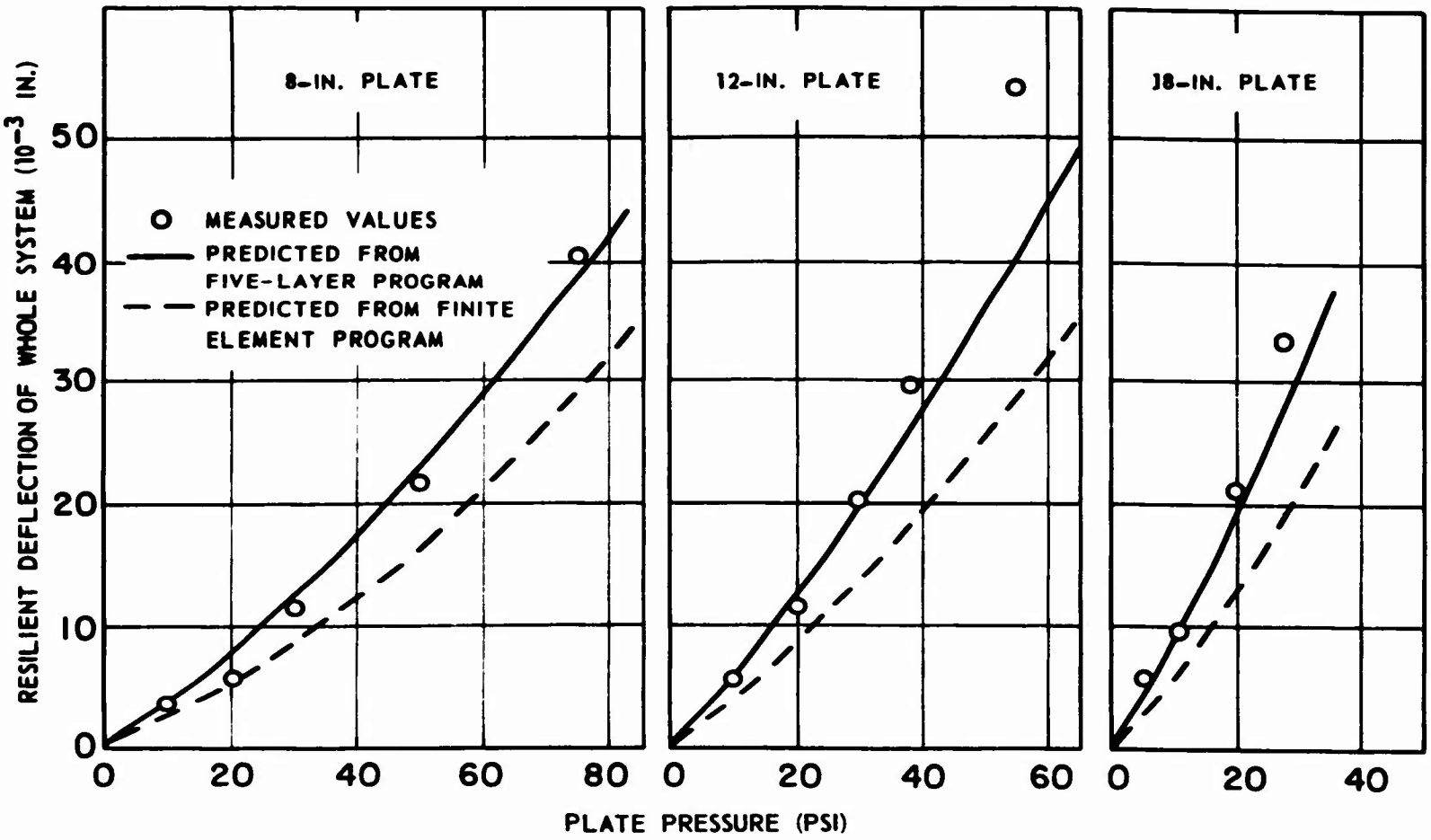

Fig. C1 Comparison of predicted and measured resilient surface deflection for pavement 1 after 2-day curing

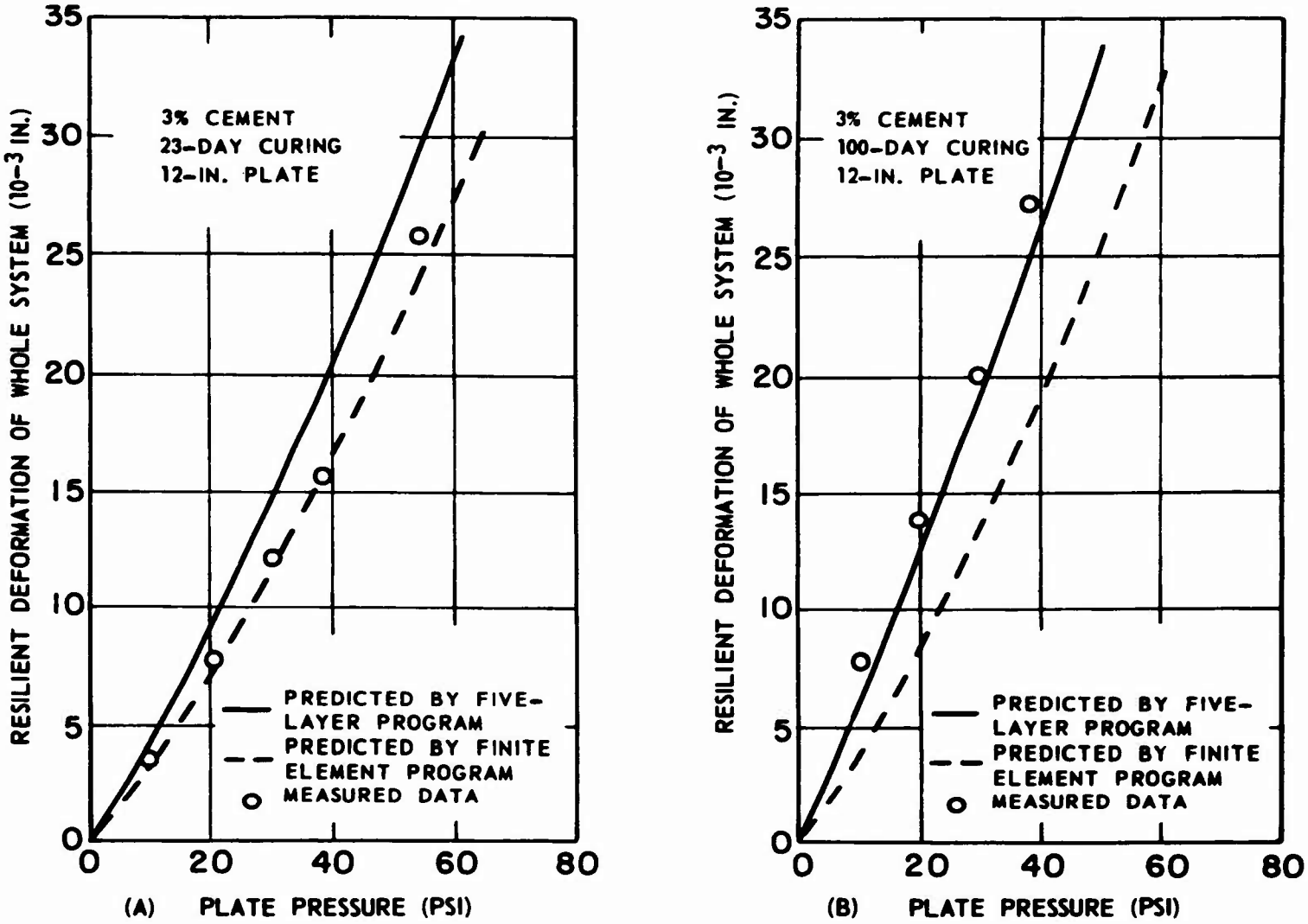

Fig. C2 Comparison of predicted and measured resilient surface deflection for pavement 1 after 23- and 100-day curing periods

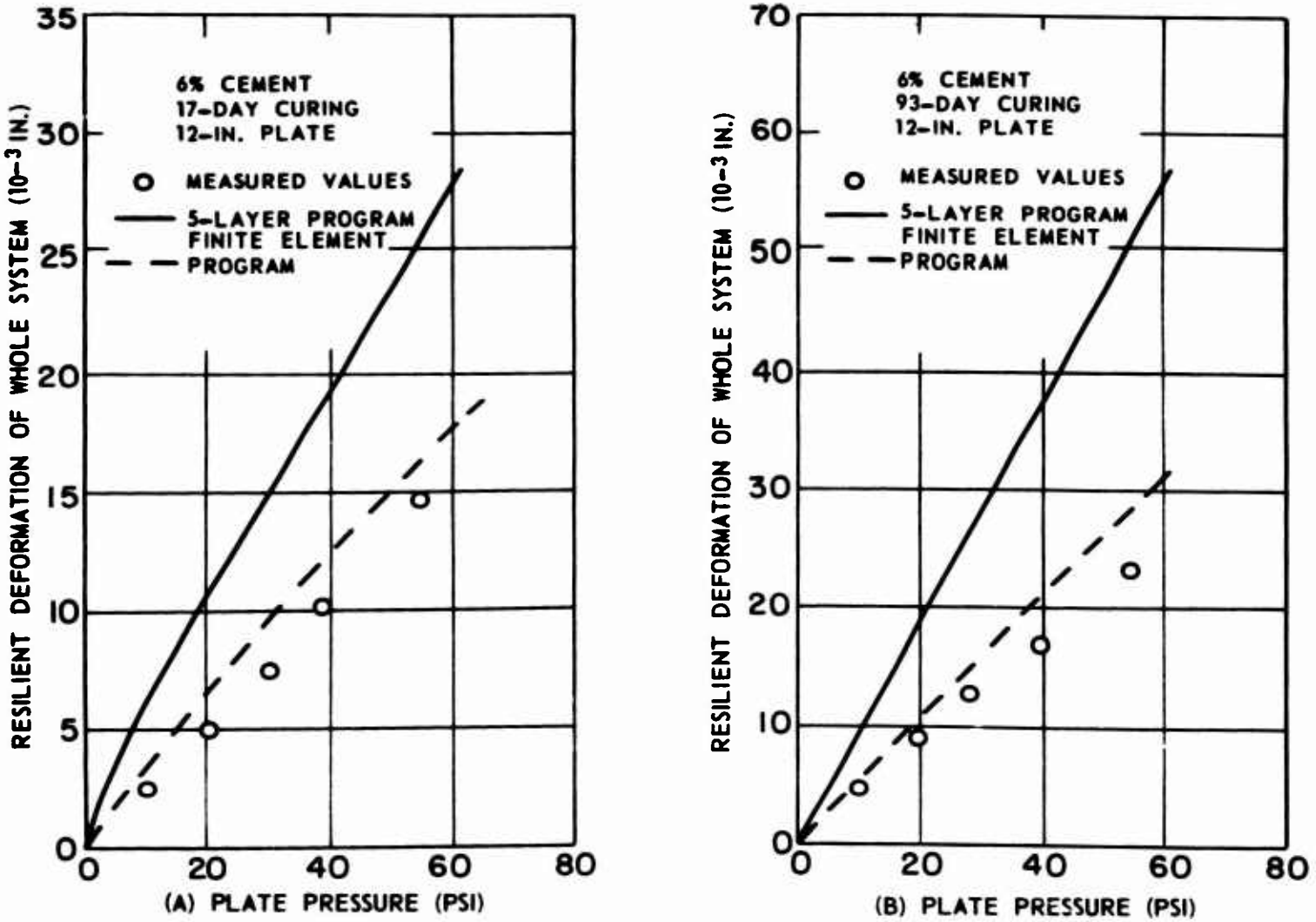

Fig. C3 Comparison of predicted and measured resilient surface deflections for pavement 2 after 17- and 93-day curing periods

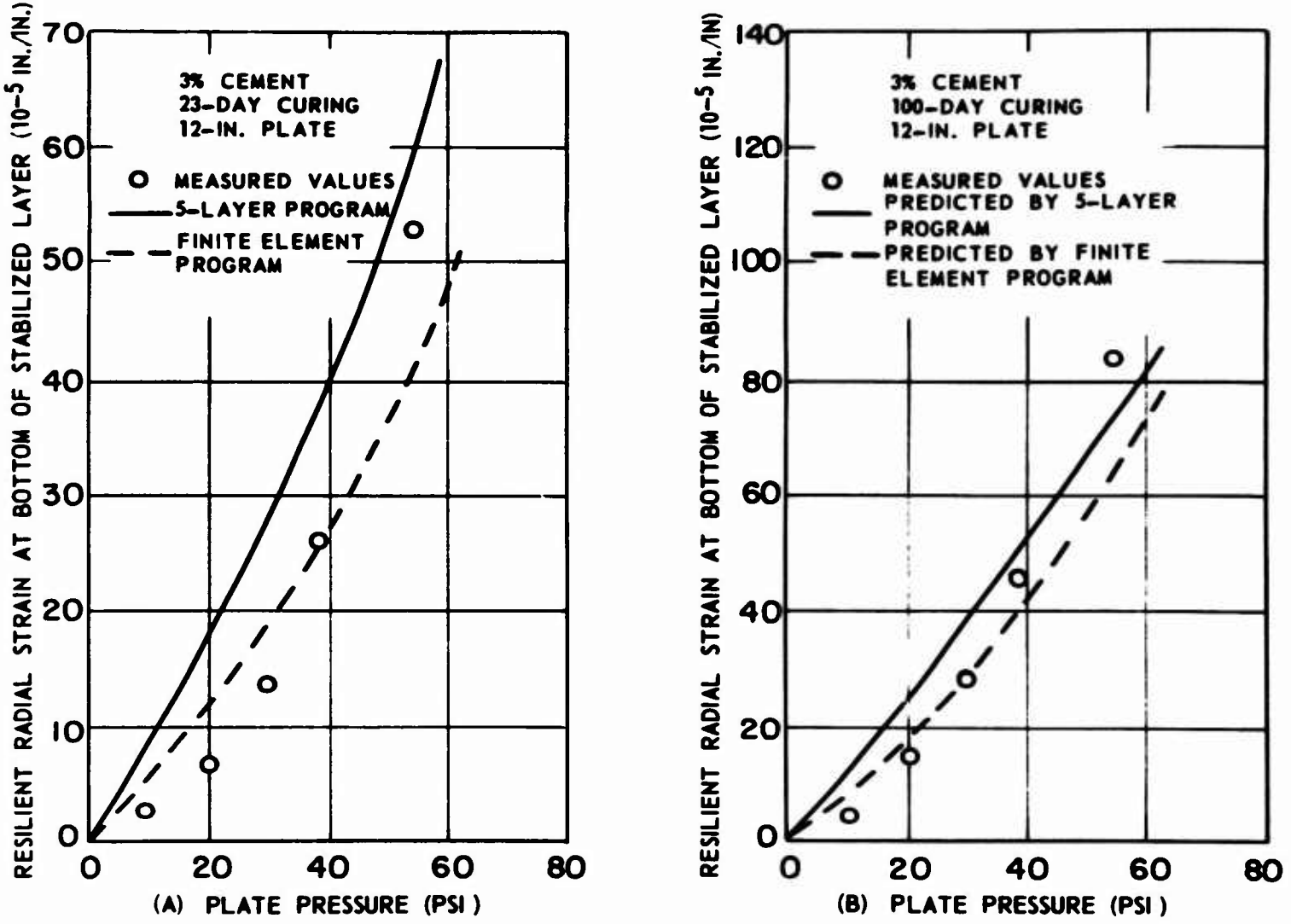

Fig. C4 Comparison of predicted and measured resilient radial strain at bottom of stabilized layer in pavement 1

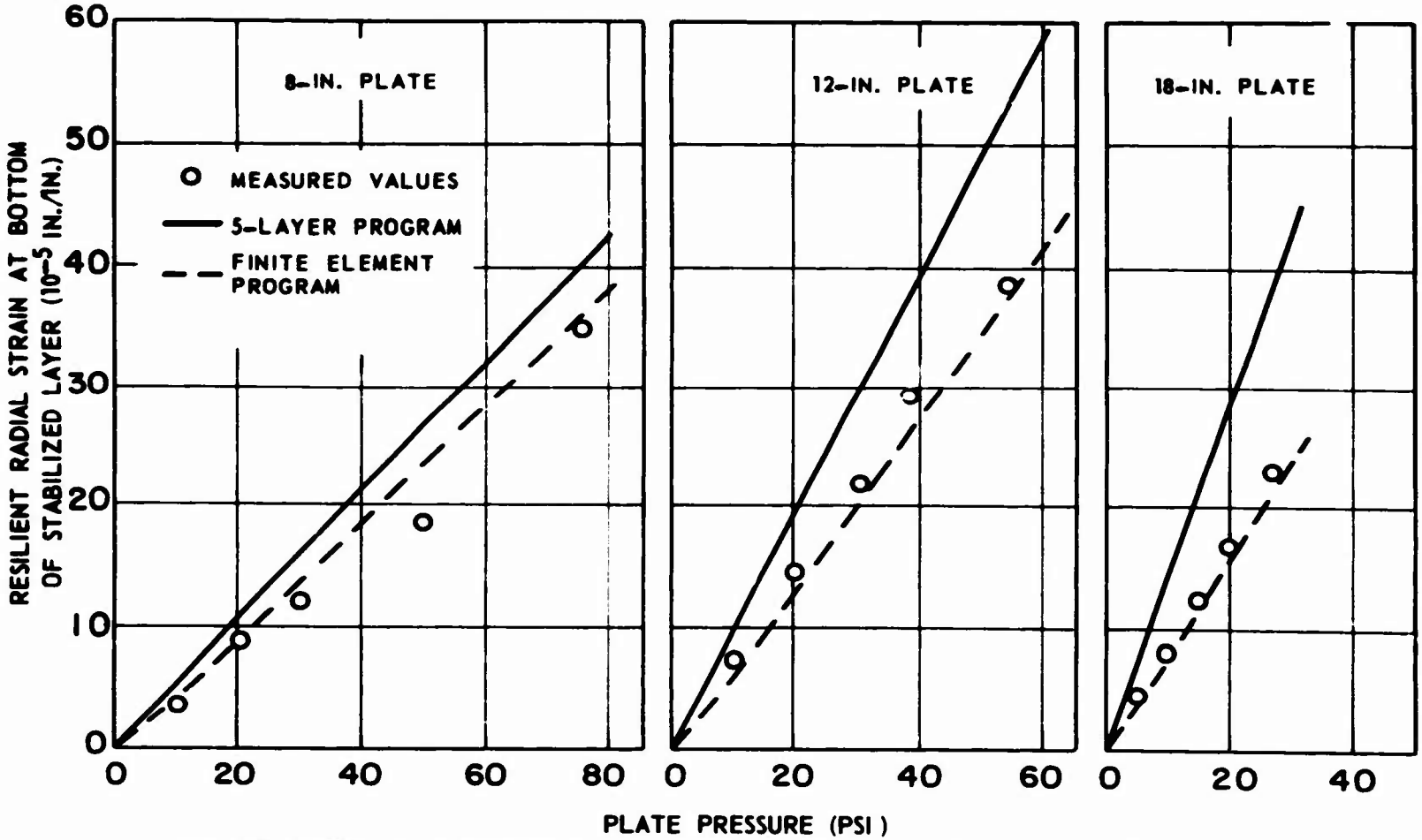

Fig. C5 Comparison of predicted and measured resilient radial strain at bottom of stabilized layer in pavement 2 after 4-day curing period

5-LAYER SYSTEM, LINEARLY ELASTIC MATERIALS

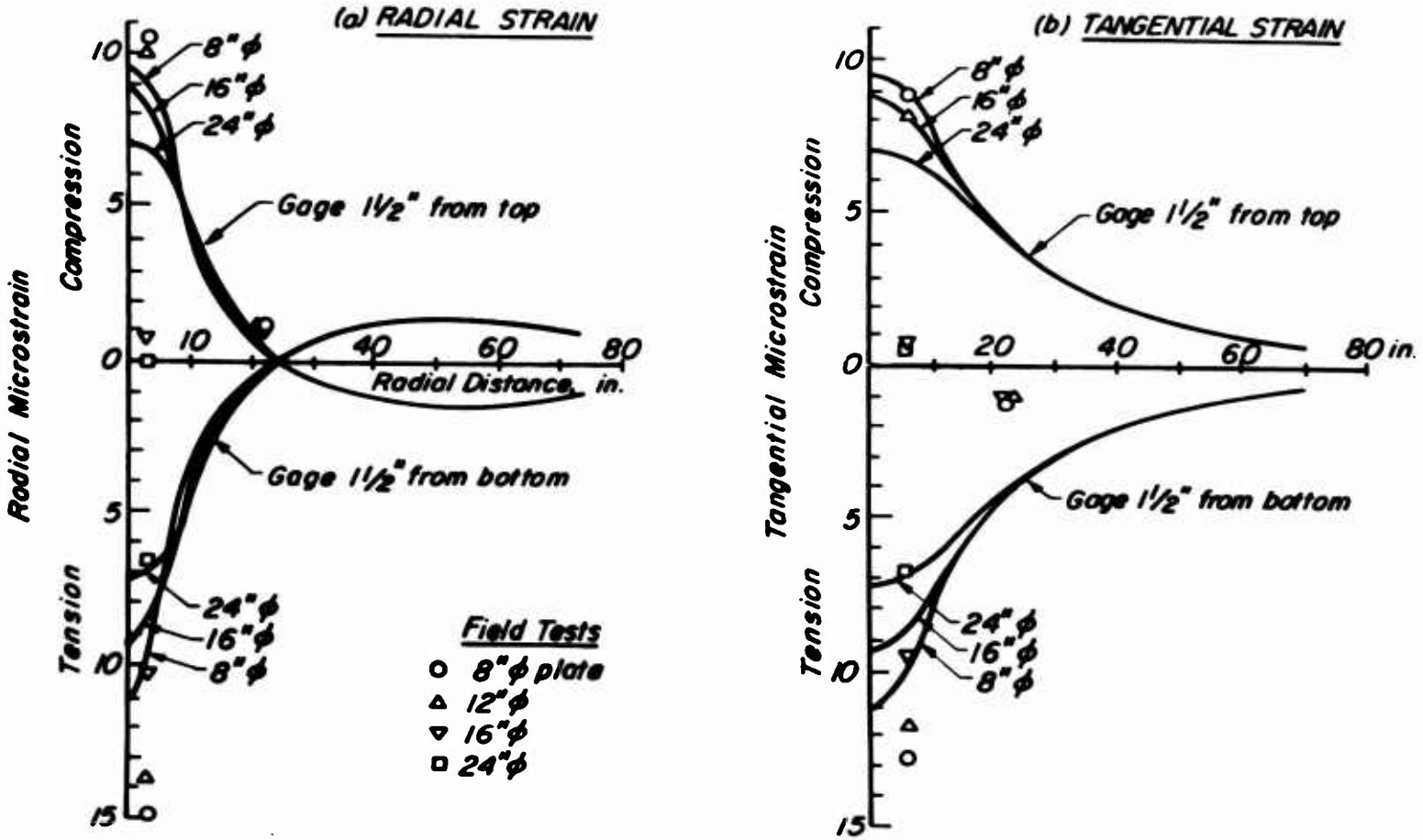

Fig. C6 Radial and tangential strains 1-1/2 in. from top and 1-1/2 in. from bottom of soil-cement base, at various distances from the center of the load (3,400 lb.). Comparison based on 5-layer system, linearly elastic materials

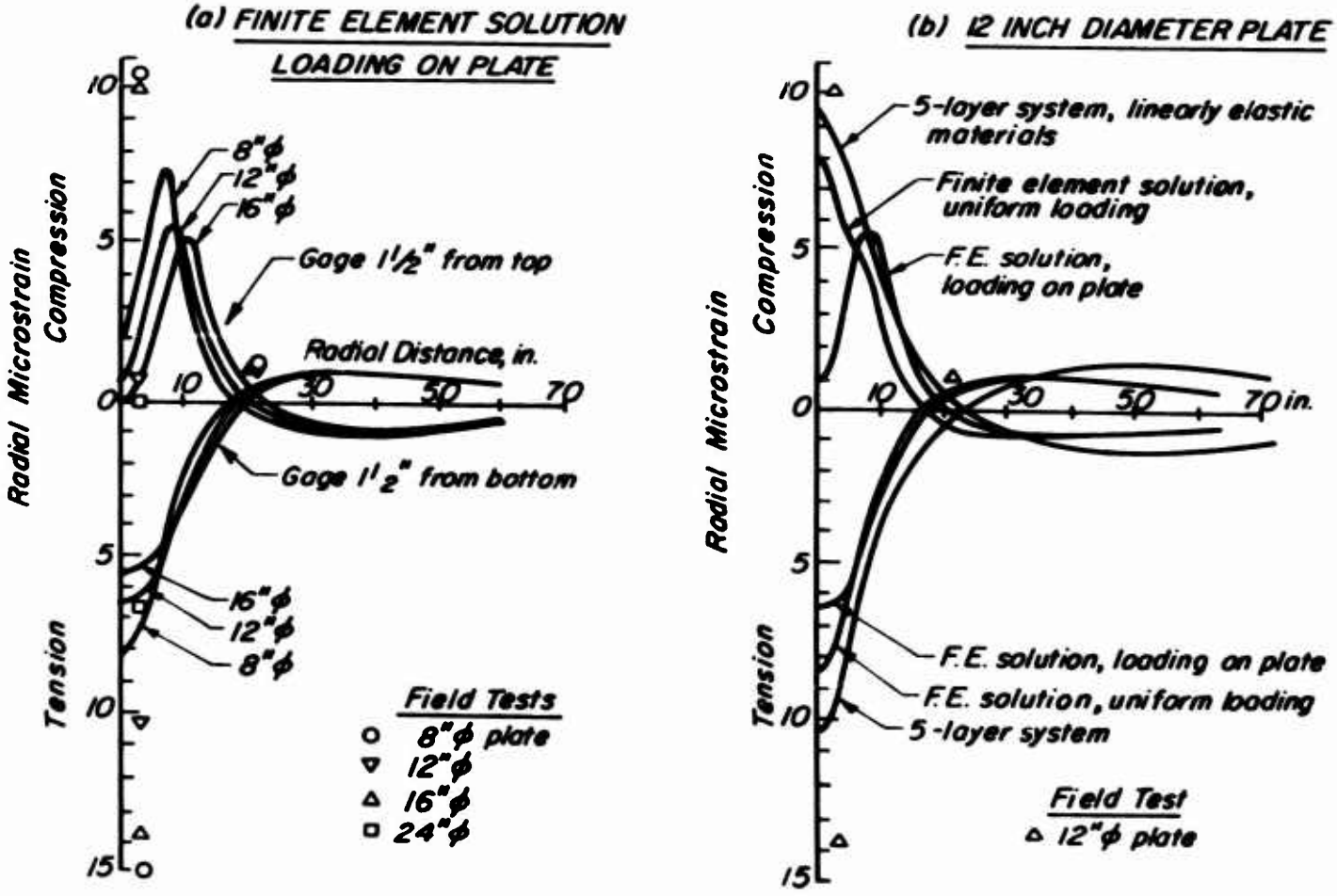

Fig. C7 Radial strains 1-1/2 in. from top and 1-1/2 in. from bottom of soil-cement base at various distances from the center of the load (3,400 lb). Comparisons based on finite element solution

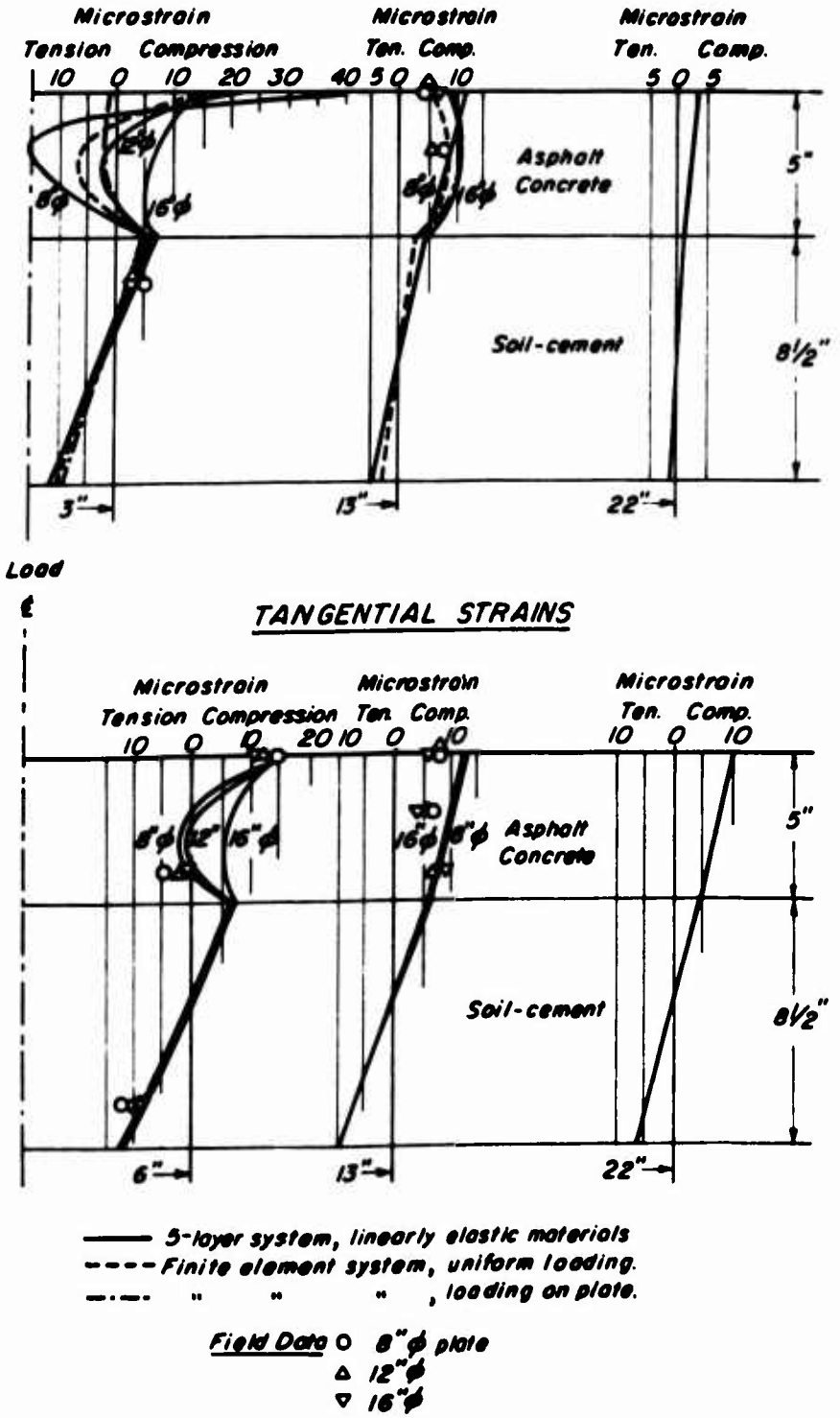

Fig. C8 Measured and predicted radial and tangential strains in 5 in. asphalt concrete surfacing and 8-1/2 in. soil-cement base at various distances from the center of 4,000 lb plate loads

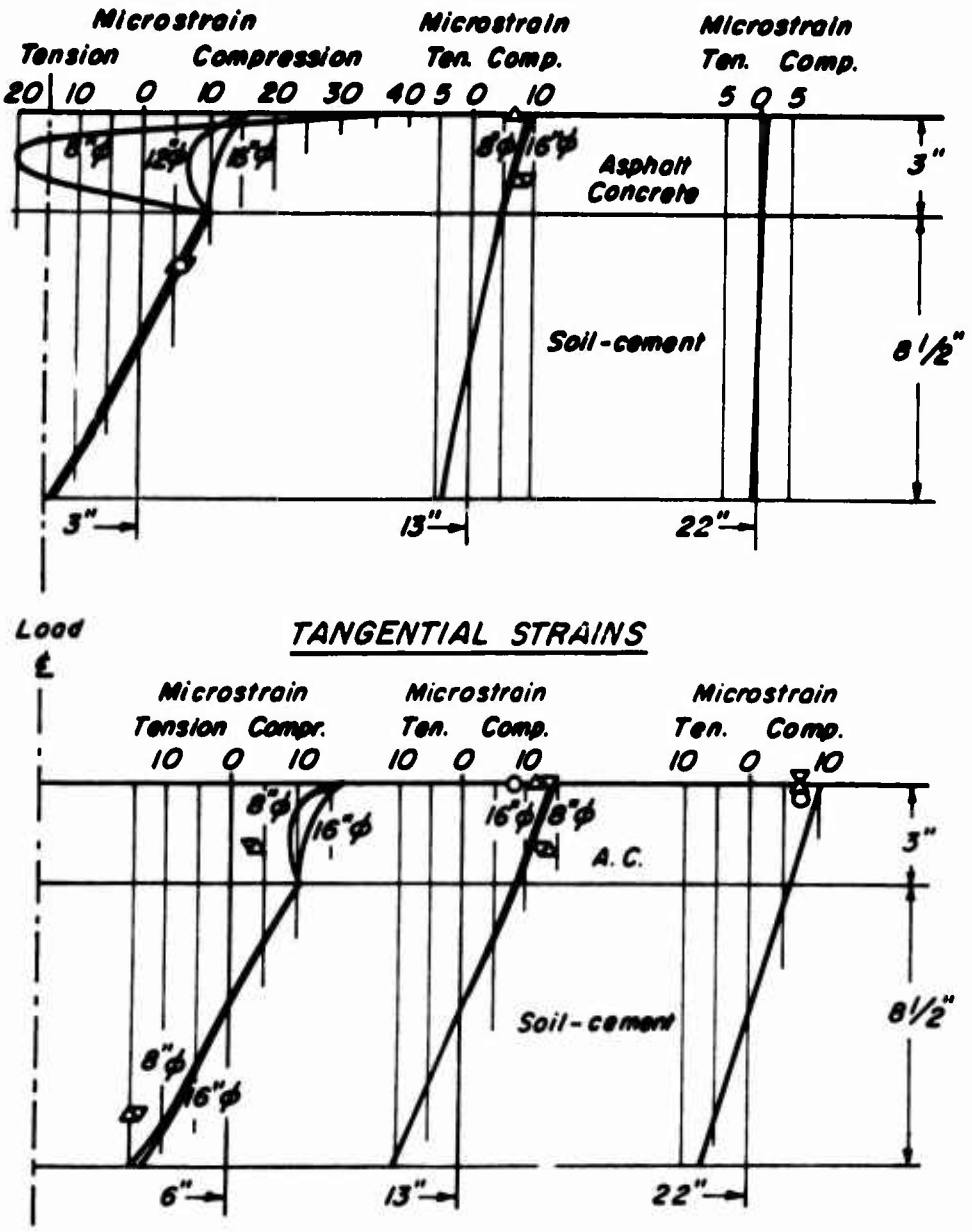

16"ϕ — Prediction by 5-layer system, linearly elastic materials (with indication of plate diameter)

Field Data ○ 8"ϕ plate
△ 12"ϕ
▽ 16"ϕ

Fig. C9 Measured and predicted radial and tangential strains in 3 in. asphalt concrete surfacing and 8-1/2 in. soil cement base at various distances from the center of 4,000 lb plate loads

APPENDIX D: THERMAL STRESSES

1. Cement-treated bases, like concrete slabs, are subjected to stresses caused by the effects of temperature and temperature gradients. There are two ways in which these stresses can be developed:

a. Overall change in length due to change in mean temperature

If the base is free to expand or contract, no thermal stresses will be developed; if, however, the base is restrained by the subgrade and/or by an overlying layer, stresses will develop which will be compressive when the base expands and tensile when the base contracts. Large values will be obtained in long uncracked slabs (Lister, 1972).

Subsequent to the development of shrinkage cracks, which occur shortly after construction, the stresses are probably small since little restraint is provided. For a 10 ft crack spacing, these stresses will be less than 10 psi even for the stiffest material (Lister, 1972) and can be,therefore, assumed negligible in the design procedure.

b. Differential changes due to temperature gradient through the base

A temperature gradient will cause the base to curl or warp; if the base is restrained by its own weight and possibly also by the presence of a surface layer, thermal stresses will be developed. The most critical case occurs when the top of the base is at a higher temperature than the bottom; under these circumstances resulting temperature stresses will be tensile at the bottom and therefore additive to traffic stresses.

2. Under some circumstances thermal stresses caused by temperature gradients across the base can be an appreciable proportion of the total stresses due to temperature and traffic stresses. This point is illustrated in Fig. D1 for an 8-in. cement-treated base covered by a four-inch asphalt surface layer (LIster, 1972). The temperature conditions are those of the early afternoon of a hot summer's day. From this figure it can be seen that for stiffer bases, thermal stress may be as much as one-third of the total stress.

3. A comparison between thermal and traffic stresses in a two-layered system (cement-treated base over a subgrade) is shown in Fig. D2. The pavement system was subjected to an 18,000 lb axle load on dual wheels and the principal horizontal tensile stress at the bottom of the cement-treated base was calculated. This stress for interior loading was then increased by 50 percent to account for edge loading. The edge thermal stresses were calculated for a linear temperature gradient of 3F deg/in. and a crack spacing of 20 ft, which should be approrpiate for a sand treated with cement. As can be seen from Fig. D2, the thermal stresses may be insignificant for very low modulus cement-treated bases or they may be comparable in magnitude to the traffic stresses for high modulus bases; for most practical cases, the thermal stresses will probably be about 30 to 50 percent of the traffic stresses. Therefore, it is necessary to include them in the design.

4. Using the Bradbury equations (equations III-4 to III-8) involves some assumptions, namely:

a. The temperature gradient is linear

b. All materials are elastic

c. The subgrade behaves as a Winkler foundation

d. The cement-treated base remains at all times in full contact with the subgrade.

5. Of these assumptions, the first two are of concern. Results of Barber's method for calculating temperature distributions in pavement systems and also those of the finite element solution show that the temperature gradient is not linear (Fig. A5 and A6). The warping stresses are higher for nonlinear temperature gradients than for linear ones. Offsetting these higher stresses, is the time-dependent response that cement-treated soils may exhibit which means that the potential exists for stress relaxation under sustrained loads. Although these assumptions will not be discussed in detail here, it is believed that the Bradbury equations are adequate and that their use is warranted, particularly considering their simplicity. For a more detailed discussion of temperature stresses and the viscoelastic properties of cement-treated soils, the reader is referred to Thomlinson (1940); Harr and Leonards (1959); Reddy et al., (1963);and Pretorius (1970).

6. In the computation of thermal stresses the dimensions of the slabs have been assumed to be 10 ft by 10 ft for cement-treated clays and 20 ft x 20 ft for cement-treated sands. Generally crack spacing will have no influence on the upper bound thermal stresses. Only for slabs with large values of radius of relative stiffness can the crack

spacing be important. For values of L_x/ℓ or L_y/ℓ less than seven the thermal stresses will be less than the upper bound stresses (see Fig. 5 of the main text).

7. To use the Bradbury equations it is also necessary to have a measure of the modulus of subgrade reaction, k, rather than subgrade modulus E. The modulus of subgrade reaction can be estimated from:

$$k(psi) = 0.0565\ E\ (psi) \qquad (D\text{-}1)$$

which was developed using elastic theory.

8. A comparison of stresses computed by layered elastic theory and stresses computed by Westergaard theory using equation D-1 is shown in Fig. D3. The two-layered pavement system (cement-treated base over subgrade) was subjected to an 18,000 lb axle load on dual wheels. The base modulus was varied from 100,000 to 1,000,000 psi; the subgrade modulus was varied from 1,000 to 10,000 psi; and the thickness of the cement-treated base was varied from 6 to 36-in. Over this wide range of parameters, the tensile stresses computed by both methods are in good agreement -- thus verifying the relation between k and E in equation D-1.

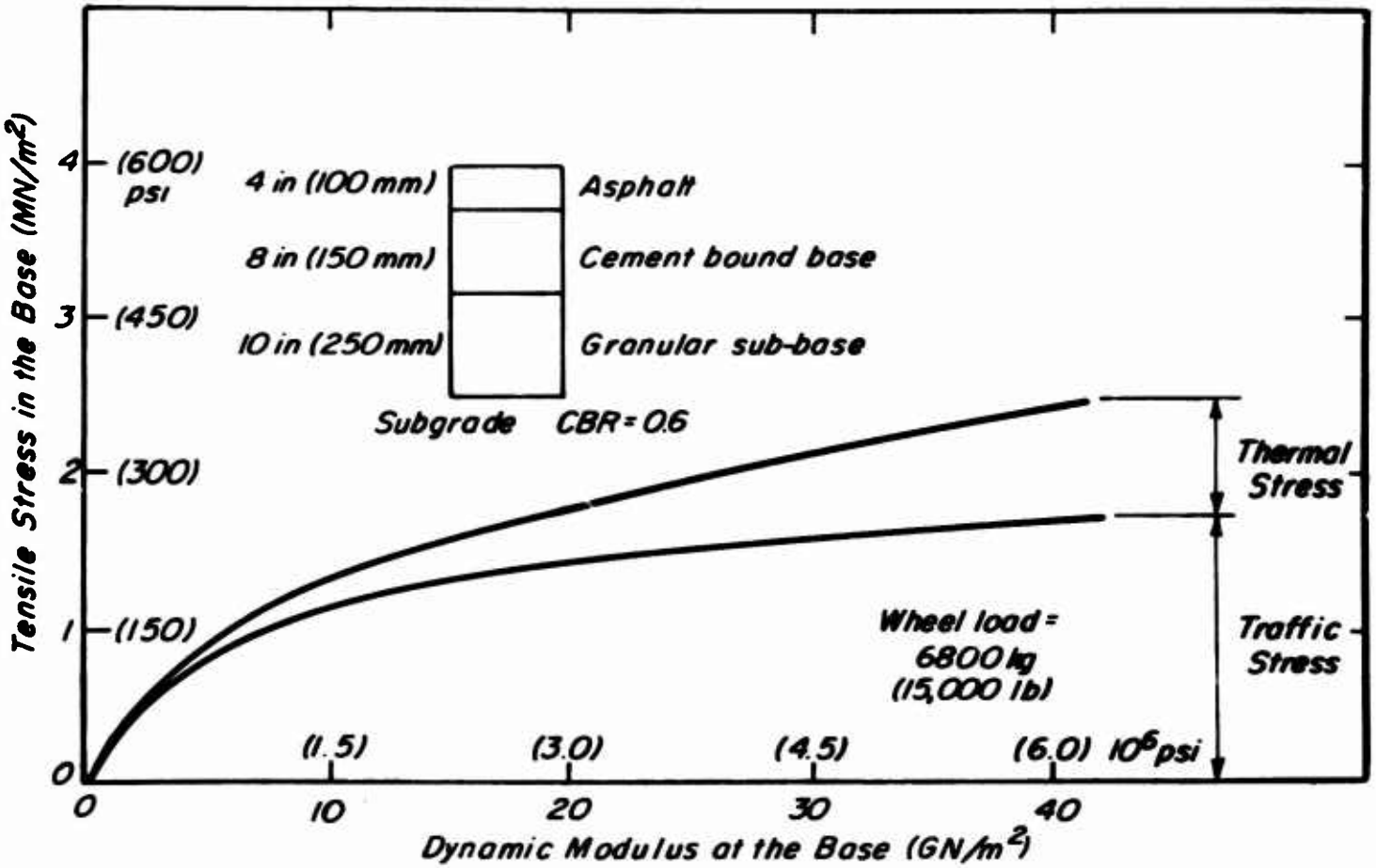

Fig. D1 Stress due to traffic and temperature in pavements with cement-bound bases of varying stiffness (After Lister, 1972)

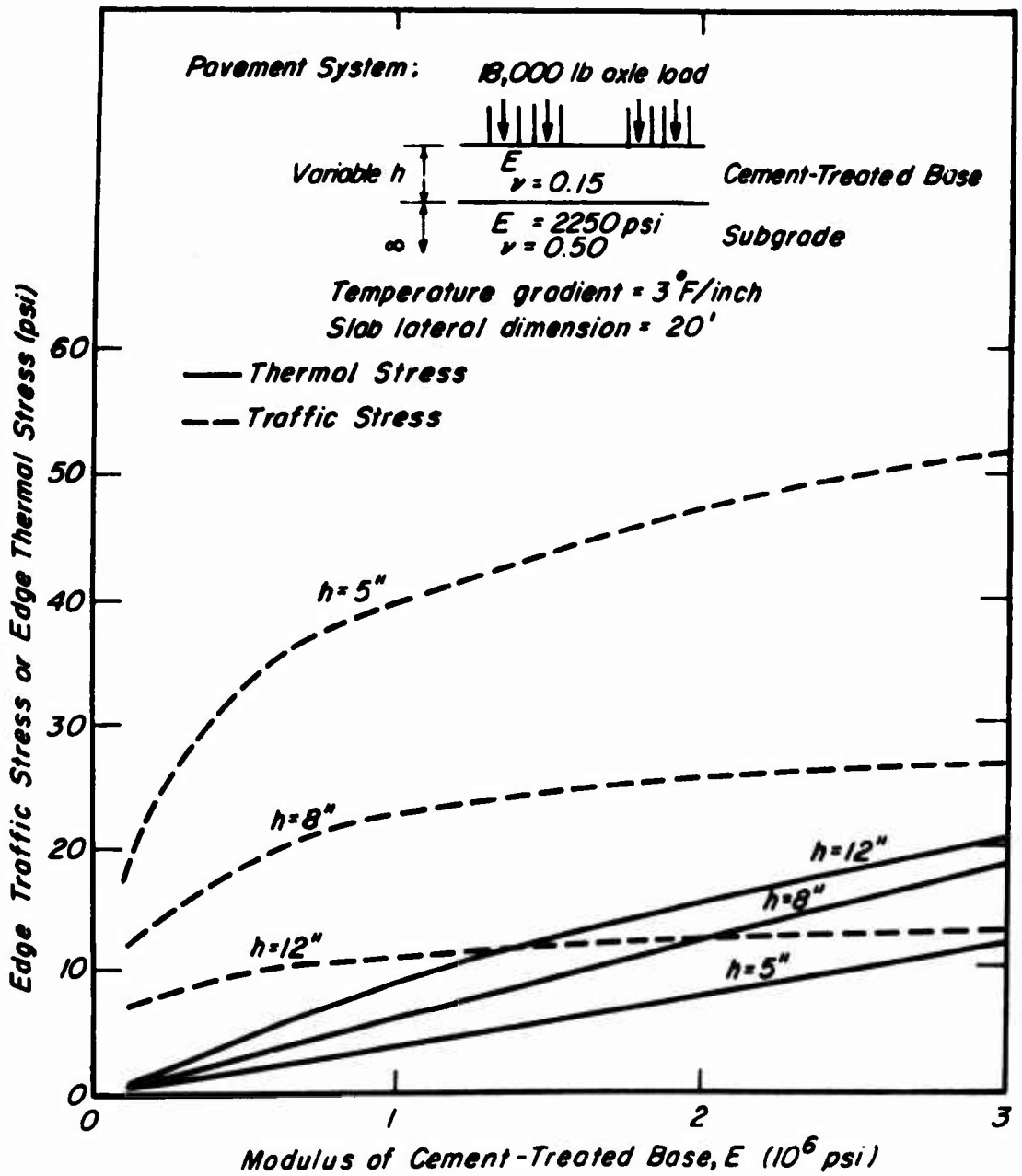

Fig. D2 Comparison of thermal and traffic stresses

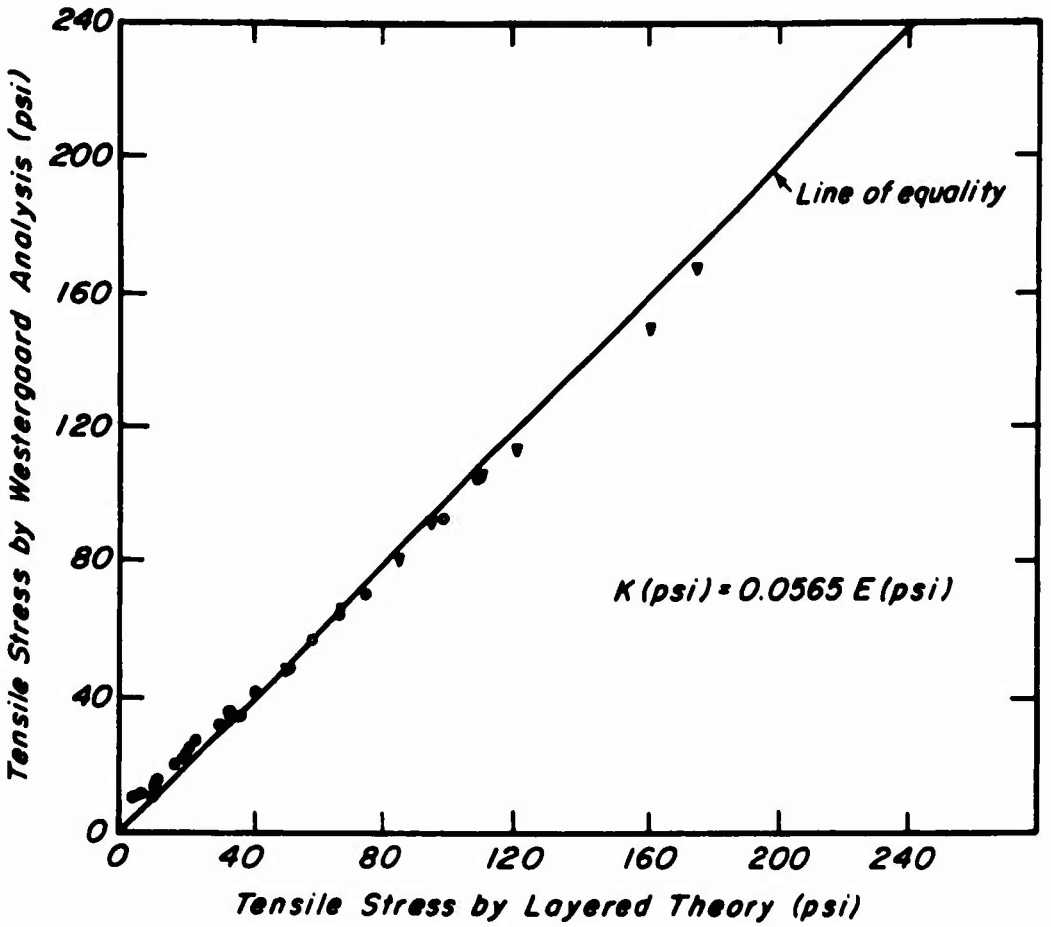

Fig. D3 Comparison of tensile stresses calculated by layered elastic theory and Westergaard's theory

APPENDIX E: FATIGUE CONSIDERATIONS

1. In the design procedure recommended in the main text, a relatively simple procedure to incorporate the influence of fatigue was presented. This procedure considers the tensile strain in the cement stabilized layer as the damage determinate.

2. While the procedure is limited to design for a two-layer system, an analysis is included in this section to indicate that the same procedure can be applied to a three layer system consisting of asphalt concrete, cement-stabilized base, and an untreated subgrade. In addition, since Shell has recommended that the vertical compressive strain at the subgrade surface should not exceed some limiting value -- to preclude the subgrade from contributing to permanent deformation at the pavement surface, analsyses have been included to indicate that the fatigue criterion for the cement-stabilized layer remains the governing factor in design.

3. Some considerations are included relative to cumulative damage, the superposition of steady state stresses (e.g., thermal stresses) on repetitive stresses,and a summary of available fatigue data for cement stabilized material to permit assessment of the values which were selected for the design.

Analysis of Limiting Distress Conditions

4. For the pavement system shown in Fig. E1, a series of analyses were made to assess which of the damage determinates shown in this figure would be most critical.

5. For a given pavement system (i.e., thickness and modulus of asphalt concrete, modulus of cement-treated base, and modulus of subgrade), the thickness of cement-treated base was determined which would limit the critical stresses and strains to acceptable values.

6. A design loading of 10^6 repetitions of a 9,000 lb dual wheel load (18,000 lb axle load) was used. The dual wheel loading was approximated by two circular loaded areas, each with a radius of 4.25 in. and a uniform stress intensity of 80 psi with centers of the loaded areas 12 in. apart.

7. The stiffness modulus of the asphalt concrete was taken as 900,000 psi under cold weather conditions (used for determining tensile strains in the asphalt concrete) and 175,000 psi under warm weather conditions (used for determining the tensile stresses and strains in the cement-treated base and compressive strains in the subgrade). Poisson's ratio for the asphalt concrete was 0.35.

8. Poisson's ratios for the base and subgrade layers were taken as 0.15 and 0.50, respectively. Based on analysis of available data the flexural strength of the base course material was taken as 0.025 percent of its modulus.

Permissible stress levels and strains in the different layers for 10^6 loading repetitions are given in the accompanying tabulation:

Material	Maximum Stress Level $\left(\frac{\text{tensile stress}}{\text{flexural strength}}\right)$	Maximum Strain
Asphalt concrete	-	70×10^{-6} (tensile)
Cement-treated base	0.50	50×10^{-6} (tensile)
Subgrade	-	650×10^{-6} (compressive)

10. Computations of stresses and strains were made using the ELSYM5 computer program. Results of the analyses are given in Table E1. In the table are shown the thicknesses of cement-treated base required to ensure that the permissible stress and strain values are not exceeded.

11. From Table E1 it can be seen that the tensile strain in the base always governed the required thickness of the cement-treated bases for the pavement systems analyzed. This finding is a direct result of the allowable maximum tensile strain value of 50×10^{-6} that was imposed on the cement-treated base. While this strain limit may be too small, others have suggested values also in this range. For example, Otté (1973) recommended strain values of 38×10^{-6} and 60×10^{-6} for two cement-treated crusher-run bases for 10^6 load repetitions, and 28×10^{-6} and 45×10^{-6} for unlimited life. Also, Hadley et al. (1972) recommended a strain value of 20×10^{-6} (based on a study of the fatigue life of portland cement concrete) for unlimited life. The question of acceptable tensile strains in the cement-treated base will be addressed later, but it is evident that the tensile strain in the base will govern the fatigue life of the pavement section.

TABLE E1 REQUIRED BASE THICKNESS TO LIMIT CRITICAL STRESSES AND STRAINS

Number	Pavement System		Asphalt Concrete Thickness in.	Base Thickness Required for Condition Indicated in.			
	Subgrade Modulus, E_3 psi	Base Modulus, E_2 psi		ε in Asphalt Concrete	ε in base	σ in base	ε in subgrade
1	3,750	500,000	3	2.5	17.5	10.3	3.1
2	3,750	500,000	6	N.C.*	15.5	8	1
3	3,750	500,000	15	N.C.	7.5	1.2	N.C.
4	3,750	500,000	18	N.C.	6.0	N.C.	0.8
5	3,750	1,000,000	10	0.4	8.1	2.2	N.C.
6	3,750	1,000,000	12	0.1	6.7	1.0	N.C.
7	7,500	1,000,000	2	5	12.0	N.C.	N.C.
8	15,000	250,000	9	N.C.	14	6	N.C.
9	15,000	500,000	6	2.6	12.5	5.8	0.4
10	15,000	500,000	8	1.8	10.9	4.3	0.3

* Not critical.

Superposition of Load and Thermal Stresses

12. To study the fatigue life of a cement-treated base subjected to loading due to traffic and temperature gradients, the strain criterion can no longer be used. Since thermal stresses result from restraint of deformation. While this may indicate that fatigue life must be analyzed in terms of stress, it will be demonstrated that the thermal stresses will not affect fatigue life significantly, and hence tensile strain can still be used as the design criterion.

13. The influence of a residual stress,thermal stress in this case, on fatigue is treated most conveniently by conducting fatigue tests for a range in conditions where steady state and fluctuating stresses are superimposed. When this is done it is convenient to introduce the stress ratio, R, defined as the ratio of the minimum stress to the maximum stress. Values for R resulting from various loading conditions are:

Loading	R = min. stress/max. stress
Zero-to-max.	R = 0/1 = 0
Complete reversal	R =-1/1 = 1
Steady state	R = +1/1 = 1
Fluctuating tension-tension or compression-compression	0<R<1

14. The spectrum of R values is conveniently presented on a modified Goodman diagram as shown in Fig. E2. This diagram allows rapid interpolation of N for various values of R.

15. Murdock and Kesler (1958) ascertained that a stright line relationship for R ranging from 0 to +1 could represent the fatigue response of plain

concrete beams. This means that one fatigue curve together with the static strength values will cover all positive R values; indications are that an extrapolation to negative values for R is also possible.

16. To illustrate the approach, consider a pavement system in which the extreme fiber tensile stress is 100 psi due to traffic loading. The value for R is zero (no steady state stress superimposed) and the fatigue life is approximately 10^6 load repetitions (case a, Fig. E2). Assume now that a thermal stress is superimposed on the traffic stress. As noted earlier the thermal stress will be tensile (positive) when the top of the slab is at a higher temperature than the bottom and compressive (negative) when the opposite occurs. Further assume that the thermal stress is ±50 psi. For the worst condition, the maximum stress is 150 psi and the minimum stress is 50 psi (R = 1/3). From Fig. E2 the resulting fatigue life is 600,000 load repetitions (point b). For the best condition, the maximum stress is 50 psi and the minimum stress is -50 psi (R =-1). The resulting fatigue life is slightly greater than 10^6 load repetitions (Case c).

Cumulative Damage Considerations

17. Although fatigue lives for three conditions have been calculated, the actual fatigue life of the pavement system is unknown, because it is dependent on many variables. Some of these variables are:

a. Variation of thermal stresses throughout each day, season and year

b. Mixed traffic loading

c. Sequence of traffic loading

d. Frequency of traffic load

e. Frequency and length of rest periods between loading.

Also, there is no reliable method for determining cumulative damage. Usually to analyze spectrum loading, the linear summation of cycle ratios cumulative damage hypothesis is used. This hypothesis assumes that the fraction of fatigue life consumed at a particular stress (or strain) level is the ratio of the number of cycles actually applied at that stress (or strain) to the total number of stress (or strain) cycles which would produce failure. Under random cycles of stress or strain, failure will occur if the damage accumulated adds up to 1.0 or:

$$\sum_{i=1}^{P} \frac{n_i}{N_i} = 1.0 \qquad \text{(E-1)}$$

where:

n_i = number of applications of stress or strain at level i

N_i = number of applications of stress or strain at level i that would lead to failure.

18. This appears to be a reasonable relationship for compound loading and is suggested for use if the design is to be based on mixed traffic.

Fatigue Criteria

19. Establishing the magnitude of allowable tensile strains for cement stabilized materials is difficult since little work has been done

in this area. Thus at this time only guidelines will be provided which can be modified as more data becomes available.

20. The most direct way of obtaining tensile strain for a given fatigue life is by testing beam specimens under repeated loading and measuring the strain. However, this testing is difficult, time consuming and also expensive.

21. One of the most comprehensive fatigue studies on cement-treated soils was done by Larsen and Nussbaum (1967). Their results were reported in terms of radius of curvature, which is related to the strain by the following equation:

$$R = \frac{h}{\varepsilon_t + \varepsilon_c} \qquad \text{(E-2)}$$

Where:

R = radius of curvature

h = specimen thickness

ε_t, ε_c = tensile and compressive extreme fiber strain respectively.

22. While Larsen and Nussbaum's results cannot be used to estimate strain vs cycles to failure relationships directly, they can be compared with the data of Pretorius (1970) as seen in Fig. E3. In this figure it will be noted that the results for A-1-a cement treated soil compares well with Larsen and Nussbaum's data for an A-1-B cement treated material.

23. In another study, Otté (1973) stated that a cement-treated material will have unlimited life if the induced flexural strain does not exceed 25 percent of the strain at failure in bending and will have

a fatigue life of 10^6 load repetitions if the induced flexural strain does not exceed 33 percent of the strain at failure in bending. This agrees well with Pretorius' findings. For 10^6 load repetitions, the strain is 54×10^{-6} which is 36 percent of strain at failure in bending (150×10^{-6}). Using Otté guidelines, a fatigue curve can be easily constructed by just performing one flexural strength test and measuring the strain at failure.

24. Based on this information the fatigue curve in terms of strain shown in Fig. 6 of the main text is recommended for use in conjunction with the design curves.

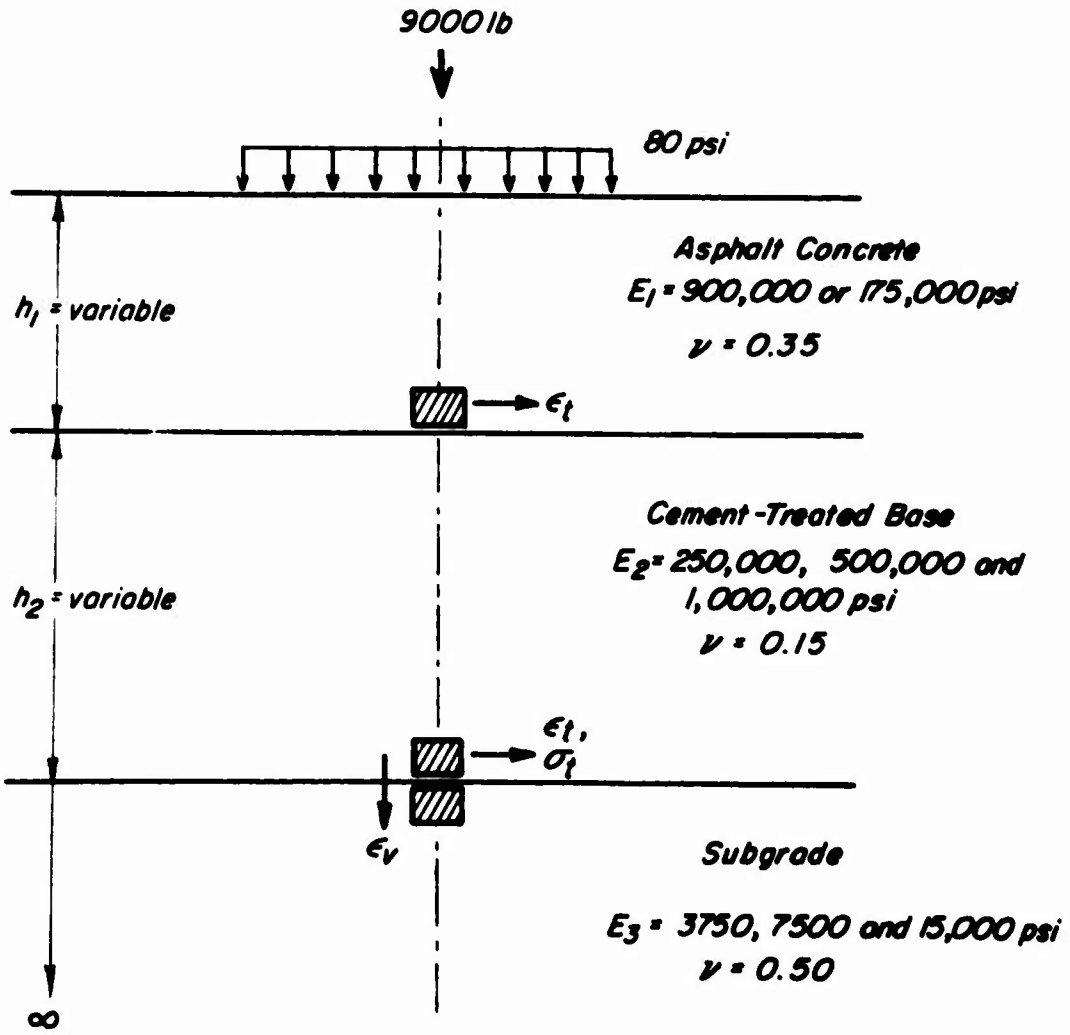

Fig. E1 Three-layered pavement system

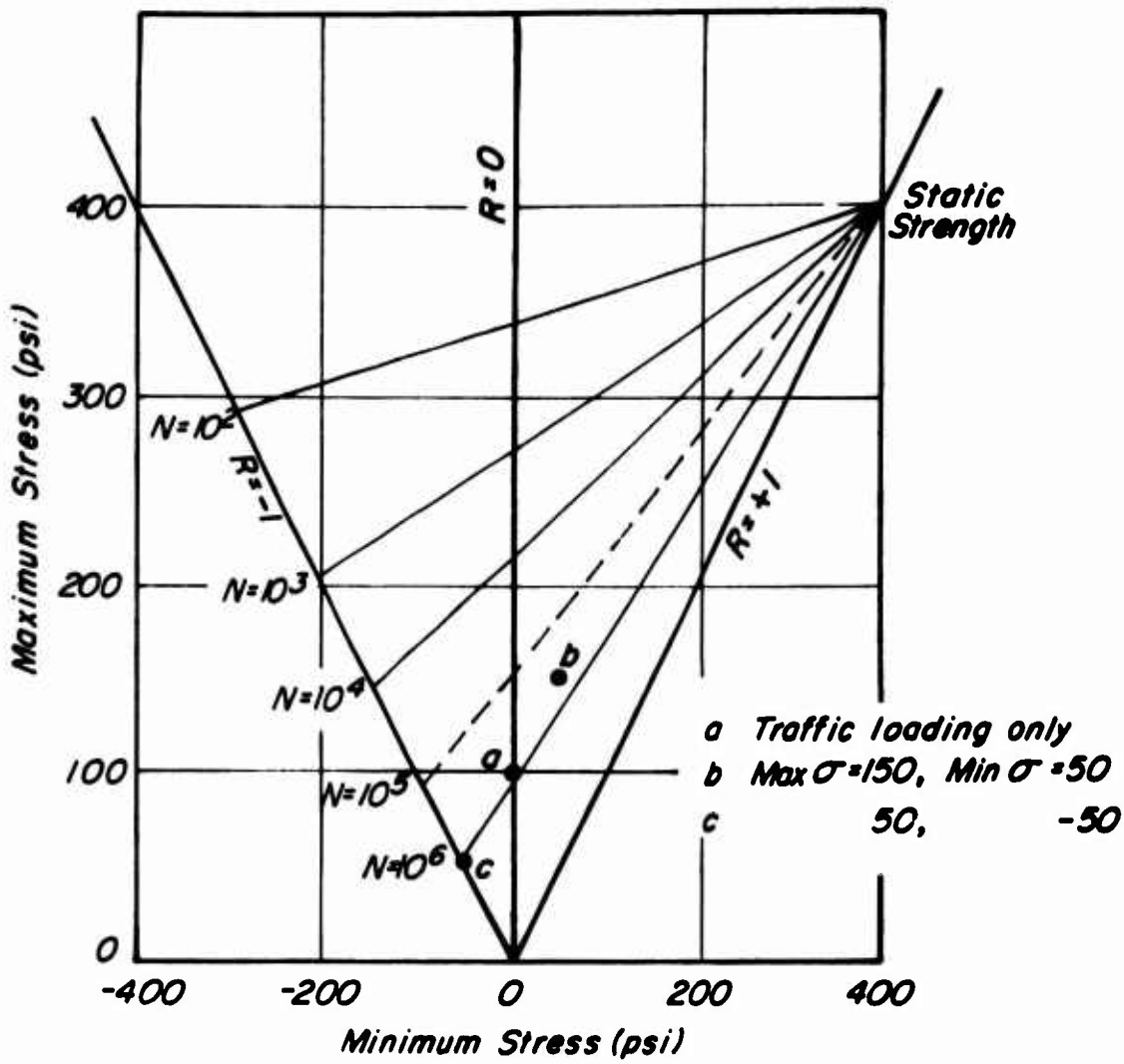

Fig. E2 Modified Goodman Diagram for a soil-cement (After Pretorius, 1970)

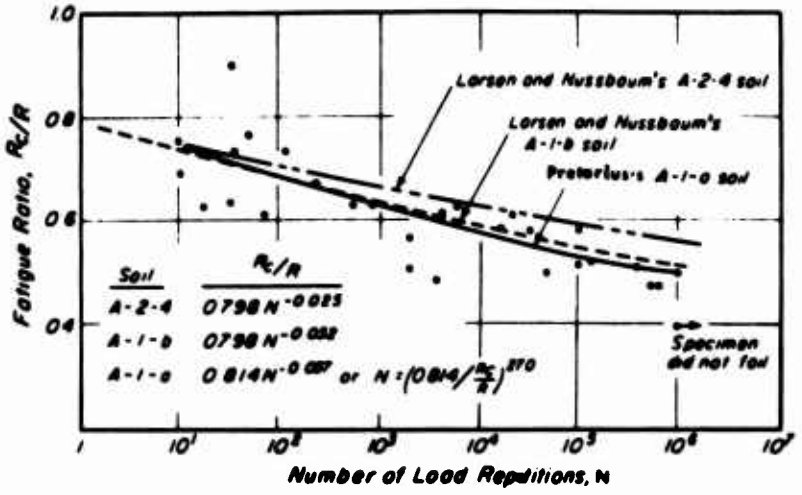

Fig. E3 Comparison of fatigue results with data presented by Larsen and Nussbaum (1967) (After Pretorius, 1970)

APPENDIX F: DEVELOPMENT OF DESIGN CHARTS

1. The design curves presented in Section IV, Figs. 9-16, assume the pavement to be represented as a two-layer elastic system and incorporate the following variables:

a. Flexural strain on the underside of the cement-stabilized base.

b. Modulus of the stabilized base

c. Thickness of stabilized base

d. Modulus of the subgrade

e. Traffic type

Poisson's ratios for the stabilized layer and subgrade were assumed to be 0.15 and 0.50 respectively.

2. Using the computer program ELSYM5 the maximum tensile strains for a range in pavement thicknesses were determined for a specific traffic type, base modulus, and subgrade modulus. For the multiple wheel loads this necessitated computations at a number of points to insure that the maximum value was obtained.

3. It will be noted that each design chart has been developed for a specific base course modulus and is similar to these developed by the Portland Cement Association for Airfield Pavements (Packard, 1973).

4. To establish a particular design chart:

a. A suitable flexural strain scale was established for the left ordinate and a suitable thickness scale for the stabilized base was drawn for the right ordinate.

b. For a particular traffic type (e.g., 18,000 lb axle load) a diagonal straight line was drawn from the origin of the flexural strain scale to the thickness scale. Essentially, the scales of the two ordinates and the placement of the diagonal line is done by trial to obtain a well proportioned design curve.

c. Subgrade curves were established by:

(1) Drawing a horizontal line from a particular base thickness to the specific diagonal traffic load line,

(2) At the intersection of the horizontal line and the diagonal line, drawing a vertical line, and

(3) Intersecting this vertical line with a horizontal line from the corresponding flexural strain to establish one point on the subgrade curve.

d. This procedure was repeated for different base thicknesses until sufficient points were established to define the curve for a particular subgrade stiffness.

e. Steps c. and d. were repeated to obtain all of the subgrade stiffness curves shown in the design charts.

f. Having established the subgrade curves for a specific vehicle (or aircraft) type, other traffic curves were plotted as follows:

(1) A horizontal line was drawn from the flexural strain computed for a particular set of conditions - base

thickness, traffic type, and subgrade stiffness - to the appropriate subgrade curve.

(2) A vertical line was drawn through the point defined in (1).

(3) The intersection of a horizontal line from the base thickness with the vertical line established one point for the specific traffic type.

(4) Repeating these steps to obtain sufficient points permitted definition of the desired traffic line. It should be noted that for the pavements analyzed herein the traffic lines were always linear.

5. The above procedure was repeated for each base modulus and an additional ordinate was added to recognize the 50% increase for edge stresses compared to those developed in the interior.

6. The curves of Figs. 17-24 in terms of stress were developed by the same procedure.

APPENDIX G: SUMMARY OF OTHER DESIGN PROCEDURES

Highway Pavements

AASHO Interim Guide

1. The AASHO Interim Guides are based on data developed from the AASHO Road Test and modified by other experience (Liddle, 1963). Recently the Guides (for both asphalt and portland cement concrete pavements) have been modified and updated (McCullough et al., 1968); the material presented herein was obtained from a report prepared by Materials Research and Development (Materials Research and Development, 1971).

2. Principal design considerations. The design chart shown in Fig. G1 (for a Terminal Serviceability Index* of 2.5) is based on the

---

*Serviceability - the ability at time of observation of a pavement to serve high-speed, high-volume automobile and truck traffic.
Present Serviceability Rating (PSR) - the mean value of the independent subjective ratings by members of a special Panel for the AASHO Road Test as to the serviceability of a section of highway. The members of the Panel included highway specialists representing many fields of interest and concern in highways.
Serviceability Index (PSI) - a number derived by formula for estimating the serviceability rating from measurements of certain physical features of the pavement.

assumptions that the equations developed from the AASHO Road Test are a valid representation of the relationship between loss in serviceability, traffic, and pavement thickness and that the equations developed:

a. for a single type of subgrade soil, may be extended to apply to any subgrade by means of a soil support scale developed for this purpose.

b. for repeated applications of uniform traffic loads may be extended to apply to mixed traffic by conversion to equivalent 18,000 lb single-axle loads.

c. for a single environmental condition may be extended to apply to other environmental conditions by means of an appropriate regional factor.

d. for subbase, base, and surfacing materials used in constructing the test road may be extended to apply to other materials by assignment of appropriate layer coefficients (a_1, a_2, a_3).

e. for accelerated applications of traffic during the two-year test period may be extended to apply to repetitions of traffic during an extended period of time (up to 20 years).

Moreover, it is assumed that uniform and high-quality construction will be obtained.

3. Use of the design equations represented graphically in Fig. G1 thus requires an evaluation of:

a. Terminal Serviceability Index, p_t (p_t = 2.5 in Fig. G1).

b. Number of equivalent 18,000 lb single axle loads anticipated during the design period.

c. Soil support value, S.

d. Regional factors, R.

e. Structural number, SN.

f. Layer coefficients, a_1, a_2, a_3.

4. Detailed discussion and appropriate developments of these factors for use in conjunction with the design chart, Fig. G1, are included in the Material Research and Development Report (1971). In this report only the structural number and layer coefficients will be discussed with particular reference to the coefficients pertaining to cement-treated base.

5. The structural number, SN, for the entire pavement can be obtained from Fig. G1 for a particular set of conditions. This number is represented by the equation:

$$(SN)_{total} = a_1D_1 + a_2D_2 + a_3D_3 \qquad (G1)$$

a_1, a_2, a_3 = layer coefficients, surface, base and subbase, respectively

D_1, D_2, D_3 = thickness in inches, surface, base, and subbase, respectively.

6. Values of layer coefficients obtained for the materials used in the factorial sections of the AASHO Road Test are as follows:

asphalt concrete surface course	0.44
crushed stone base course	0.14
sandy gravel subbase course	0.11

Coefficients for other materials are shown in Table G1 as proposed by the AASHO Committee.

7. A number of agencies have modified these values somewhat in the light of their own experiences. A summary of such practices is also included in Materials Research and Development report (1971).

8. Applicability to sections with cement-treated base. The use of the Interim Guide for asphalt concrete pavements to design sections containing cement-stabilized layers merely requires the determination of the structural number from Fig. G1 and the use of the appropriate coefficient a_2 or coefficients a_2 and a_3 if different treatments are contemplated with depth. While such a procedure has appeal because of its simplicity,there are a number of limitations; from the standpoint of treatment level, for example, the coefficient a_2 or a_3 will vary considerably depending on soil type and cement content. Moreover, the procedure is limited to highway-type loadings.

State of California Method

9. The State of California method of asphalt concrete pavement design was first presented by Hveem and Carmany (1948) and then adopted by the California Division of Highways in 1950. Over the years the procedure has been modified as performance data from in-service highways in California together with that from the WASHO and AASHO test roads have become available (Hveem, 1955; Sherman, 1958; Hveem and Sherman, 1963). The present procedure is detailed in the Materials Manual of the State of California Division of Highways (State of California, 1964).

10. Principal design considerations. Pavement thickness is a function of:

TABLE G1 STRUCTURAL LAYER COEFFICIENTS

PROPOSED BY AASHO COMMITTEE ON DESIGN, OCTOBER 12, 1961*

Pavement Component	Coefficient+
Surface Course	
Road mix (low stability)	0.20
Plantmix (high stability)	0.44**
Sand Asphalt	0.40
Base Course	
Sandy Gravel	0.07++
Crushed Stone	0.14**
Cement-Treated (no soil-cement)	
Compressive strength at 7 days	
650 psi or more†	0.23++
400 psi to 650 psi	0.20
400 psi or less	0.15
Bituminous-Treated	
Course-Graded	0.34++
Sand Asphalt	0.30
Lime-Treated	0.15-0.30
Subbase Course	
Sandy Gravel	0.11**
Sand or Sandy-Clay	0.05-0.10

* Adapted from material presented by Materials Research and Development (1971).
** Established from AASHO Road Test Data.
+ It is expected that each state will study these coefficients and make such changes as experience indicates necessary.
++ This value has been estimated from AASHO Road Test data, but not to the accuracy of those factors marked with a double asterisk.
† Compessive strength at 7 days.

TABLE G2 GRAVEL EQUIVALENT FACTORS

FOR COMMON PAVEMENT AND BASE MATERIALS

Type of Material	Gravel Equivalent Factor, G_f
Cement Treated Base - Class A	1.7
Cement Treated Base - Class B	1.5
Asphalt Concrete	$2.5\left[\frac{5.14}{TI}\right]^{0.5} \leq 2.5$
Traffic Index: 0 - 5.0	2.50
7.5 - 8.0	2.01
10.5 - 11.0	1.71
12.5 - 13.0	1.57
Untreated Aggregate Base	1.1
Aggregate Subbase	1.0

12. For expansive soils, the thickness of the structural section must also be sufficient to insure that the weight of the pavement structure will be equal to the expansion pressure of the soil developed under expected field conditions. Thickness to prevent expansion is determined from the relationship:

$$T(ft) = \frac{\text{Expansion pressure (psf)}}{\text{Unit weight of cover materials (lb per cu ft)}} \qquad (G4)$$

13. Material properties. The material properties used to select a pavement thickness by this method are:

a. Resistance (R) value.

b. Tensile strength of paving components as measured by the gravel equivalent factor, G_f, and obtained from a consideration of cohesiometer test values and road test data. Design values for G_f for various materials are listed in Table G2.

c. Expansion pressure.

14. Normally a particular material is prepared at a series of water contents such that an R-value may be obtained over a range in water contents and dry densities. The design thickness is usually determined using an R-value selected at a specified exudation pressure (a pressure required to exude water from the sample after preparation by kneading compaction) which represents some future saturated condition. If the material is very expansive, an equilibrium thickness is used for design and is determined both from a consideration of the expansion pressure and the R-value by the exudation pressure.

15. Applicability to sections with cement-treated base. This method can be used for design of sections containing cement-stabilized materials by using the appropriate gravel equivalent factors obtained from Table G2.

Asphalt Institute Procedure

16. This method was developed from analyses of data from the AASHO Road Test (Shook and Finn, 1963); however, data from the WASHO Road Test, various British test roads, previous Asphalt Institute design considerations, together with a range of existing design experiences from throughout the United States influenced development of the present procedure (Shook, 1972; Asphalt Institute, 1964) first published in 1963 (Asphalt Institute, 1963) and revised slightly in 1970 (Asphalt Institute, 1970).

17. Principal design considerations. Adequacy of a structural design is defined in terms of the Present Serviceability Index (PSI) of the pavement with a terminal value set at 2.5.

18. As in the AASHO procedure, the number of applications of various wheel loads are expressed in terms of an equivalent number of 18,000 lb single-axle-load applications:

$$\frac{W_{18}}{W_L} = 10^{0.118(L-18)} \qquad \text{(G5)}$$

where:

L = single axle load or 0.57 x tandem axle load (must be > 10,000 lb)

$W_{18,L}$ = repetitions of 18,000 lb wheel load or wheel load of magnitude L.

and

$$DTN = \frac{W_{18}}{7300} \qquad (G6)$$

where:

DTN = Design traffic number and represents the average daily equivalent 18,000 lb single-axle load applications for a design period of 20 years.

19. Thickness of asphalt concrete T_A, may be determined from either:

$$T_A = \frac{9.19 + 3.97 \log DTN}{(CBR)^{0.4}} \qquad (G7)$$

where:

CBR = Design California Bearing Ratio of subgrade

or:

$$T_A = 6.37 + 2.75 \log DTN - 0.0893 \cdot DTN^{0.119}(R - 12) \qquad (G8a)$$

$$T_A = 6.37 + 2.75 \log CTN - 0.117\ DTN^{0.0279}(R - 12) \qquad (G8b)$$

where:

R = Stabilometer "R" value.

Design charts representing equations G7 and G8 are shown in Figs. G2 and G3.

20. For convenience, in the western United States, approximate relationships between DTN and Traffic Index (TI) have been established and thicknesses of asphalt concrete for a range in "R" values, DTN's and TI's are shown in Table G3.

21. For pavements consisting of granular materials as well as asphalt concrete the concept of equivalent thickness (or substitution

TABLE G3 ASPHALT CONCRETE THICKNESS GUIDE
ASPHALT CONCRETE THICKNESS (ft) FROM THICKNESS DESIGN MANUAL*

DESIGN TRAFFIC NUMBER (AI)	TRAFFIC INDEX (CA)	R VALUE (CALIFORNIA) OF UNDERLYING SOIL															
		5	10	15	20	25	30	35	40	45	50	55	60	65	70	75	80
0.14	4.0	0.40	0.40	0.35	0.35	0.35	0.35	0.35	0.35	0.35	0.35	0.35	0.35	0.35	0.35	0.35	0.35
0.39	4.5	0.50	0.50	0.45	0.40	"	"	"	"	"	"	"	"	"	"	"	"
0.95	5.0	0.60	0.55	0.50	0.50	0.45	0.40	0.40	"	"	"	"	"	"	"	"	"
2.11	5.5	0.70	0.65	0.60	0.55	0.50	0.45	0.40	"	"	"	"	"	"	"	"	"
4.40	6.0	0.75	0.70	0.65	0.60	0.60	0.55	0.50	0.45	0.40	"	"	"	"	"	"	"
8.62	6.5	0.85	0.80	0.75	0.70	0.65	0.60	0.55	0.50	0.45	0.40	"	"	"	"	"	"
16.08	7.0	0.90	0.85	9.80	0.75	0.70	0.65	0.60	0.55	0.50	0.45	0.40	0.40	0.40	0.40	0.40	0.40
29	7.5	0.95	0.90	0.85	0.80	0.75	0.70	0.65	0.60	0.55	0.50	"	"	"	"	"	"
49	8.0	1.0	0.95	0.90	0.85	0.80	0.75	0.70	0.65	0.60	0.55	0.50	0.45	"	"	"	"
82	8.5	1.05	1.00	0.95	0.90	0.85	0.80	0.75	0.70	0.60	0.55	0.50	0.50	0.45	0.45	0.45	0.45
133	9.0	1.10	1.05	1.00	0.95	9.90	0.85	0.80	0.70	0.65	0.60	0.55	0.50	"	"	"	"
209	9.5	1.15	1.10	1.05	1.00	0.95	0.85	0.80	0.75	0.70	0.65	0.60	0.55	"	"	"	"
322	10.0	1.20	1.15	1.10	1.00	0.95	0.90	0.85	0.80	0.75	0.70	0.65	0.55	0.50	0.50	0.50	0.50
486	10.5	1.25	1.20	1.10	1.05	1.00	0.95	0.90	0.85	0.80	0.70	0.65	0.60	0.55	"	"	"
718	11.0	1.30	1.20	1.15	1.10	1.05	1.00	0.95	0.85	0.80	0.75	0.70	0.66	0.60	"	"	"
1043	11.5	1.30	1.25	1.20	1.15	1.10	1.00	0.95	0.90	0.85	0.80	0.75	0.65	0.60	0.60	0.60	0 60
1491	12.0	1.35	1.30	1.25	1.20	1.10	1.05	1.00	0.95	0.90	0.80	0.75	0.70	0.65	0.60	"	"
2101	12.5	1.40	1.35	1.25	1.20	1.15	1.10	1.05	0.95	0.90	0.85	0.80	0.75	0.65	0.60	0.60	0.60
2922	13.0	1.45	1.35	1.30	1.25	1.20	1.10	1.05	1.00	0.95	0.90	0.80	0.75	0.70	0.65	"	"
4150	13.5	1.45	1.40	1.35	1.25	1.20	1.15	1.10	1.05	0.95	0.90	0.85	0.80	0.70	0.65	0.60	"
5800	14.0	1.50	1.45	1.35	1.30	1.25	1.20	1.10	1.05	1.00	0.95	0.85	0.80	0.75	0.70	0.60	"

NOTE: To use Chart, use TI to left - R-Value across - at intersection, read thickness of asphalt concrete required.

When no further reduction in thickness is indicated, it may be assumed the minimum recommended thickness has been reached.

* Asphalt Institute, 1970.

ratio) has been utilized. For high quality granular materials the substitution ratio is 2.0 in. of granular material for 1.0 in. of asphalt concrete, while this ratio is 2.7 in. for low-quality untreated base.

22. Material properties. Characteristics of the subgrade soil may be determined by either the CBR or R value procedure. No determinations of the properties of the other pavement components are required; although the assumption is made that all structural section components meet certain minimum quality standards normally specified for these materials.

23. Applicability to sections with cement-treated base. While the procedure as published does not include provision for the use of cement-treated base courses, data obtained from the AASHO Road Test could be used to develop an equivalent thickness just as described above for untreated granular materials. The ratio of granular base thickness to that for cement-treated base is approximately 1.7 for equivalent performance. (Note: Coefficient a_2 in AASHO design procedure is 0.14 for granular base and 0.23 for cement-treated base); accordingly one could use a substitution ratio of 1.2 in.* of cement-treated base for 1.0 in. of asphalt concrete.

---

*Note: The quotient of a_2 for cement-treated base to that for untreated base is about 1.7. In the Asphalt Institute design procedure the equivalency of asphalt concrete to granular base is 2 to 1; accordingly the ratio of 2 to 1.7 is about 1.2, the number suggested above.

Shell Method

24. This method of pavement design has been developed for highway pavements (Dormon and Metcalf, 1965; Klomp and Dormon, 1964; Dormon et al., 1964; Lettier and Metcalf, 1964; and Heukelom and Klomp, 1968) and later adapted to airfield pavement design (Edwards and Valkering, 1970) and is applicable for situations with asphalt concrete resting on granular material and in turn on subgrade soils whose strength index can be defined by the CBR procedure (either by measurement or estimation). In addition, the procedure is applicable for selecting the thickness of asphalt pavements resting directly on subgrade soils. Although not a part of the original design procedure the use of the substitution ratio-concept would permit the inclusion of cement stabilized materials.

25. Principal design considerations. The pavement structure is represented by a three-layer elastic system (full friction at interfaces of layers) and the critical conditions for design are:

a. Horizontal tensile radial strain on the underside of the asphalt bound layer; if excessive, cracking may occur on the asphalt layer.

b. Vertical compressive strain in the surface of the subgrade; if excessive, permanent deformation may occur at the top of the subgrade leading, in turn, to permanent deformation at the surface of the pavement.

26. An 18,000-lb single axle load (9,000-lb wheel load) was used as the basis for design charts distributed in the United States. Because of limitations in computer solutions for multi-layer elastic systems at

the time the procedure was developed (1962) (Dormon and Metcalf, 1965), subgrade strains were determined for a load applied to a single circular area with radius of 6 in. and a contact pressure of 80 psi; tensile strains were, on the other hand, determined using a circular area with a radius of 4.2 in. and a contact pressure of 80 psi (equivalent to 4,500 lb on one wheel of dual tires). Repetitions of the 18,000 lb axle load are considered as a part of the design process and the allowable strains associated with various numbers of repetitions are shown in Table G4 and G5.

27. Material Properties. Materials in each of the three layers are assumed to be homogeneous, isotropic and elastic.

a. Asphalt concrete. The time-of-loading and temperature dependency of asphalt concrete are recognized. Tensile strains in the asphalt concrete are determined for an assumed stiffness in this layer of 900,000 psi (corresponds to a temperature of 50°F and a time of loading of 0.02 sec.). For determination of subgrade strain, the air temperature is assumed to be 95°F, and effective stiffness modulus (depending on the thickness of asphalt concrete - h) is selected from Fig. G4.

b. Untreated aggregate base. The modulus of the granular base is expressed in terms of the subgrade modulus and is dependent on the thickness of the base layer, Fig. G5.

c. Subgrade soil. From dynamic (vibratory) tests in-situ, an approximate relationship between subgrade modulus (E_3) and CBR was established (Klomp and Dormon, 1964):

TABLE G4 ALLOWABLE TENSILE STRAIN IN ASPHALT-BOUND LAYER CORRESPONDING TO DIFFERENT LOAD APPLICATIONS*

Weighted Load Applications	Tensile Strain in. per in.
10^5	2.3×10^{-4}
10^6	1.45×10^{-4}
10^7	9.2×10^{-5}
10^8	5.8×10^{-5}

* From Dormon and Metcalf (1965).

TABLE G5 ALLOWABLE SUGRADE COMPRESSIVE STRAIN VALUES CORRESPONDING TO DIFFERENT LOAD APPLICATIONS*

Weighted Load Applications	Compressive Strain on Subgrade in. per in.
10^5	1.05×10^{-3}
10^6	6.5×10^{-4}
10^7	4.2×10^{-4}
10^8	2.6×10^{-4}

* From Dormon and Metcalf (1965).

$$E_3 = 1500 \cdot CBR \text{ (psi)} \qquad \text{(G9)}$$

28. Since the computations were developed in the early 1960's at a time when solutions were available only for a Poisson's ratio of 0.5 in each of the three layers, the design charts are based on this value for all the materials.

29. Materials tests. In this procedure the only test potentially required is a CBR test on the subgrade soil to permit estimation of the modulus from equation (G8).

30. Typical design relationship. Design curves for a range in subgrade moduli are shown in Fig. G6 for 10^6 repetitions of an 18,000 lb axle load. In this procedure, the design process simply consists of selecting a combination of thicknesses of asphalt concrete and untreated granular material from the appropriate relationship.

31. Thick-lift asphalt concrete sections. From curves such as those shown in Fig. A6 it is possible to select, for a specific subgrade modulus, thicknesses of asphalt concrete corresponding to a thickness of the granular layer equal to zero. Alternatively, Heukelom and Klomp (1968) have formulated a relationship developed from the design chart which is plotted in Fig. G7* and has the form

---

* This design chart was presented in metric units and no attempt has been made to replot it in English units. Note that 1 Kg per sq cm is about 15 psi.

$$h = 10\ (2/3\ \log N - \text{Log}\ E_s) + 13 \qquad \text{(G10)}$$

where:

h = thickness of asphalt-bound layer, cm. (h > 6 cm.)

N = number of repetitions of axle load

E_s = subgrade modulus, kg per sq cm (E_3 in previous section)

32. Use with cement-stabilized layers. Like the other design procedures a substitition ratio could be utilized with a value for cement-stabilized material being selected from available data.

Airfield Pavements (Shell Method)

Principal design criteria

33. As with highway pavements the pavement is represented as a multilayer elastic structure. While the same criteria are chosen, different levels for each of the conditions has been selected (Edwards and Valkering, 1970).

a. Horizontal tensile radial strain on the underside of the asphalt-bound layer - increased the value at 10^6 repetitions from 1.45×10^{-4} to 2.3×10^{-4} since this appeared to produce thickness requirements in line with experience with conventional structures.

b. Vertical compressive strain in the surface of the subgrade - increased the value at 10^6 repetitions from 6.5×10^{-4} to 10.3×10^{-4}. Value changed because of change in Poisson's ratio from 0.5 to 0.35 in analyses.

34. For the vertical strain in the subgrade, principal strains under various wheel load configurations were examined using BISTRO* (Peutz et al., 1966). For the actual design curve development, superposition of vertical rather than principal strains was used since the vertical strain was determined to be nearly equal to the principal strain.

35. From an examination of various gear configuration, it was concluded that the maximum principal tensile strain occurred under any one wheel** e.g., Fig. G8***.

Typical design relationships

36. Design curves for the B707-320B and the B747 are shown in Figs. G9a and b for a range in subgrade moduli.

Use with cement-stabilized layers

37. As with highway pavement design procedures, the substitution ratio concept could be used. At this time, however, data are not available for substitution ratios for loadings associated with aircraft.

---

* Computer program to determine stresses, strains, and displacements in a multilayer elastic structure.

** For the Boeing 747 aircraft this analysis did not consider the effects of the other gears; Shell is examining this problem at this date (1974).

*** Note 1MN per sq m is about 150 psi.

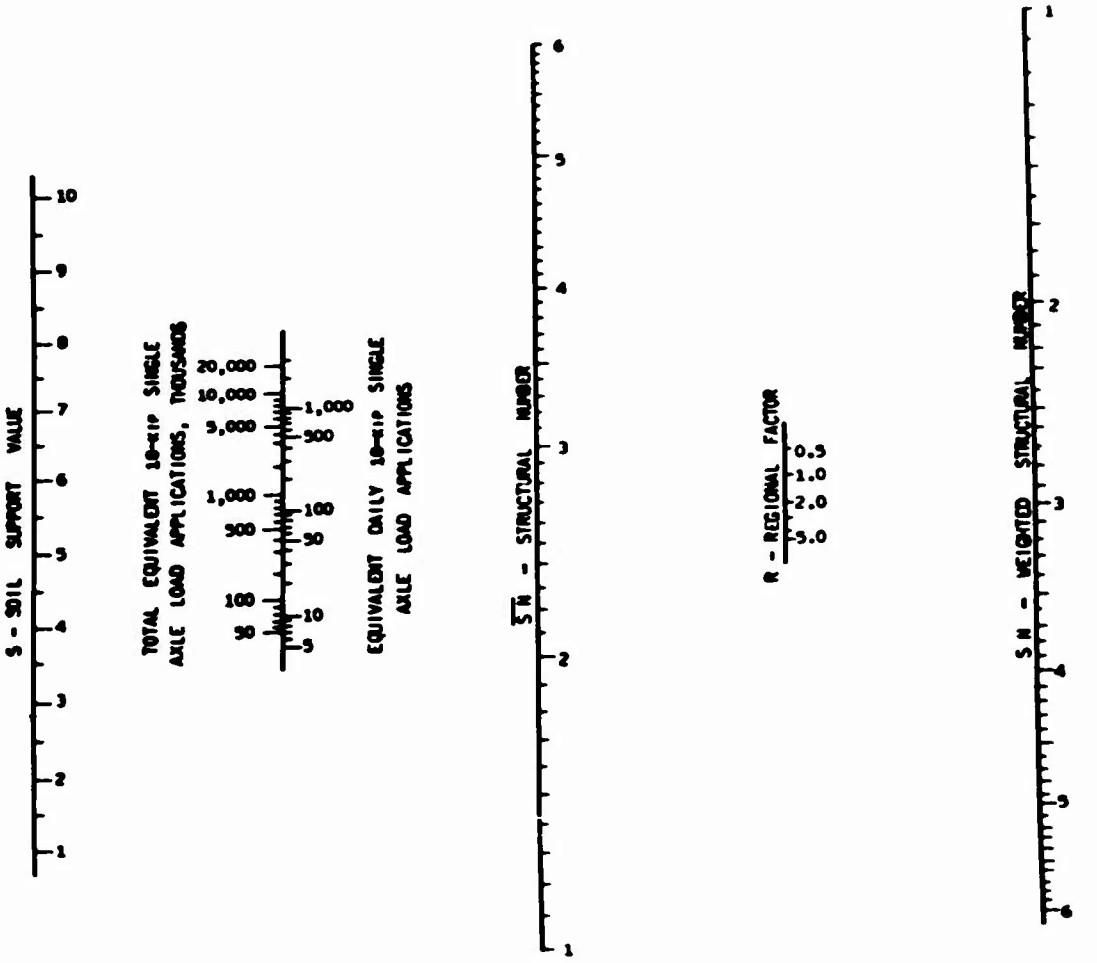

Fig. G1 AASHO Interim Guide, design chart for flexible pavements, terminal serviceability index = 2.5 (Materials Research and Development, 1971)

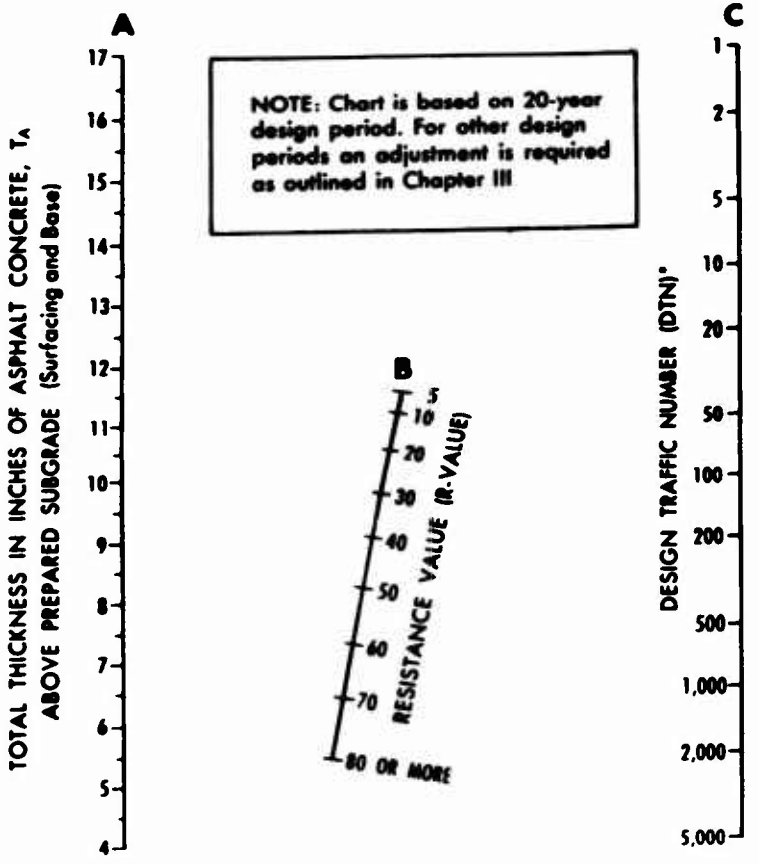

Fig. G2 Thickness design chart for asphalt pavement structures using subgrade soil R-value (Asphalt Institute, 1970)

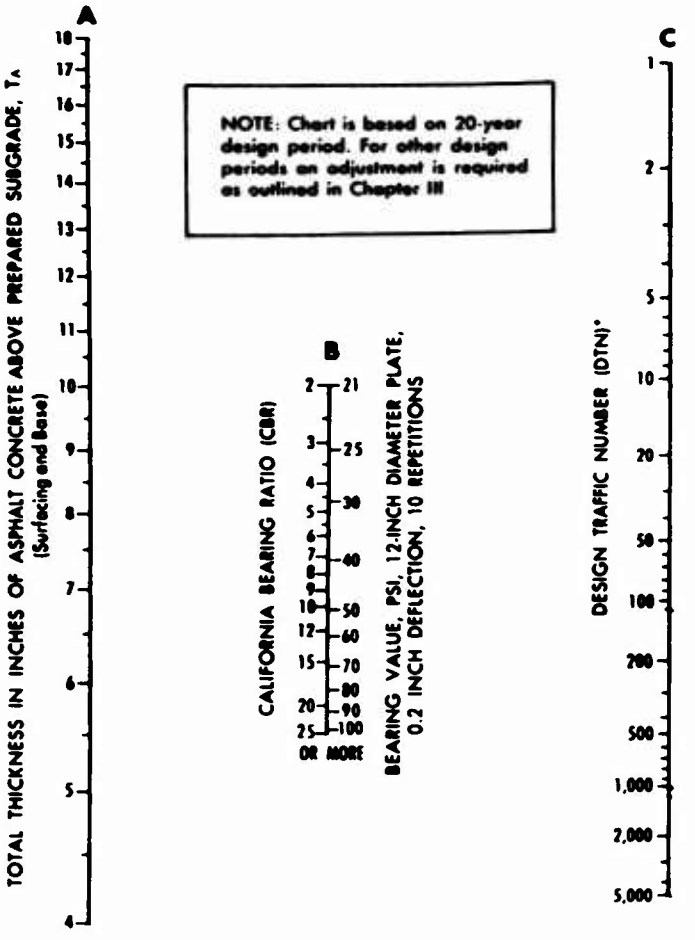

Fig. G3 Thickness design chart for asphalt pavement structures using subgrade soil CBR or Plate-Bearing values (Asphalt Institute, 1970)

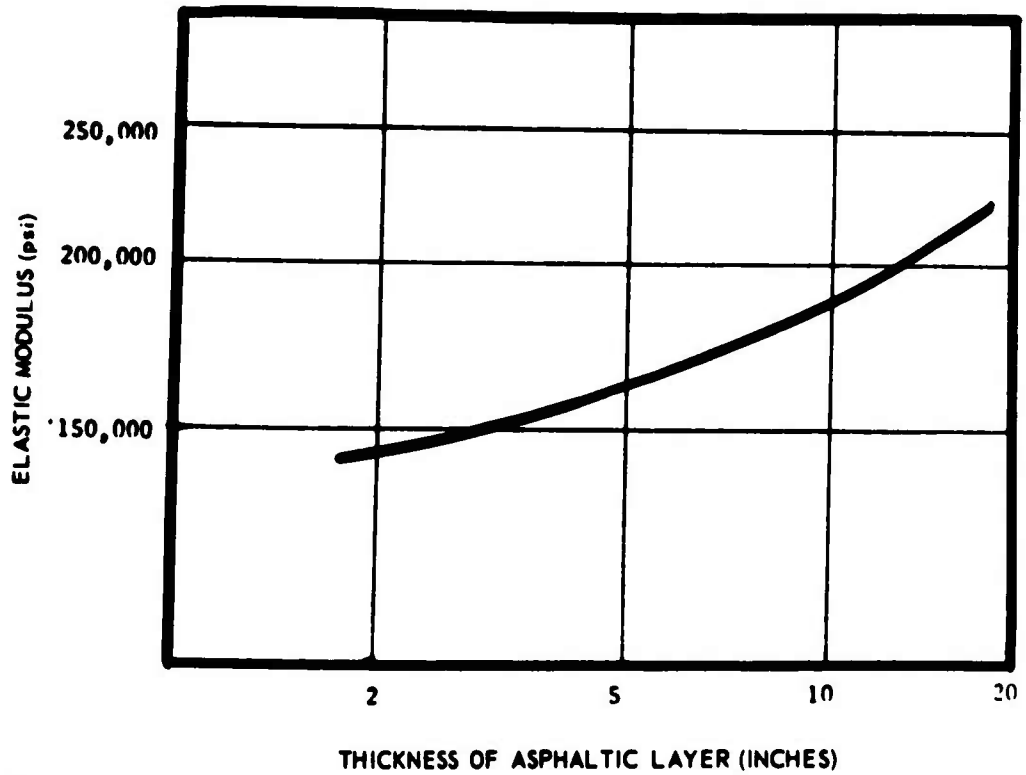

Fig. G4 Relation of asphaltic layer modulus to thickness of layer (air temperature of 95°F) (Lettier and Metcalf, 1964)

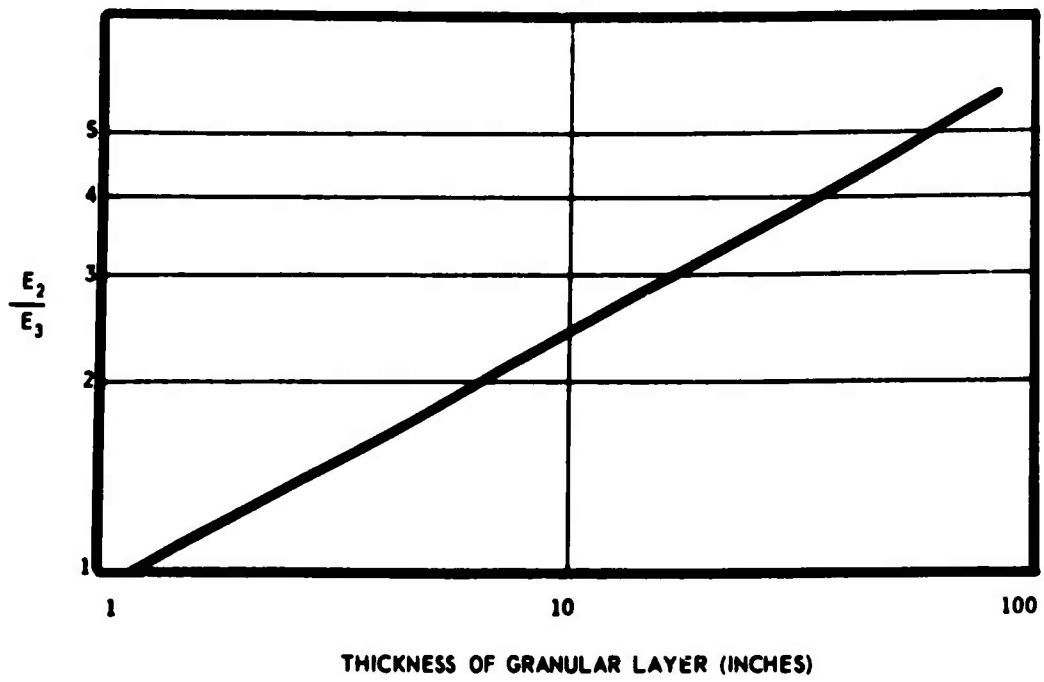

Fig. G5 Relation of modular ratio to granular base thickness. (Lettier and Metcalf, 1964)

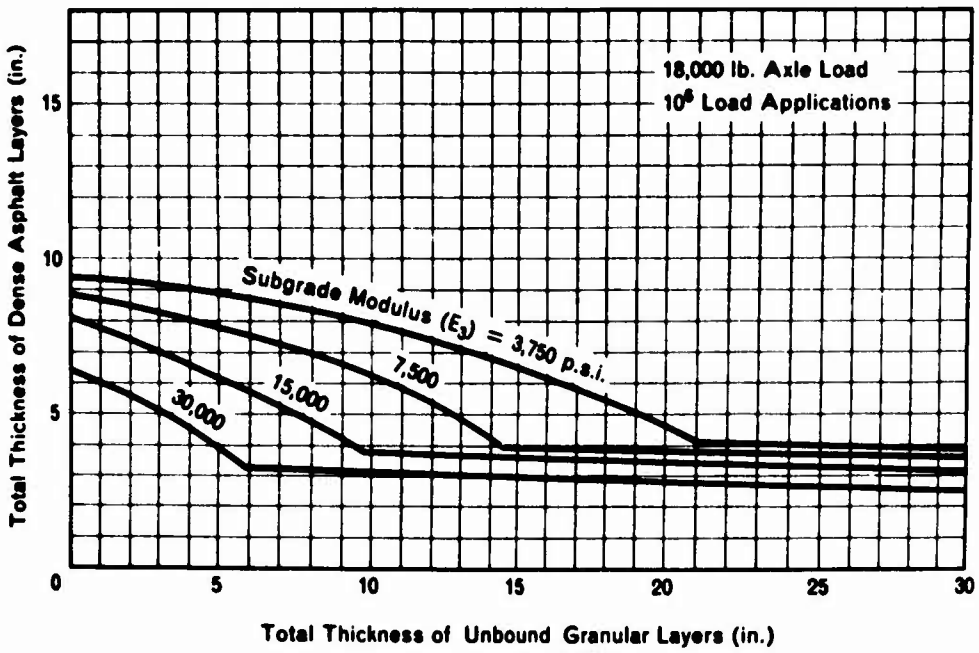

Fig. G6 Design curves for 10^6 load applications (Shell Oil Company, 1963)

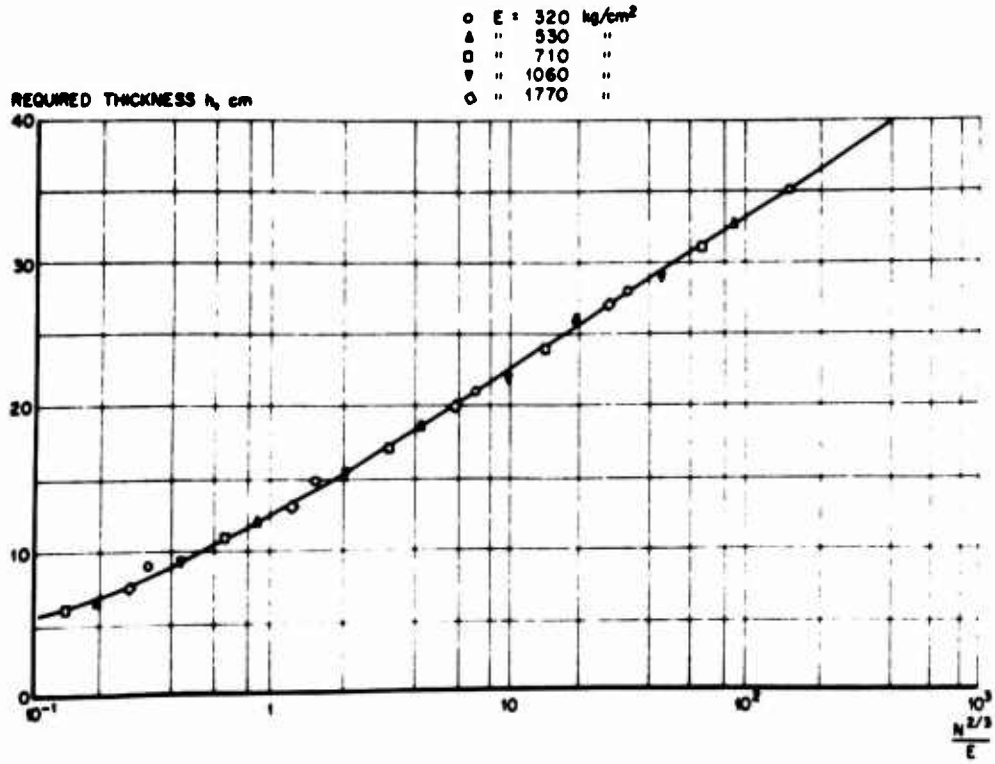

Fig. G7 Design of thickness, h, of asphalt concrete layer resting directly on the subgrade as a function of the design number, N, and the subgrade modulus, E (Heukelom and Klomp, 1968)

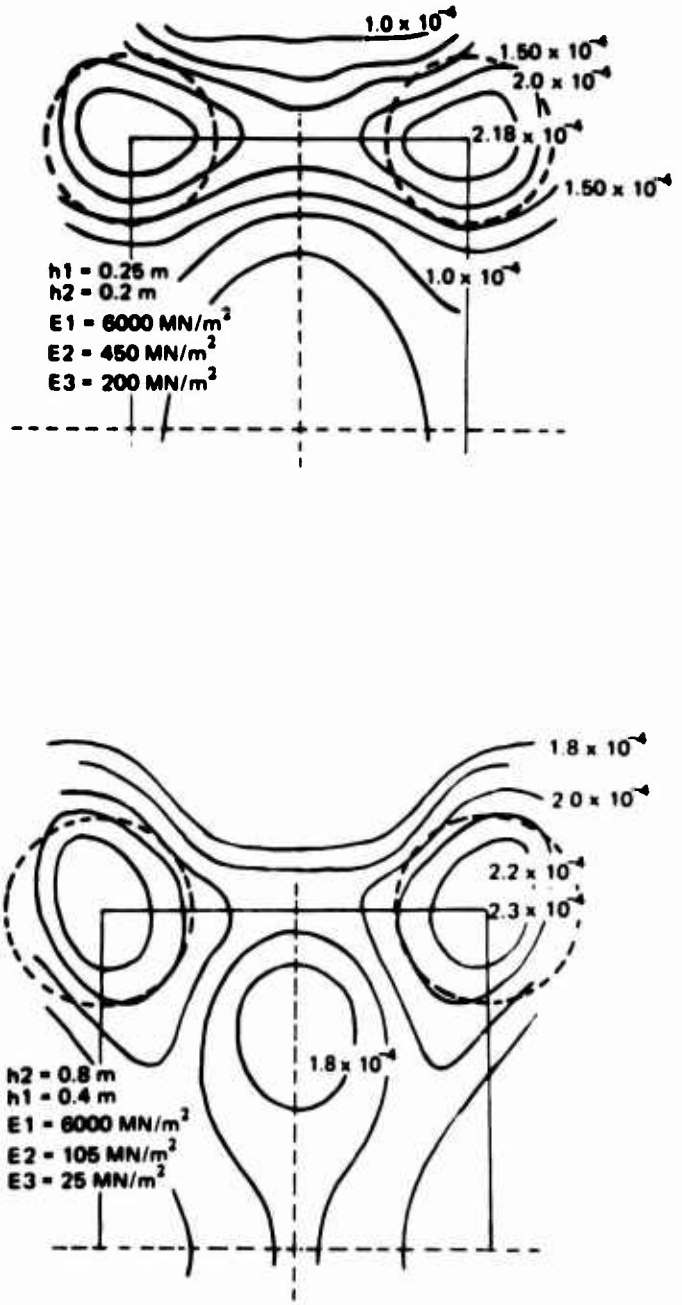

Fig. G8 Asphalt strain pattern under B707 (Edwards and Valkering, 1970)

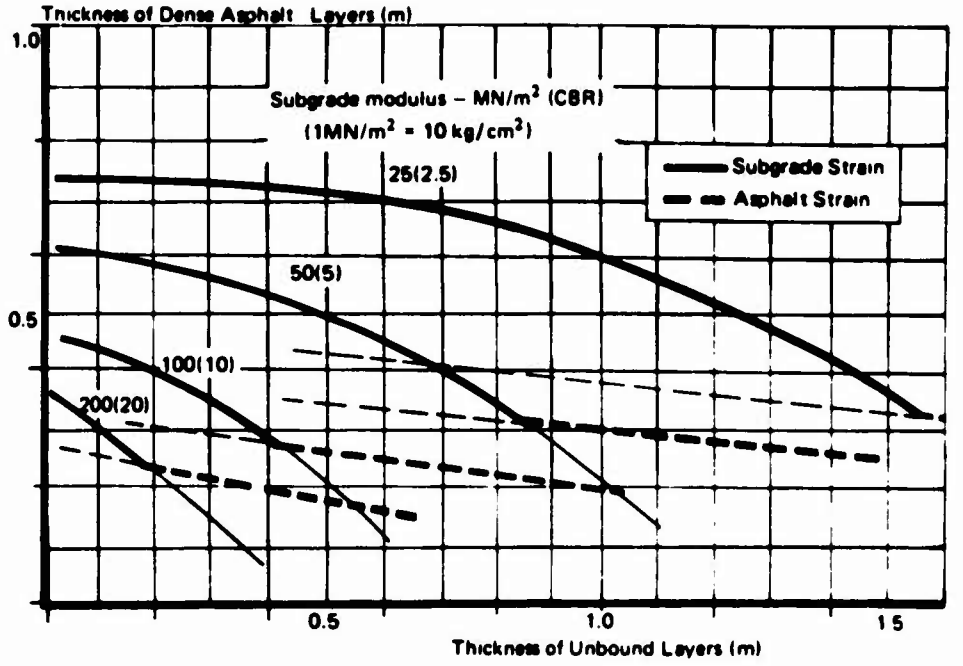

Fig. G9a Design curves for B707-320B
(Edwards and Valkering, 1970)

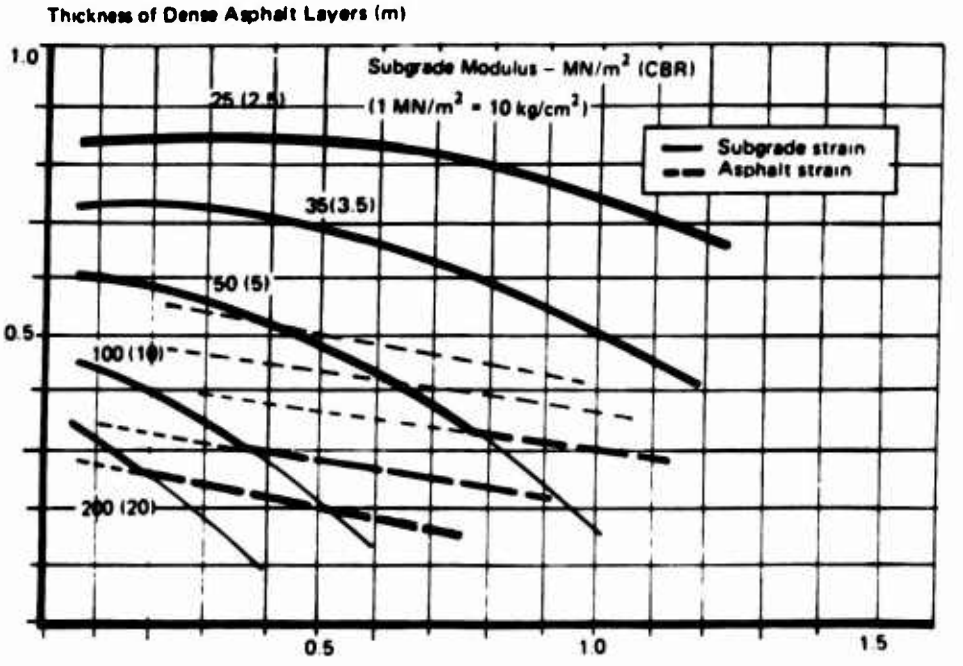

Fig. G9b Design Curves for B747 (Edwards and Valkering, 1970)